-THÈSE-

DOCTEUR ÈS SCIENCES

SPECIALITE : PHYSIQUE DE L'ATMOSPHERE

Présentée et soutenue le vendredi 18 septembre 2020 par :

JEAN-MAURICE CADET

Le rayonnement solaire ultraviolet de surface en région tropicale, validation instrumentale, climatologie et impacts sur la santé

JURY

Pr. Colette BROGNIEZ	LOA, Lille, FR	Examinateur
Dr. Fabrice JEGOU	LPC2E, Orléans, FR	Examinateur
Pr. Thierry PORTAFAIX	LACy, Saint-Denis, RE	Examinateur
Dr. Nathalie SULTAN-BICHAT	CHOR, Saint-Paul, RE	Examinateur
Dr. Sophie GODIN-BEEKMANN	LATMOS, Paris, FR	Rapporteur
Pr. Marcelo de PAULA CORREA	IRN, Itajubà, BR	Rapporteur
Pr. Hassan BENCHERIF	LACy, Saint Denis, RE	Directeur de thèse
Dr. Caradee WRIGHT	MRC, Pretoria, ZA	Co-directrice de thèse

ÉCOLE DOCTORALE, SPECIALITE :
Sciences Technologies Santé (ED542), Physique de l'Atmosphère

UNITE DE RECHERCHE :
Laboratoire de l'Atmosphère et des Cyclones – LACy UMR 8105

DIRECTEUR ET CO-DIRECTRICE DE THESE :
Hassan BENCHERIF et Caradee WRIGHT

« Là où est ton trésor, là aussi sera ton cœur »

Matthieu 6:21

REMERCIEMENTS

LETTRE D'ENGAGEMENT DE NON-PLAGIAT

Je soussigné CADET Jean-Maurice, en ma qualité de doctorant de l'Université de La Réunion, déclare être conscient que le plagiat est un acte délictueux passible de sanctions disciplinaires. Aussi, dans le respect de la propriété intellectuelle et du droit d'auteur, je m'engage à systématiquement citer mes sources, quelle qu'en soit la forme (textes, images, audiovisuel, internet), dans le cadre de la rédaction de ma thèse et de toute autre production scientifique, sachant que l'établissement est susceptible de soumettre le texte de ma thèse à un logiciel anti-plagiat.

Fait à Saint-Denis, le 18/09/2020

Extrait du Règlement intérieur de l'Université de La Réunion

(Validé par le Conseil d'Administration en date du 11 décembre 2014)

Article 9. Protection de la propriété intellectuelle – Faux et usage de faux, contrefaçon, plagiat

L'utilisation des ressources informatiques de l'Université implique le respect de ses droits de propriété intellectuelle ainsi que ceux de ses partenaires et plus généralement, de tous tiers titulaires de tels droits.

En conséquence, chaque utilisateur doit :

- utiliser les logiciels dans les conditions de licences souscrites ;

- ne pas reproduire, copier, diffuser, modifier ou utiliser des logiciels, bases de données, pages Web, textes, images, photographies ou autres créations protégées par le droit d'auteur ou un droit privatif, sans avoir obtenu préalablement l'autorisation des titulaires de ces droits.

La contrefaçon et le faux

Conformément aux dispositions du code de la propriété intellectuelle, toute représentation ou reproduction intégrale ou partielle d'une œuvre de l'esprit faite sans le consentement de son auteur est illicite et constitue un délit pénal.

L'article 444-1 du code pénal dispose : « Constitue un faux toute altération frauduleuse de la vérité, de nature à causer un préjudice et accomplie par quelque moyen que ce soit, dans un écrit ou tout autre support d'expression de la pensée qui a pour objet ou qui peut avoir pour effet d'établir la preuve d'un droit ou d'un fait ayant des conséquences juridiques ».

L'article L335_3 du code de la propriété intellectuelle précise que : « Est également un délit de contrefaçon toute reproduction, représentation ou diffusion, par quelque moyen que ce soit, d'une œuvre de l'esprit en violation des droits de l'auteur, tels qu'ils sont définis et réglementés par la loi. Est également un délit de contrefaçon la violation de l'un des droits de l'auteur d'un logiciel (…) ».

Le plagiat est constitué par la copie, totale ou partielle d'un travail réalisé par autrui, lorsque la source empruntée n'est pas citée, quel que soit le moyen utilisé. Le plagiat constitue une violation du droit d'auteur (au sens des articles L 335-2 et L 335-3 du code de la propriété intellectuelle). Il peut être assimilé à un délit de contrefaçon. C'est aussi une faute disciplinaire, susceptible d'entraîner une sanction.

Les sources et les références utilisées dans le cadre des travaux (préparations, devoirs, mémoires, thèses, rapports de stage…) doivent être clairement citées. Des citations intégrales peuvent figurer dans les documents rendus, si elles sont assorties de leur référence (nom d'auteur, publication, date, éditeur…) et identifiées comme telles par des guillemets ou des italiques.

Les délits de contrefaçon, de plagiat et d'usage de faux peuvent donner lieu à une sanction disciplinaire indépendante de la mise en œuvre de poursuites pénales.

VALORISATION SCIENTIFIQUE

Articles en premier auteur

- **Cadet, J.-M.**; Bencherif, H.; Portafaix, T.; Lamy, K.; Ncongwane, K.; Coetzee, G. J. R.; Wright, C. Y. Comparison of Ground-Based and Satellite-Derived Solar UV Index Levels at Six South African Sites. *Int. J. Environ. Res. Public Health* 2017, *14(11)*, 1384. doi: 10.3390/ijerph14111384
- **Cadet, J.-M.**; Bencherif, H.; Du Preez ; D.; Portafaix, T.; Sultan-Bichat, N.; Belus, M.; Brogniez, C.; Auriol, F.; Metzger, J.-M.; Ncongwane, K.; Coetzee, G. J. R.; Wright, C. Y.; Solar UV Radiation in Saint-Denis, La Réunion and Cape Town, South Africa: 10 years Climatology and Human Exposure Assessment at Altitude. *Atmosphere* 2019, *10(10)*, 589. doi: 10.3390/atmos10100589
- **Cadet, J.-M.**; Portafaix, T.; Bencherif, H.; Lamy, K.; Brogniez, C.; Auriol, F.; Metzger, J.-M.; Wright, C. Y.; Inter-comparison campaign of solar UVR instruments under clear sky conditions at Reunion Island (21°S, 55°E). *Int. J. Environ. Res. Public Health* 2020, *17(8)*, 2867. doi: 10.3390/ijerph17082867
- **Cadet, J.-M.**; Bencherif, H.; Wright, C. Y.; We found high UV doses at high-altitude hiking trails in Reunion and Cape Town. *The Conversation* 2020 (https://theconversation.com/we-found-high-uv-doses-at-high-altitude-hiking-trails-in-reunion-and-cape-town-136890)
- **Cadet, J.-M.**; Bencherif, H.; Cadet, N.; Lamy, K.; Portafaix, T.; Belus, M.; Wright, C. Y.; Solar UV radiation in the tropics: human exposure at Reunion Island (21°S, 55°E) during summer outdoor activities, *Int. J. Environ. Res. Public Health,* 2020 (**SUBMITTED**)

Article en co-auteur

- Du Preez, D.; Ajti, J.; Bencherif, H.; Bègue, N.; **Cadet, J. M.**; Wright, C.; Ajtić, J.; Spring and summer time ozone and solar ultraviolet radiation variations over Cape Town, South Africa. Annales Geophysicae 2019, 37(2), 129-141. doi: 10.5194/angeo-37-129-2019

Conférences

- **Cadet, J.-M.**; Portafaix, T.; Bencherif, H.; Brogniez, C.; Sébastien, N.; Lallemand, C.; Wright, C. Y.; Inter-comparison campaign of solar UVR instruments at Réunion Island (21.0° S, 55, 5° E): findings and recommendations. In *European Conference on solar UV Monitoring*, Vienna, Austria, 2018
- **Cadet, J.-M.**; Bencherif, H.; du Preez, D. J.; Portafaix, T.; Brogniez, C.; Auriol, F.; Metzger, J.-M.; Ncongwane, K.; Coetzee, G. J. R.; Wright, C. Y.; Solar UV Radiation in Saint-denis, La Réunion and Cape Town, South Africa: 10 years climatology and trends (2009-2018). In *French – South African Science and Innovation Days*, Pretoria, South Africa, 2019
- Bencherif, H.; Techer, L.; Vescovini, T.; Sivakumar, V.; Begue, N.; Revillion, C.; **Cadet, J.-M.**; Mbatha, N.; George, M.; Coheur, P.-F.; Variability and distributions of carbon monoxide and fires in southern Africa from ground based and satellite observations. In *French – South African Science and Innovation Days*, Pretoria, South Africa, 2019
- Wright, C. Y.; Bencherif, H.; Venkataram, S.; Du Preez, D. J.; **Cadet, J.-M.**; Research, collaboration and friendship in atmospheric science and public health. In *French – South African Science and Innovation Days*, Pretoria, South Africa, 2019
- **Cadet, J.-M.**; Solar UV radiation in tropical region, instruments validation, climatology and human health. in Workshop IRP ARSAIO December 2019, Pretoria, South Africa, 2019

SOMMAIRE

TABLE DES ACRONYMES ET ABREVIATIONS

AERONET	Aerosol Robotic Network
ALB	Albédo
AOD	Aerosol Optical Depth
AOT	Aerosol Optical Tickness
CF	Cloud Fraction
CFC	Chlorofluorocarbure
CIE	Commission Internationale de l'Eclairage
COV	Composé Organique Volatile
ETS	Extraterrestrial Spectrum
LACy	Laboratoire de l'Atmosphère et des Cyclones
LER	Lambertian Equivalent Reflectivity
MAPE	Mean Absolute Percentage Error
MED	Minimal Erythemal Dose
NDACC	Network for the Detection of Atmospheric Composition Change
OMI	Ozone Monitoring Instrument
OP	Ozone Profil
OPAR	Observatoire de Physique de l'Atmosphère
QASUME	Quality Assurance of Spectral Ultraviolet Measurements in Europe
RD	Relative Difference
RSME	Root Mean Square Error
RSD	Relative Standard Deviation
SAWS	South African Weather Service
SED	Standard Erythemal Dose
SSA	Single-Scattering Albedo
SZA	Solar Zenith Angle
TNO_2	Total Nitrogen Dioxide column
TO_3	Total Ozone column
TOMS	Total Ozone Mapping Spectrometer
TP	Temperature Profil
TUV	Tropospheric Ultraviolet Visible
UV	Ultraviolet
UVI	UV Index
UVR	Ultraviolet Radiation
WHO	World Health Organization

TABLE DES FIGURES

Chapitre 4

Chapitre 5

INTRODUCTION

Le rayonnement ultraviolet a été mis en évidence pour la première fois en 1801 par le physicien allemand Johann Wilhelm Ritter, en étudiant son action sur le chlorure d'argent. Cependant, ce n'est que dans les années 1970 que les connaissances sur le rayonnement ultraviolet ont été approfondies, après la découverte du trou d'ozone en Antarctique et ses conséquences directes sur la biosphère. Le rayonnement ultraviolet (UV) est aujourd'hui bien connu et défini, autant pour son caractère néfaste pour la biosphère terrestre que par sa nécessité vitale.

La principale source naturelle de rayonnement ultraviolet est le soleil. Le rayonnement UV représente environ 5% du rayonnement solaire total, la majeure partie étant le rayonnement infrarouge et visible, et s'étend des longueurs d'onde 100 nm à 400 nm. Il est divisé en plusieurs bandes, les UVA (315-400 nm), UVB (280-315 nm) et UVC (100-280 nm) (CIE I. 1., 1999).

Le rayonnement UV subit de nombreuses atténuations ou augmentations d'intensité avant d'arriver à la surface. Différents paramètres environnementaux modulent l'intensité UV. Parmi eux, nous pouvons noter l'ozone stratosphérique, l'angle solaire zénithal ou encore la nébulosité. Le rayonnement UV permet la réalisation des réactions de photolyses du dioxygène et de l'ozone selon le cycle de Chapman (**Figure 1**) (Bais, Zerefos, Meleti, Ziomas, & Tourpali, 1993). Ainsi, après la couche d'ozone, le rayonnement UV se retrouve diminué en raison de son absorption par les réactions du cycle de l'ozone. L'importance de l'évolution de la quantité d'ozone stratosphérique est alors déterminante, tout comme l'équilibre entre l'ozone et l'oxygène. D'autres gaz traces absorbent et diffusent également le rayonnement ultraviolet, comme le dioxyde d'azote ou le dioxyde de souffre (Diaz, et al., 2014).
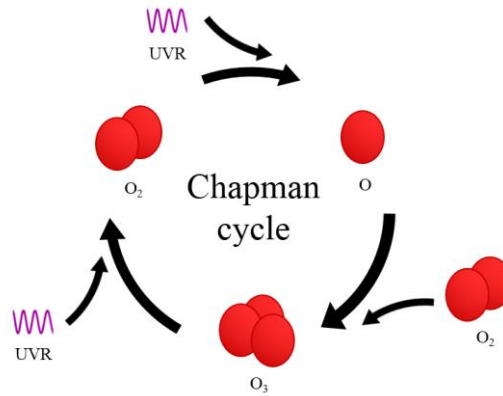
Figure 1 : Le cycle de Chapman

De manière générale, plus la longueur d'onde associée à un rayonnement est courte, plus ce rayonnement est dangereux pour la santé, car il peut détruire l'ADN. Pour le cas de la bande UV, les longueurs d'onde les plus courtes et les plus dangereuses sont les UVC et sont totalement arrêtées par la couche d'ozone. Les UVB sont absorbés à 95% par l'atmosphère et 95% des UVA arrivent à la surface de la Terre. Les UVA sont les moins dangereux, mais entrainent toutefois quelques effets pernicieux : ils sont responsables du vieillissement cutané. Les UVB, quant à eux, sont responsables des coups de soleil ou dommages cutanés à plus long termes, mélanomes, cancer, immunodéficience, cataracte (Gallagher & Lee, 2016). Chaque année, un nombre toujours croissant de cancers, mélanomes ou autres est enregistré. Une trop longue exposition aux UV engendre 90% des problèmes de peau (Sitas, 1994) (Armstrong & Kricker, 1993).

Au-delà de la dangerosité, le rayonnement UV est aussi une nécessité par l'intermédiaire de la vitamine D (McKenzie, Liley, & Björn, 2009). Le rayonnement UV permet la synthèse de vitamine D, un facteur incontournable dans le cycle du calcium, mais est également connu pour son action dans la diminution du risque de certaines maladies (Holick, 2001). La vitamine D intervient également dans de nombreuses réactions chimiques telles que la production de sérotonine (Lansdowne & Provost, 1998) (Shipowick, Moore, Corbett, & Bindler, 2009).

Cette ambivalence des UV se retrouve chez les végétaux (Caldwell, 1971), ou encore dans la biosphère marine (Vernet, Brody, Holm-Hansen, & Mitchell, 1994).

Les enjeux environnementaux sont donc majeurs, notamment dans le domaine de la santé publique. L'évaluation régulière et précise de l'intensité du rayonnement ultraviolet est donc nécessaire. L'instrumentation des villes ou sites très fréquentés, où la population est

susceptible de s'exposer au soleil, devient particulièrement importante. A plus grande échelle, l'installation de réseau de mesures, comme le réseau UV-Indien (Lamy K. , Portafaix, Forestier, Rakotoniaina, & Amélie, 2019), est pertinente (Schmalwieser, et al., 2017).

Il existe différents moyens de quantifier le rayonnement ultraviolet : la spectrométrie, qui mesure l'irradiance par longueur d'onde, la radiométrie, qui mesure l'irradiance erythemale ou autre sur une bande de fréquence. Ces instruments peuvent être localisés sur des stations fixes au sol, destinées à la mesure à long termes. Ils peuvent également être embarqués à bord de satellites, par exemple le spectromètre OMI (Ozone Monitoring Instrument) embarqué à bord du satellite Aura. Le niveau d'ultraviolet peut également être obtenu par la modélisation, via des modèles de transfert radiatif.

Les instruments de mesure nécessitent un suivi et une calibration régulière. Les calibrations peuvent être faites par des lampes de références (Brogniez, et al., 2016) ou lors de campagnes de calibrations avec des instruments de référence (Gröbner, et al., 2006) (Hülsen & Gröbner, 2017). Des corrections sont alors appliquées, notamment une correction en ozone ou en angle zénithal.

Ce travail de thèse est organisé en 5 chapitres. Le premier chapitre est consacré à la présentation générale du sujet. Le second chapitre est consacré à l'évaluation de différents instruments de mesure du rayonnement ultraviolet. Lors d'une campagne d'inter-comparaison, quatre radiomètres larges bandes UV ont été comparés à un spectroradiomètre de référence. La référence utilisée est un spectroradiometre Bentham DTMc300 calibré tous les trois mois, considéré comme étant à la pointe de la mesure UV. L'objectif est d'évaluer les performances de ces instruments, ces derniers étant de qualités et de coûts différents. L'exercice de comparaison s'est déroulé à La Réunion sur une période d'une année. Afin d'améliorer la précision des résultats, les comparaisons ont été effectuées par ciel clair. Le filtrage a été réalisé à l'aide des données de fraction nuageuse mesurées par une caméra imageur de ciel co-localisée.

Le troisième chapitre présente, quant à lui, une évaluation de l'instrument satellitale OMI. Les données d'indice UV issue du capteur OMI à bord du satellite Aura ont été comparés à un réseau de six instruments opérationnel sur différents sites en Afrique du Sud. Ce réseau instrumental, composé de six radiomètres large bande Solar light SL501, est géré par le South African Weather Service (SAWS). La comparaison a été effectuée à l'heure du passage au

nadir du satellite et par ciel clair. Le filtrage en ciel clair a été réalisé en utilisant la réflectivité du capteur OMI.

Le quatrième chapitre de ce manuscrit de thèse est consacré à la climatologie, à l'estimation des tendances et à la mesure de l'exposition. Les climatologies sur la période 2009-2018 ainsi que les tendances des indices UV ont été calculées pour les sites de Saint-Denis à La Réunion et à Cape Town en Afrique du Sud. Les climatologies obtenues étant révélatrices d'un niveau d'exposition extrême, des mesures d'exposition UV ont été réalisées dans des endroits très prisés par les touristes et locaux et où la population est susceptible de s'exposer au rayonnement solaire, particulièrement à La Réunion, où de nombreuses activités se font à la plage ou en montagne.

Chapitre 1   LE RAYONNEMENT SOLAIRE ULTRAVIOLET

1.1 DEFINITION

Le rayonnement ultraviolet que nous recevons sur terre nous vient du soleil. Il représente une petite partie du spectre d'émission solaire, environ 5%, allant des longueurs d'onde 100 nm à 400 nm.

La Commission Internationale de l'Eclairage (CIE) a défini un découpage de la bande de longueur d'onde UV en 4 parties (Barth, et al., 1999) (WHO, 1994), en fonction de leur propriété physique, notamment de leur capacité de propagation dans l'atmosphère, mais aussi de leurs effets biologiques sur l'Homme (discutées au §1.3) (Figure 2) :

- UV-C : de 100 nm à 280 nm. Les UV-C sont les plus énergétiques et sont les plus dangereux pour la biosphère, même à très faible dose. Cependant, ils n'atteignent pas la surface de la Terre, car ils sont totalement absorbés par l'atmosphère.

- UV-B : de 280 nm à 315 nm. Ils sont en grande partie filtrés par l'atmosphère, 95%. Les UVB ne pénètrent que les couches superficielles de la peau, mais sont responsables du bronzage à long terme et des problèmes de peau, coups de soleil, cancers.

- UV-A : de 315 nm à 400 nm, sont quant à eux très peu absorbés par l'atmosphère, ils représentent la quasi-totalité du rayonnement UV atteignant le sol. Ils sont de plus faible énergie et sont responsable du bronzage immédiat, du vieillissement et des cancers de la peau. On distingue 2 sous-classes dans les UV-A :

    - UV-A1 : de 340 nm à 400 nm

    - UV-A2 : de 315 nm à 340 nm

Cependant, d'autres classifications existent, notamment celle définie par la norme ISO 21348 de 2007, avec un découpage plus fin.
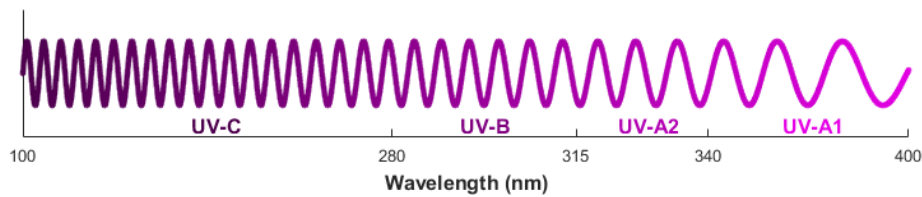
Figure 2 : Découpage de la bande UV selon la CIE

Il existe également le rayonnement ultraviolet extrême (*V-UV – Vaccum UV*), situé entre 10 nm et 100 nm. Ce rayonnement est complètement arrêté par l'atmosphère, il ne peut se propager que dans le vide. Il n'est donc communément pas pris en compte dans l'étude de l'ultraviolet sur Terre. Plus généralement, la surface de la Terre est protégée par l'atmosphère du rayonnement dont les longueurs d'onde sont inférieures à 290 nm (Kerr & Fioletov, 2008).

1.2 FACTEURS ENVIRONNEMENTAUX

De nombreux facteurs environnementaux modulent l'intensité du rayonnement ultraviolet solaire atteignant la surface de la Terre.

1.2.1 LE CYCLE SOLAIRE

Le rayonnement ultraviolet reçu au sol nous vient du Soleil. L'intensité de son activité périodique, dont la modulation par le cycle de 11 ans, a donc un rôle à jouer (Shindell, Rind, Balachandran, Lean, & Lonergan, 1999). D'autre part, il a été montré que le cycle solaire a un impact important sur la stratosphère, notamment sur la circulation de Brewer-Dobson et sur le cycle de l'ozone qui, nous le verrons par la suite, est un paramètre déterminant la quantité de rayonnement UV reçu au sol (Marchand, et al., 2012). Cependant, il a été montré que la variabilité des UVA et UVB due à l'activité solaire restait faible, <1% (Kerr & Fioletov, 2008).

1.2.2 LES SAISONS

L'intensité du rayonnement ultraviolet mesuré au sol dépend de la période de l'année. En effet, le rayonnement à une distance donnée du soleil est inversement proportionnel au carré de la distance au soleil. La trajectoire de la Terre autour du Soleil étant elliptique, le rayonnement ultraviolet est maximal quand la Terre est au périhélie de sa trajectoire, point le plus proche du soleil, et minimal lorsque la Terre est l'aphélie, point le plus éloigné. Entre ces 2 points, le rayonnement global varie d'environ 7% (Kerr & Fioletov, 2008).

Une des conséquences directes de l'orbite terrestre autour du Soleil et de l'inclinaison de l'axe de rotation de la Terre est la différence d'intensité du rayonnement dans les 2 hémisphères. En effet, lorsque la Terre est au périhélie, l'hémisphère Sud est orienté face au Soleil (été austral) et lorsque la Terre est à l'aphélie, c'est l'hémisphère Nord qui est orienté face au Soleil (été boréal). L'intensité du rayonnement est donc plus importante durant l'été austral que l'été boréal. De ceci résulte un niveau UV globalement plus élevé dans l'hémisphère Sud (illustration en **page 47**, **Figure 11**).

1.2.3 LA LATITUDE

La latitude est un élément important qui détermine le flux de rayonnement UV atteignant la surface. En effet, aux faibles latitudes, proche de l'équateur, le rayonnement traverse l'atmosphère avec un faible angle d'incidence. L'énergie solaire reçue est élevée. Plus on s'éloigne de l'équateur, plus le trajet optique de la lumière dans l'atmosphère augmente, entrainant une plus grande absorption, et plus l'énergie se répartie sur de plus grandes surfaces qu'aux latitudes équatoriales et tropicales. Ceci implique une diminution de l'irradiance à surfaces égales, **Figure 3** (illustration en **page 47**, **Figure 11**).
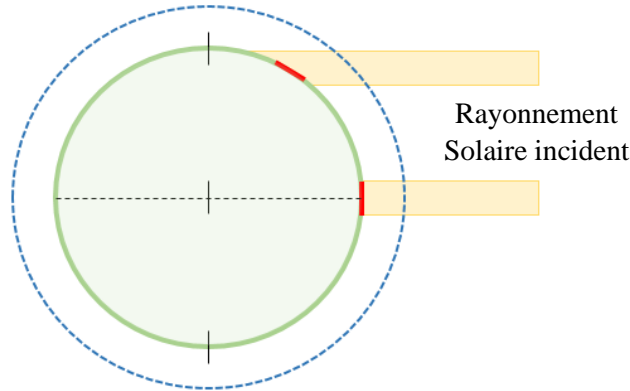
Figure 3 : Atténuation du rayonnement solaire incident en fonction de la latitude

1.2.4 LA LONGITUDE

Le rayonnement UV est maximal au moment du midi solaire, lorsque le soleil est au plus haut dans le ciel. L'heure (légale) du midi solaire (locale) dépend de la longitude et du fuseau horaire. Cette heure n'est pas constante au cours de l'année à cause de l'inclinaison du plan de l'écliptique par rapport à l'équateur mais aussi en raison de la trajectoire elliptique de la Terre autour du Soleil, et doit donc être corrigée de « l'équation du temps vrai » (Chambelin, 2013).

Ainsi, en fonction de la longitude, par rapport au méridien d'origine et vers l'Est, le midi local est calculé suivant la formule suivante :

$$H_{12h\ solaire} = 12[h] + F[h] - \frac{L[°]}{15[°.h^{-1}]} + E_{tv}[h] \qquad (1)$$

où *F* est le nombre de fuseaux horaires comptés positivement vers l'Est, *L* la longitude du site considéré et E_{tv} l'équation du temps.

La **Figure 4** ci-dessous montre l'heure à laquelle le soleil est au zénith à Saint-Denis de La Réunion.
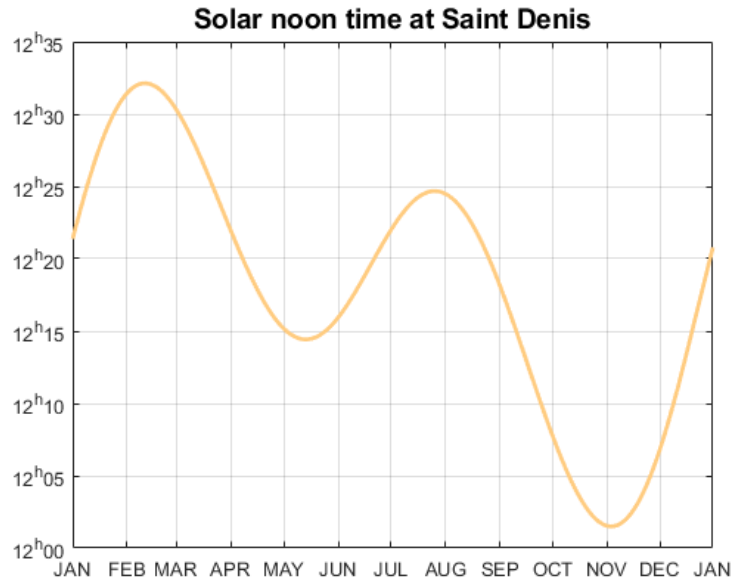
Figure 4 : Heure du midi solaire à Saint-Denis

1.2.5 L'HEURE DE LA JOURNEE

Le moment de la journée détermine également le niveau du rayonnement ultraviolet. L'incidence du rayonnement solaire, mesurée par l'angle solaire zénithal, module fortement l'intensité perçue à la surface : plus le soleil est haut dans le ciel, plus l'énergie est répartie sur une petite surface et moins cette énergie est absorbée par l'atmosphère, la distance parcourue dans celle-ci étant plus courte.
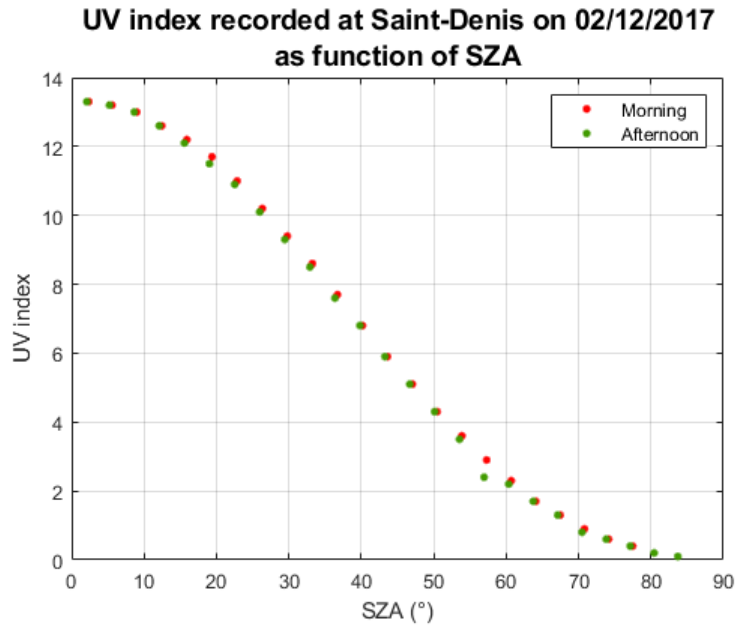
Figure 5 : Indice UV en fonction de l'angle solaire zénithal mesuré à Saint-Denis le 02/12/2017

1.2.6 LA COUVERTURE NUAGEUSE

La couverture nuageuse joue un rôle primordial sur le rayonnement atteignant le sol. Bien que difficilement quantifiable, étant donné la variabilité spatiale et temporelle de la nébulosité, les nuages peuvent être quasi-transparent ou fortement, voire complètement opaque, selon le type de nuage, la forme et l'empreinte spatiale. Les nuages peuvent également augmenter le rayonnement par diffusion multiple dans des cas particuliers lors de la présence de brume ou de cirrus, ou encore lors de couverture nuageuse fragmentée (5-7 octas) (Jégou, et al., 2011) ; (Calbo, Pagès, & Gonzalez, 2004) ; (Cede, Blumthaler, Luccini, Piacentini, & Nuñez, 2002) ; (Bessemoulin & Oliviéri, 2000) ; (Bais, Zerefos, Meleti, Ziomas, & Tourpali, 1993).

1.2.7 L'ALTITUDE

L'altitude a un effet sur le rayonnement UV : la distance parcourue dans l'atmosphère étant plus courte en altitude, le rayonnement subit moins de diffusion. Ainsi une augmentation d'altitude entraine une augmentation de rayonnement UV. La diffusion dépendant de la

quantité, ainsi que du type d'aérosols, l'augmentation d'UV varie : +7%/1000m dans des situations de ciel clair et +15%/1000m dans les cas de fortes pollutions, notamment dans les basses couches de la troposphère (Blumthaler, Ambach, & Ellinger, 1996) ; (Krotkov, Bhartia, Herman, Fioletov, & Kerr, 1998) ; (Pfeifer, Koepke, & Reuder, 2006). Illustration en **page 47**, **Figure 11**.

1.2.8 L'ALBEDO

L'albédo, compris entre 0 et 1, définit la réflectivité d'une surface. Très variable en fonction des surfaces, le rayonnement peut être complètement absorbé ou fortement renvoyé **(Tableau 1)**. Par exemple, sur une surface enneigée, pour un albédo de 0,6 – 0,8, on observe une augmentation d'environ 40% du rayonnement UV (McKenzie, Paulin, & Madronich, 1998) ; (Bessemoulin & Oliviéri, 2000). Illustration en **page 47**, **Figure 11**.

Tableau 1 : Albédos typiques de différents types de surfaces (Bessemoulin et Oliviéri, 2000)

Type de surface	Albédo
Neige fraîche	0,8 à 0,9
Neige ancienne	0,5 à 0,7
Sol rocheux	0,15 à 0,25
Sol cultivé	0,07 à 0,14
Forêt	0,06 à 0,20
Etendue d'eau	0,05

1.2.9 L'OZONE

L'effet de l'ozone sur le rayonnement ultraviolet de surface est bien documenté, notamment à cause du trou d'ozone et de l'impact environnemental pouvant être engendré (Bais, et al., 2018). L'ozone et le rayonnement UV de surface sont anti corrélés (Zerefos, 2002).

De manière générale, l'ozone peut être « bon » ou « mauvais ». Le « bon » ozone se situe dans la stratosphère et constitue la couche d'ozone. Il représente 90% de l'ozone total. L'ozone stratosphérique joue le rôle de filtre du rayonnement UV par absorption et diffusion, seulement 3% de l'irradiance érythémale arrivent à atteindre la troposphère. Le rayonnement

UV permet l'activation des réactions de photolyse de l'ozone et de photolyse du dioxygène. Ces réactions se produisent continuellement en présence d'ultraviolet (cycle de Chapman) et leur équilibre est très fragile. La production d'ozone peut être stoppée par différents composés et aérosols, comme par exemple les chlorofluorocarbures (CFC). La prolifération de ces derniers est à l'origine du trou d'ozone dans la région du pôle Sud. C'est dans l'objectif de réduire les émissions des ODS (*ozone-depleting substance*) qu'a été signé le protocole de Montréal, 1987, afin de protéger la couche d'ozone, et à long terme, permettre sa restauration (Slaper, Velders, Daniel, de Gruilj, & van der Leun, 1996) (WMO, 1975).

Le « mauvais » ozone se trouve dans les basses couches de l'atmosphère, dans la troposphère. Il peut être formé suite à des réactions chimiques initiées par le rayonnement ultraviolet avec la présence d'oxyde d'azote (NO_x) ou de composés organiques volatiles (COV). NO_x et COV sont connus pour être des traceurs de pollutions et ont très souvent une origine anthropogénique. L'ozone tropospherique peut également être transporté depuis la stratosphère. L'ozone est un puissant oxydant et peut engendrer des problèmes médicaux chez l'homme, irritation des voies respiratoires, affaiblissement du système immunitaire, … mais aussi chez les animaux et les végétaux (Lippmann, 1989). C'est aussi un gaz à effet de serre.

(Guarnieri, et al., 2003) ; (McKenzie, Connor, & Bodeker, 1999) ; (Kerr & McElroy, 1993) ;

1.2.10 LES AEROSOLS

Certains aérosols, telles que le SO_2, NO_2, HNO_3 ou encore les poussières désertiques, absorbent et diffusent également dans la bande ultraviolette. Ces aérosols sont bien souvent d'origine anthropogéniques, mais peuvent aussi être naturels. Bien qu'ayant un effet moindre que l'ozone, leurs impacts peuvent être clairement identifiables dans les zones très industrialisées ou lors d'évènements de très forte pollution urbaine, avec des réductions de l'ordre de 10 à 15% du rayonnement UV, ou lors d'évènement tels que les feux de forêts ou panaches volcaniques. Il a été montré que certaines éruptions volcaniques peuvent emmètre suffisamment de SO_2 pour pouvoir absorber jusqu'à 50% de l'UV erythemal. (Tarasick, et al., 2010) (Diaz, et al., 2014) (Krueger, et al., 1995)

1.3 IMPACTS SUR LA SANTE

Le rayonnement solaire ultraviolet est nécessaire pour la bonne santé de l'homme. En effet, il permet la synthèse de la vitamine D par le corps humain, connue pour de nombreux bienfaits sur la santé. En revanche, une trop longue exposition au rayonnement UV peut causer des dommages importants pour l'homme, à court et long termes.

1.3.1 LES PHOTOTYPES

Chaque individu ne réagit pas de la même manière à une exposition au rayonnement ultraviolet. Le phototype permet de classifier les types de peaux en fonctions de leur résistance au rayonnement solaire (coup de soleil) et à leur capacité de pigmentation (bronzage). Le **Tableau 2** ci-dessous montre la classification des phototypes les plus utilisés (Fitzpatrick, 2002) :

Phototype	Caractéristiques	Brule au soleil	Bronzage
I	Peau sensible, ne produisant pas assez de mélanine	Toujours	Rare
II		Habituellement	Parfois
III	Peau normale, produisant assez de mélanine	Parfois	Habituellement
IV		Rare	Toujours
V	Peau protégée par la mélanine qu'elle contient	Très rare	Naturellement foncée
VI		Jamais	Naturellement foncée

Tableau 2 : Classification des différents phototypes selon Fitzpatrick. (Tableau extrait du guide pratique sur le rayonnement UV de l'OMS, 2002)

1.3.2 LES SPECTRES D'ACTION ERYTHEMALE ET VITAMINE D

Les spectres d'action (érythémale, vitamine D ou autres) sont des courbes de pondération qui, convoluées au spectre d'irradiance solaire, déterminent l'action réelle du rayonnement UV du phénomène associé, en fonction de la longueur d'onde. Il existe de nombreux spectres d'action, pour les animaux, les végétaux, le phytoplancton, les réactions chimiques, …

Pour l'homme, les 2 spectres d'action principaux sont le spectre d'action érythémale et le spectre d'action vitamine D, **Figure 6**.

Ainsi, on peut constater que la synthèse de vitamine D est optimale pour des longueurs d'onde autour de 300 nm (UV-B) et n'est quasiment pas produite sous un éclairement UVA. En revanche, la peau est très sensible aux longueurs d'onde croissantes jusqu'à 328 nm, ensuite l'action du rayonnement UV est exponentiellement décroissante pour les longueurs d'onde supérieures.

Reference: (Webb, Slaper, Koepke, & Schmalweiser, 2011) ; (Fioletov, McArthur, Mathews, & Marrett, 2008)
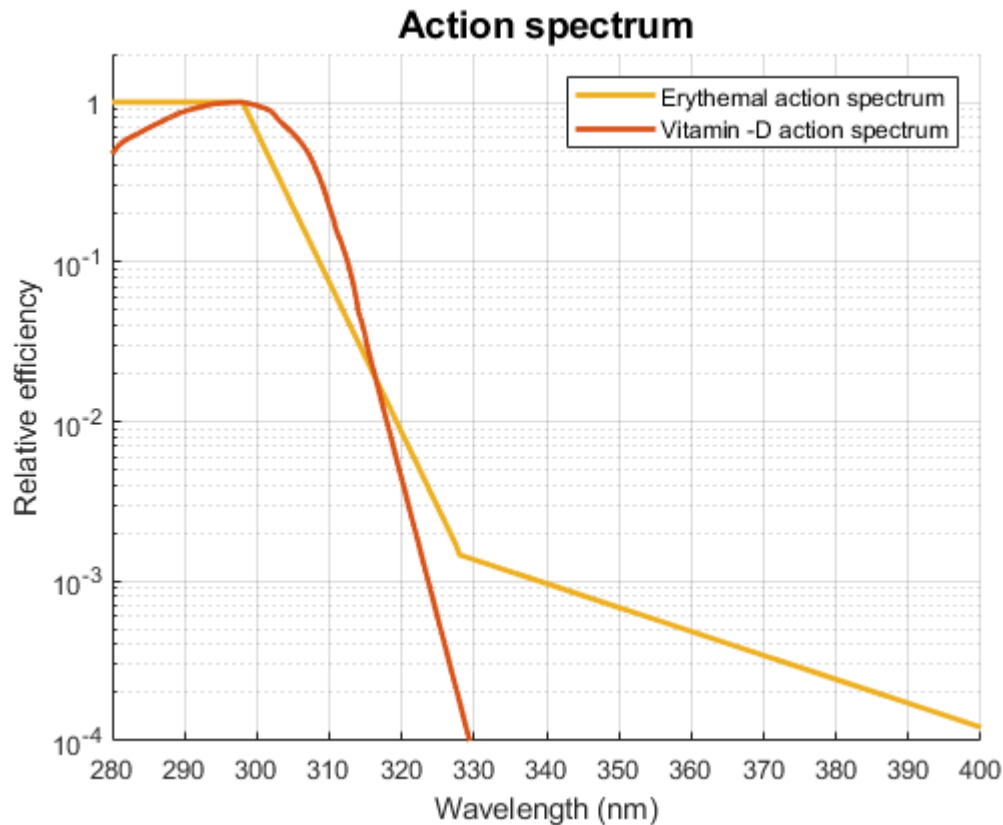
Figure 6 : Spectre d'action érythémale (jaune) et spectre d'action vitamine D (rouge) - La courbe montre le niveau de réaction de la peau en fonction de la longueur d'onde

1.3.3 LES EFFETS DU RAYONNEMENT UV

Le rayonnement ultraviolet joue un rôle central dans la biosphère terrestre, notamment pour l'Homme. Son action est à la fois positive et négative, dépendant du temps d'exposition (Matsumura & Ananthaswamy, 2004).

Les effets bénéfiques du rayonnement UV

Le rayonnement UV-B est nécessaire à la production de vitamine D. En effet, le rayonnement UV-B permet la transformation des molécules de 7-déhydrocholestérol en vitamine D3 inactive, puis par l'action du foie et des reins, en vitamine D3 active (cholécalciférol). (Webb, Kline, & Holick, 1988).

La vitamine D est connue pour son rôle dans le cycle du calcium et la robustesse osseuse, mais aussi pour diminuer le risque cardiovasculaire, le risque de sclérose en plaque, et de certains cancers (Holick, 2001).

La vitamine D est également un facteur affectant le comportement. En effet, elle intervient dans la chimie du cerveau, notamment pour la production de sérotonine, connu pour ses effets antidépresseurs et son lien avec la bonne humeur ! (Lansdowne & Provost, 1998) (Shipowick, Moore, Corbett, & Bindler, 2009).

Le rayonnement ultraviolet est également utilisé en photothérapie, prophylaxie, ou en médicine préventive. Il a été montré son efficacité contre différentes maladies, comme la tuberculose cutanée (Prix Nobel de Finsen, 2003), le rachitisme, *etc*. (Albert & Ostheimer, 2003) (Rajakumar, Greenspan, Thomas, & Holick, 2007)

Les effets délétères de l'exposition aux UV

Les effets néfastes du rayonnement ultraviolet sont nombreux. Les dommages sur la peau sont les plus fréquents : coup de soleil, mélanome cutané, cancer de la peau. Les personnes les plus touchées sont les phototypes I et II. 90% des problèmes de peau sont liés au rayonnement ultraviolet (Armstrong & Kricker, 1993).

Le bronzage et l'épaississement des couches externes de la peau, synonymes de lésions cutanées, sont les mécanismes de défense du corps, retardant ainsi les effets néfastes d'une exposition prolongée rayonnement solaire UV (OMS, 2002). Il est à noter que le bronzage, qui est la synthèse de mélanine par les UVB, protège temporairement du rayonnement UV. A l'inverse, le « bronzage » causé par les UVA, qui est l'oxydation de la mélanine, ne protège aucunement du rayonnement UV (Coelho, et al., 2014).

L'utilisation des crèmes solaires depuis les années 1960 a permis de réduire de risque lié aux expositions UV, mais peut cependant avoir un effet négatif. En effet, l'usage de crème solaire induit généralement une modification du comportement humain liée à un sentiment de sécurité, entrainant de fait une exposition plus longue au soleil. Certaines crèmes solaires ne protégeant que des UVB, et une longue exposition aux UVA peut, entre autres, entrainer un vieillissement prématuré de la peau (Gallagher & Lee, 2016) (Fisher, et al., 1997). De plus,

les crèmes solaires sont aujourd'hui connues pour leur impact négatif sur la biodiversité marine, notamment sur les coraux, autant par leur mauvaise utilisation que par les quantités utilisées (ARVAM, 2015).

Parmi les effets délétères des UV, on note également les dommages causés aux yeux, très sensibles à ce rayonnement : mélanome oculaire, kératites, cataractes, ptérygium, *etc* (Tucker, et al., 1985) (Gallagher, et al., 1985).

L'effet immunosuppresseur causé par le rayonnement ultraviolet est aussi très bien connu. Même à faible dose, le rayonnement UV entraine une diminution des cellules de Langerhans, la première défense immunitaire, et réduis le pouvoir des lymphocytes T. Par ailleurs, l'irradiance UV favorise les réactions photo-immunosuppresseurs et limite les processus de réparation de l'ADN (Sinha & Häder, 2002) (Cadet, Sage, & Douki, 2005) (AFSSE, 2005) (Schwarz, 2010) (Karran & Brem, 2016). Ces effets sont causés autant par les UVB que par les UVA, bien que de moindre intensité dans le cas des UVA (Tewari, Grage, Harrison, Sarkany, & Young, 2013).

Il est également à noter que le changement des comportements humains est un facteur important expliquant les surexpositions au rayonnement UV. En effet, une tendance à l'augmentation de l'exposition au soleil est à noter au cours des dernières décennies, soit par la recherche d'un bronzage pour effet esthétique, le bronzage étant synonyme de bonne apparence, soit par des activités de plein air, synonyme de bonne santé (Albert & Ostheimer, 2002) (Albert & Ostheimer, 2003) (Chaillol, 2011). Par exemple, la popularité croissante des cabines de bronzage artificiel dans un but esthétique est un facteur important de surexposition (Gallagher, Spinelli, & Lee, 2005) (Börner, Schütz, & Wiedemann, 2009) (Joel Hillhouse, Thompson, Jacobsen, & Hillhouse, 2009) et est responsable de 4% des mélanomes cutanés en France (Arnold, et al., 2018).

Les cabines de bronzage artificiel sont des lieux d'exposition extrême. En France, la législation limite l'intensité maximale des cabines UV, mais l'irradiance associée reste encore très élevée, correspondant à un indice UV maximum de 12 **(indice UV défini au §1.4.1 suivant)** (Genet, 2018). La répartition UVA/UVB n'est pas la même pour les cabines de bronzage peut monter à jusqu'à 80%. Mais cette augmentation des UVA entraine un vieillissement jusqu'à 4 fois plus rapide de la peau (Sola & Lorente, 2015), ce qui est paradoxale puisque les cabines de bronzage sont utilisés à des fins esthétiques. Enfin, il a été

aussi démontré que les cabines de bronzage ont un effet addictif, entrainant nécessairement une augmentation des durées d'exposition (Aubert, et al., 2016).

Le temps d'exposition

Comme expliqué dans les 2 paragraphes précédents, le rayonnement UV est à la fois nécessaire et dangereux. Heureusement, le temps nécessaire pour les bienfaits du rayonnement UV est inférieur au temps nécessaire pour subir les premiers effets négatifs. La durée d'exposition optimale dépend bien entendu du niveau de rayonnement UV, mais aussi du phototype de chaque individu. (**Figure 7**)

Il est à noter que la surface de peau exposée au soleil est importante pour la synthèse de vitamine D. Plus la surface exposée est grande, plus la synthèse de la vitamine D sera grande. A l'inverse, la surface de peau exposée n'intervient pas dans le temps d'apparition des problèmes liés à la surexposition aux UV. Un coup de soleil, par exemple, mettra autant de temps pour apparaitre sur tout le corps que sur 1 cm² de peau. (McKenzie, Liley, & Björn, 2009) (Lucas, McMichael, Smith, & Armstrong, 2006) (Lucas & Ponsonby, 2002)
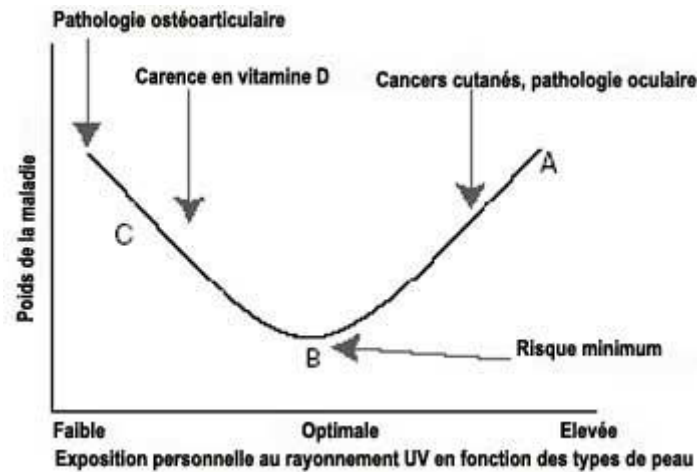
Figure 7 : Risques liés au rayonnement UV en fonction du temps d'exposition (Image tirée du site internet de l'OMS : http://www.who.int/uv/health/fr/)

1.4 QUANTIFICATION DU RAYONNEMENT UV

Il existe différentes manières de quantifier le rayonnement ultraviolet, en fonction de la finalité recherchée. Dans cette partie seront présentés les différents indices et unités de quantification de l'ultraviolet érythémale uniquement, bien que d'autre indices et unités de mesure existent pour des domaines d'étude différents.

1.4.1 L'INDICE UV

Défini et utilisé au Canada depuis 1992 et adopté par l'Organisation Mondiale de la Santé (OMS) en 1994, l'indice UV est une valeur simple, sans unité, destinée à quantifier le rayonnement ultraviolet érythémale. Cet indice UV est principalement destiné à sensibiliser le grand public, afin de lui permettre d'apprécier les risques liés au rayonnement UV de manière simple. L'indice UV est aujourd'hui largement adopté (Fioletov, Kerr, & Fergusson, 2010). Un exemple de suivi temporel journalier d'indice UV est présenté ci-dessous. L'indice UV a été enregistré lors d'une randonnée en altitude à La Réunion : Maïdo – Grand Bénare **(Figure 8)**.

Extrait du guide pratique sur le rayonnement UV édité par l'OMS (OMS, 2002) :

« L'indice universel de rayonnement UV solaire (IUV) exprime l'intensité du rayonnement ultraviolet solaire qui atteint la surface terrestre. La valeur minimale de l'indice est zéro et, plus il est élevé, plus le risque de lésions cutanées et oculaires est grand, et moins il faut de temps pour qu'elles apparaissent. »
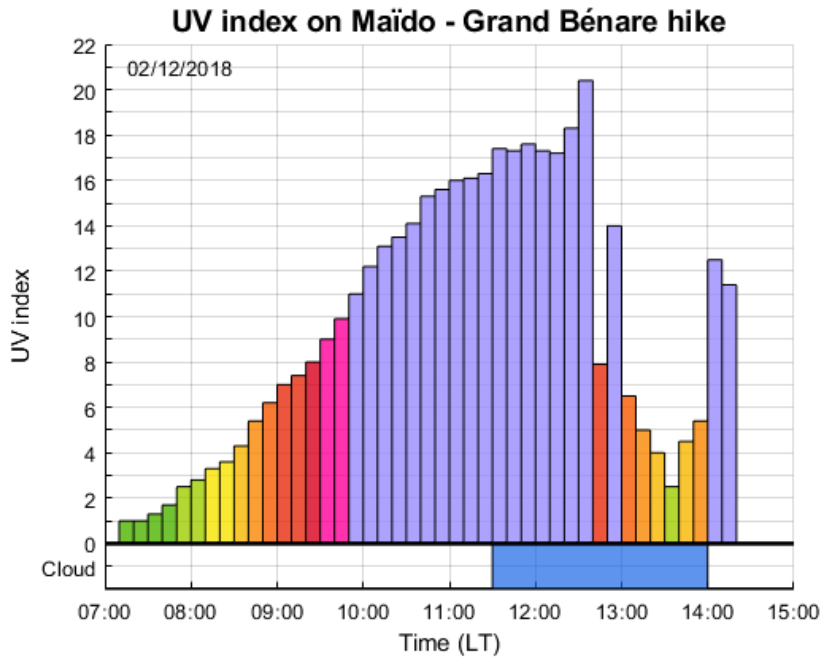
Figure 8 : Indice UV enregistré lors d'une randonnée entre le Maïdo et le Grand Bénare à la Réunion. Les couleurs représentent l'indice UV, suivant l'échelle de couleur définie par l'OMS. La présence de nuage occultant le soleil directement a été enregistrée et est représentée par la surface colorée en bleu en bas de la figure.

1.4.2 CALCUL DE L'INDICE UV

L'indice UV est obtenu en intégrant, en fonction de la longueur d'onde de 280 à 400 nm, l'irradiance solaire convoluée au spectre d'action érythémale **Equation (2)**. Rappelons que les UVC (100-280nm) n'atteignent pas la surface, ils ne sont donc pas pris en compte dans le calcul de l'indice UV.

$$UV\ index = k_{er}.\int_{280}^{400} E_\lambda.S_{er}(\lambda)\,d\lambda \qquad (2)$$

Avec :

- k_{er} une constante ; $k_{er} = 40\ m^2.W^{-1}$

- E_λ l'irradiance solaire exprimée en $W.m^{-2}.nm^{-1}$

- S_{er} le spectre d'action érythémale

La **Figure 9** montre un exemple de calcul d'indice UV.
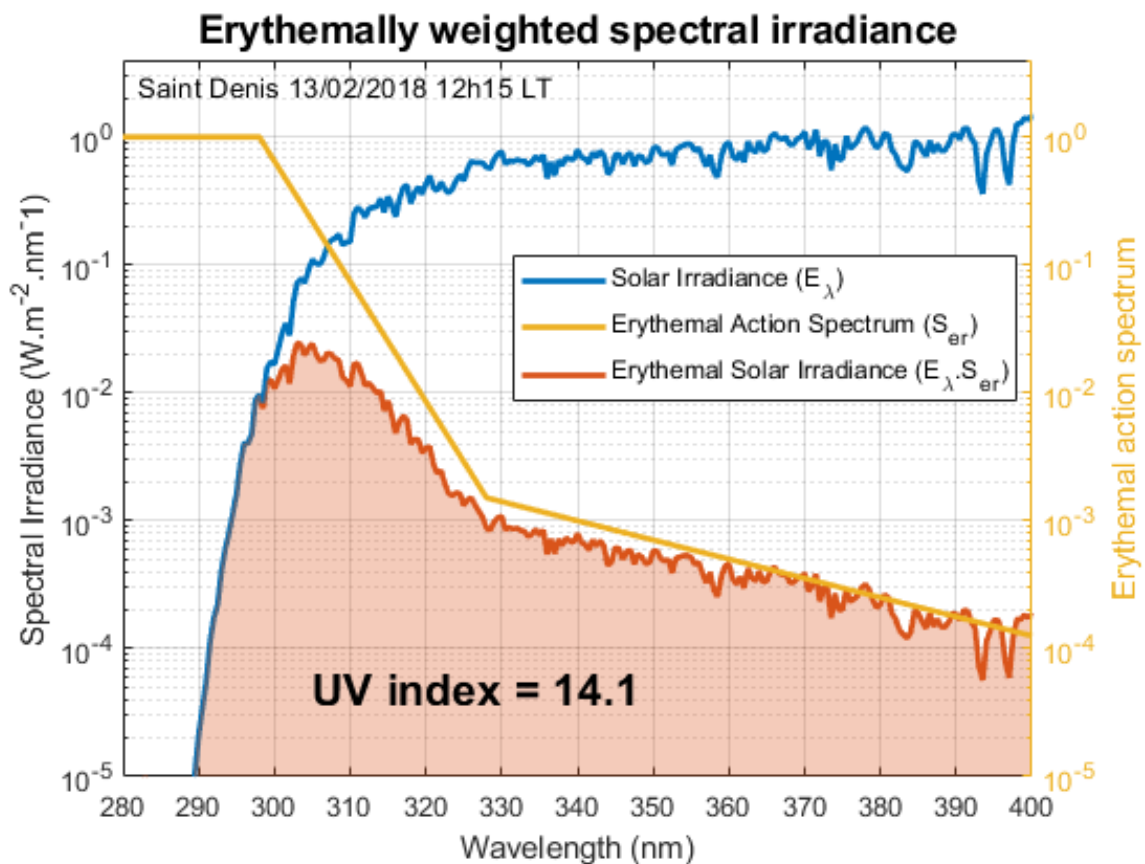
Figure 9 : Illustration du calcul de l'indice UV - La courbe bleu montre un des spectres d'irradiance solaire enregistrés à Saint-Denis le 13 février 2018, la courbe jaune montre le spectre d'action érythémale et la courbe rouge montre le spectre d'irradiance érythémale. La surface rose représente l'intégrale du spectre d'irradiance érythémale nécessaire au calcul de l'indice UV. On obtient dans cet exemple 14.1 d'indice UV.

1.4.3 ECHELLE D'INDICE UV

Comme nous l'avons précédemment dit, les indices UV sont des nombres positifs allant de 0, où il n'y a pas de rayonnement UV et augmentent en fonction de leur intensité. Différents seuils ont été établis en fonction de la dangerosité de l'exposition **(Tableau 3)**.

INTENSITE DE L'EXPOSITION	INDICE UV
FAIBLE	2
MODEREE	3 à 5
FORTE	6 à 7
TRES FORTE	8 à 10
EXTREME	11+

Tableau 3 : Intensité du rayonnement ultraviolet associée à l'échelle d'indice UV (OMS, 2002).

A ses différents seuils sont associées des recommandations, telles que le temps d'exposition maximale, le comportement à adopter, ainsi que des protections adéquates, telles que les types de vêtements, crème solaire, … (OMS, 2002).

1.4.4 LES DOSES STANDARDS ET DOSES MINIMALES

Standard Erythemal Dose (SED)

Une dose standard erythemale (SED), basé sur le spectre d'action erythemale, a été définie comme étant égale à $100 \, J.m^{-2}$ par la Commission Internationale de l'Eclairage. (CIE, 1997).

$$1 \, SED = 100 \, J.m^{-2}$$

Minimal Erythemal Dose (MED)

La dose minimale érythémale (MED) n'est pas une unité standard, bien que largement utilisée, car elle dépend de chaque phototype. La MED, exprimée en SED, donc également

basée sur le spectre d'action érythémale, représente la dose minimale qui produit une rougeur perceptible 24 heures après l'exposition. Un MED correspondra à une faible dose d'irradiation pour une personne de phototype 1 et à l'inverse, de plus forte dose pour des phototypes plus élevés **Tableau 4**.

(Webb, Slaper, Koepke, & Schmalweiser, 2011) (Diffey, Jansén, Urbach, & Wulf, 1996) (Fitzpatrick, 2002)

Phototypes	I	II	III	IV	V	VI
SED	1,5 – 3	2,5 – 4	3 – 4	4 – 6	6 – 9	9 – 15

Tableau 4 : Doses minimales érythémales en fonction du phototype.

Exemple pratique

Une personne de phototype III exposée à un indice UV de 11 pendant 20 minutes reçoit 3,3 SED. La dose minimale érythémale pour un phototype III étant de l'ordre de 3 à 4 SED, cette personne aura donc un coup de soleil.

1.5 LA MESURE DU RAYONNEMENT UV

Il existe différents moyens d'obtenir l'indice UV. La mesure de l'irradiance peut se faire par spectromètre ou par radiomètre large bande. Les instruments peuvent être installés au sol ou embarqués à bord de satellites. L'indice UV peut également être obtenu par la modélisation.

1.5.1 SPECTROMETRIE

Un spectromètre permet d'obtenir l'énergie d'un rayonnement en fonction de la longueur d'onde (courbe bleu de la **Figure 9**). Ainsi, ce spectre énergétique permet le calcul de l'indice UV via l'**équation (2)**, mais aussi le calcul d'autres indices, telle que la vitamine D, par exemple.

Les chercheurs du LACy utilisent les mesures d'un spectromètre Bentham DTM300. La base de données de cet instrument a été utilisée pour les travaux de cette thèse.

Le DTM300 est un spectromètre construit et entretenu par la société anglaise Bentham. Affilié au réseau NDACC (*Network for the detection of Atmospheric Composition Change*), le spectromètre mesurant le rayonnement UV par un double monochromateur de 280 à 450 nm par pas de 0.5 nm toutes les 15 minutes, dans sa configuration utilisateur. L'**équation (2)** permet de calculer l'indice UV pour chaque spectre enregistré.

L'instrument a été installé en janvier 2009. Depuis, il y a eu quelques arrêts, due aux calibrations, aux pannes et aux délais de réparation causés par l'éloignement de l'île de la Réunion. La **Figure 10** permet de visualiser la profondeur de la base de données Bentham DTMc300 de la Réunion, ainsi que les périodes d'arrêts et de maintenances.

Le spectromètre est calibré tous les 3 mois en intensité en utilisant une lampe tungstène-halogène de 150 W et de 1000 W et en longueur d'onde, en utilisant une lampe mercure. Les lampes sont également calibrées et suivis par le *National Institute of Standards and Technology*. L'erreur instrumentale du Bentham DTMc300 est estimée à ±5% (Brogniez, et al., 2016).

Les données du spectromètre ont été utilisées pour une étude de santé dans le but d'estimer le niveau d'exposition des personnes les plus exposées, comme les travailleurs en extérieur ou les enfants dans les écoles (Wright, et al., 2013).

Le spectromètre a été aussi utilisé pour l'évaluation de rayonnement ultraviolet obtenu par modélisation. En effet, il a été montré dans le cadre de la thèse de Kévin LAMY, que la différence entre le modèle TUV et le spectromètre était de 5% (Lamy, et al., 2016), sachant que l'incertitude instrumentale du Bentham est de ±5% et celle du modèle aussi de ±5%.
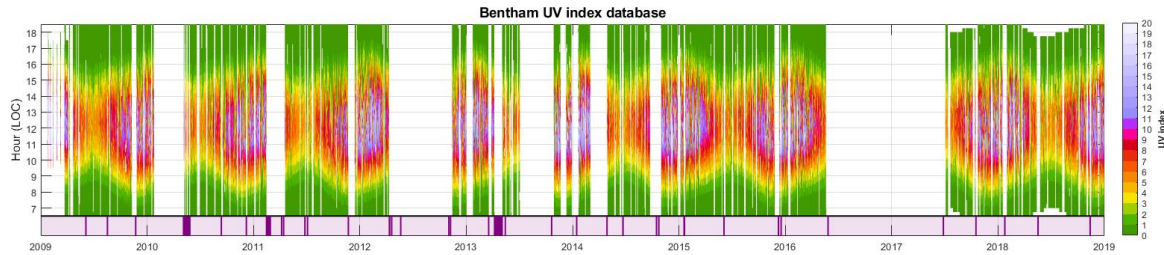
Figure 10 : Variation 2009-2019 de l'indice UV à la Réunion (site de St-Denis) à partir de la base de données des mesures UV par le spectromètre Bentham – Les calibrations et campagnes de comparaison sont indiquées en violet en bas du graphique.

1.5.2 RADIOMETRIE

Contrairement à la spectrométrie qui mesure l'irradiance par longueur d'onde, la radiométrie mesure l'intensité du rayonnement intégrée sur une bande de fréquence. De ce fait, il n'est alors pas possible de faire la convolution avec un spectre d'action quelconque. Un spectre d'action doit alors être intégré à l'instrument, faisant de celui-ci un instrument dédié à la mesure d'un éclairement type, l'éclairement érythémale par exemple.

Le LACy opère un radiomètre Kipp&Zonen UVS-E-T. Ce radiomètre large bande mesure l'irradiance érythémale conformément au spectre d'action érythémale définit par la Commission Internationale de l'éclairage (ISO 17166 : 1999 CIE S 007/E-1998) (CIE I. 1., 1999). L'irradiance est intégrée sur la bande 280-400 nm.

Le radiomètre a été calibré durant une campagne d'inter-comparaison internationale (*International UV filter Radiometer Comparison in summer 2018*) organisée par le PMOD/WRC au *World Calibration Center* à Davos (Hülsen & Gröbner, 2017). Une correction en intensité, en angle zénithal et en ozone a été calculée suivant la formule (Webb, Gröbner, & Blumthaler, 2007) :

$$E_{CIE} = (U - U_{dark}).C.f_n(\theta, TO_3).Coscor(\theta) \qquad (7)$$

où :

- E_{CIE} est l'irradiance érythémale en $[W.m^{-2}]$

- U est le signal brut en $[V]$

- U_{dark} est le signal résiduel en $[V]$

- C est le coefficient de calibration en $[W.m^{-2}.V^{-1}]$

- f_n une fonction de l'angle zénithal θ et de l'ozone total TO_3

- $Coscor$ une correction cosinus dépendant de θ

1.5.3 AUTRES

D'autres instruments existent. Ils sont conçus sur le principe de la radiométrie et mesurent l'intensité du rayonnement UV en SED, MED ou encore en indice UV. Ils sont d'usage divers, comme la dosimétrie personnel ou la mesure UV de terrain.

Par exemple :

Le radiomètre portatif *UV Index Meter* mesure l'indice UV entre les longueurs d'onde 280 et 400 nm via une photodiode UV. L'instrument mesure l'indice UV instantanément dans un but d'information et de prévention public. L'instrument est calibré par le constructeur et la précision est de 10% (Référence *National Institution of Standard and Technologies*).

L'inconvénient de ce radiomètre est l'enregistrement des données. En effet, la mesure doit être déclenchée manuellement et l'indice UV doit être lu et enregistré manuellement.

Dans une précédente étude de comparaison instrumentale (de Paula Corrêa, et al., 2010), il a été trouvé que l'instrument est fiable et stable, avec un biais inférieur à +5% comparé à un spectromètre de référence.

1.5.4 SATELLITE

La mesure du rayonnement ultraviolet peut également être effectuée à très grande distance, par des instruments installés à bord de satellite. Les satellites peuvent être héliosynchrones, comme la plateforme Aura de la NASA, ou géostationnaire, comme les satellites Météosat de l'ESA. Le rayonnement ultraviolet n'est pas directement mesuré. Il est obtenu par des modèles de transfert radiatif, à l'aide des principaux paramètres modulant le rayonnement

UV, tels que l'ozone, la nébulosité et l'albédo. Ces dernières données sont quant à elles mesurés par satellites, aussi.

Produits UV OMI

Le Capteur OMI (Ozone Monitoring Instrument) à bord du satellite Aura est dédié à la mesure de l'ozone. Les quantités d'ozone sont obtenues par analyse du rayonnement solaire rétrodiffusé par l'atmosphère dans la bande UV de 270 à 380 nm. Le rayonnement ultraviolet erythemal est ensuite obtenu à l'aide de la version améliorée de l'algorithme TOMS (Total Ozone Mapping Spectrometer) (OMI, 2002). Le processus d'évaluation du rayonnement UV prend également en compte les aérosols (AOD et SSA) issues de la modélisation ou par observations sols (AERONET).

Le satellite couvrant toute la surface de la Terre, des cartes complètes illustrant le niveau d'irradiation UV peuvent être calculées. Ci-dessous **(Figure 11)** une carte montrant la moyenne annuelle climatologique (calculée sur 14 ans, 2004-2018) des indices UV par ciel clair au midi solaire local, à partir des mesures OMI.

Une analyse rapide de la **Figure 11** montre :

- Une dépendance de l'indice UV avec la latitude : plus la latitude augmente, plus l'indice UV diminue.

- Il est à noter également que l'indice UV est globalement plus élevé dans l'hémisphère Sud que dans l'hémisphère Nord. Ceci est dû à la géométrie de l'orbite terrestre. En effet, lors de l'été austral, la Terre est au périhélie de sa trajectoire, et inversement pour l'été boréale. En somme, le rayonnement UV est donc plus important dans l'hémisphère Sud.

- Une dépendance de l'indice UV avec l'altitude : plus l'altitude augmente, plus l'indice UV augmente. Cette dépendance est clairement visible dans la région de l'Himalaya, de la Cordillère de Andes, ou des Rocheuses.

- Une dépendance de l'indice UV avec l'albédo : plus l'albédo augmente, plus l'indice UV augmente. Le cas de figure est visible au-dessus du Groenland.

- Une dépendance de l'indice UV avec les aérosols : plus la quantité d'aérosols augmente, plus l'indice UV diminue. Cette situation est visible dans la région du Sahara, où les aérosols désertiques et les aérosols issus des feux de biomasses sont importants.
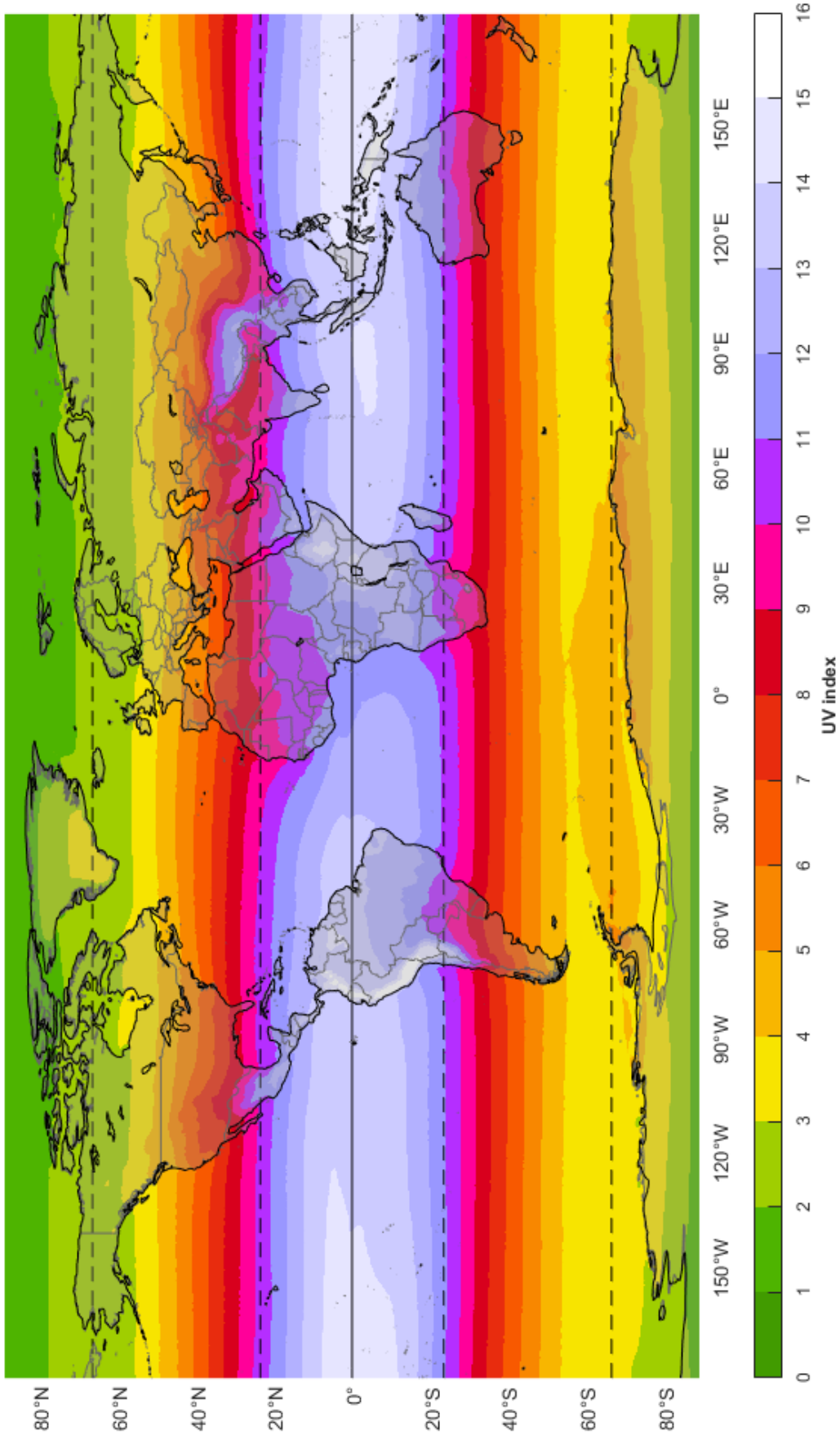
Figure 11 : Moyenne climatologique annuelle (2004 à 2018) des indices UV ciel clair au midi solaire local issue des données satellites OMI/Aura

1.5.5 MODELISATION

La modélisation est également un moyen d'obtenir une estimation du rayonnement UV, via un modèle de transfert radiatif, par exemple le modèle TUV (Tropospheric Ultraviolet Visible) (Madronich, 1993). Ce modèle prend en compte de nombreuses variables d'entrées afin de résoudre l'équation de transfert radiatif. Ces variables peuvent être :

- le spectre extraterrestre,
- l'angle solaire zénithal,
- la colonne totale d'ozone,
- le profil d'ozone,
- la colonne totale de dioxyde d'azote,
- le profil de température,
- l'épaisseur optique d'aérosols,
- le coefficient d'Ångström,
- l'albédo simple de diffusion,
- l'albédo de surface,
- ou encore l'altitude.

L'erreur résultant de la modélisation de l'indice UV par le modèle TUV a été estimée à 5% (k=2) par (Koepke, et al., 1998).

1.5.6 RESEAUX DE MESURE

De nombreux pays mettent en place des réseaux de mesures afin de mieux cartographier le risque lié aux UV dans un but de prévention et de santé publique (Cadet, et al., 2017) (Kazantzidis, et al., 2006) (Steinmetz, 1997), mais aussi à plus grande échelle telle que l'Europe (Schmalwieser, et al., 2017), ou plus récemment sur les îles de l'Ouest de l'Océan Indien.

Chapitre 2   INTER-COMPARAISON INSTRUMENTALE

2.1 ARTICLE : RESUME

Les effets du rayonnement ultraviolet, autant positifs que négatifs, sont aujourd'hui maitrisés et bien documentés. Le rayonnement solaire ultraviolet de surface est modulé par plusieurs paramètres, notamment atmosphériques, temporelles et géographiques. La Réunion est une île tropicale très exposée à ce rayonnement à cause de l'incidence du rayonnement solaire. Les effets inhérents au rayonnement sont alors de plus forte amplitude, en particulier les effets néfastes. Il devient alors primordial de mesurer précisément l'intensité du rayonnement ultraviolet.

L'objectif de cette étude est de comparer différents instruments, de différents coûts (de ~100€ à ~5000€), à un instrument de référence : le spectro-radiomètre Bentham DTMc300 de l'OPAR. Les instruments comparés sont des radiomètres larges bandes : un Kipp&Zonen UVS-E-T ; un Solarlight UV-Biometer Model 501 ; un SGLux UV Cosine ; un radiomètre DAVIS. Une caméra imageur de ciel a été utilisée afin de filtrer les données en ciel clair.

Le spectro-radiomètre Bentham est calibré par l'opérateur tous les 3 mois en amplitude et en longueur d'onde et fait partie du réseau NDACC. Les radiomètres Kipp&Zonen et Solar Light ont été calibrés durant une campagne de calibration internationale à Davos (amplitude, ozone et angle solaire zénithal). Les radiomètres SGLux et Davis ont été calibrés par le constructeur en amplitude. Le radiomètre SGLux, lui, a été calibré en angle solaire zénithal.

L'inter-comparaison s'est déroulée sur une période d'une année entre mars 2018 et février 2019. Elle eut lieu à Saint-Denis, La Réunion, sur le campus universitaire du Moufia (20.9°S, 55.5°E, 85m).

Les données de fraction nuageuse ont d'abord été analysées. Les journées de ciel clair ont été sélectionnées via 2 méthodes différentes : 1) une comparaison du modèle TUV et du spectro-radiomètre Bentham, avec une différence maximum de 5% et 2) la méthode présentée par Bodeker et McKenzie (1996). Par la suite, les fractions nuageuses associées à ces données de ciel clair ont été analysées. Un seuil de 20% maximum de fraction nuageuse a été déterminé pour le filtrage ciel clair.

L'inter-comparaison en ciel clair montre un biais relatif inférieur à 3% avec une faible dispersion pour les radiomètres Kipp&Zonen, Solar Light et SGLux, ainsi qu'une bonne stabilité temporelle et une dépendance en angle zénithale négligeable. Cependant, une faible dépendance à ±6% en angle zénithal a été trouvée pour le radiomètre Kipp&Zonen. Quant au radiomètre Davis, il a montré un biais moyen de 14%, ainsi qu'une forte dépendance en angle solaire zénithale.

La comparaison est dans l'ensemble satisfaisante excepté pour le radiomètre Davis. Il conviendra par la suite d'étudier la dérive temporelle de ces radiomètres à plus long terme. A la suite de cette étude, il est envisagé d'intégrer le radiomètre SGLux UV-Cosine dans des réseaux d'instruments, locaux ou régionaux.

2.2 ARTICLE : CADET ET AL., 2020 (IJERPH)

Article ci-dessous publié le 19 avril 2020 dans IJERPH disponible sur :

https://www.mdpi.com/697176

Article

Inter-Comparison Campaign of Solar UVR Instruments under Clear Sky Conditions at Reunion Island (21°S, 55°E)

Jean-Maurice Cadet [1],*, Thierry Portafaix [1], Hassan Bencherif [1,2], Kévin Lamy [1], Colette Brogniez [3], Frédérique Auriol [3], Jean-Marc Metzger [4], Louis-Etienne Boudreault [5] and Caradee Y. Wright [6,7]

[1] LACy, Laboratoire de l'Atmosphère et des Cyclones (UMR 8105 CNRS, Université de La Réunion, Météo-France), 97744 Saint-Denis de La Réunion, France; thierry.portafaix@univ-reunion.fr (T.P.); hassan.bencherif@univ-reunion.fr (H.B.); kevin.lamy@univ-reunion.fr (K.L.)

[2] School of Chemistry and Physics, University of KwaZulu-Natal, Durban 4041, South Africa;

[3] Université Lille, CNRS, UMR 8518, Laboratoire d'Optique Atmosphérique, F-59000 Lille, France; colette.brogniez@univ-lille.fr (C.B.); frederique.auriol@univ-lille.fr (F.A.)

[4] Observatoire des Sciences de l'Univers de la Réunion, UMS 3365, 97744 Saint-Denis de la Réunion, France; jean-marc.metzger@univ-reunion.fr

[5] Reuniwatt, 97490 Sainte Clotilde de la réunion, France; louisetienne.boudreault@reuniwatt.com

[6] Department of Geography, Geo-informatics and Meteorology, University of Pretoria, Pretoria 0002, South Africa; caradee.wright@mrc.ac.za

[7] Environment and Health Research Unit, South African Medical Research Council, Pretoria 0001, South Africa

* Correspondence: jean.cadet@univ-reunion.fr; Tel.: +262-262-93-82-97

Abstract: Measurement of solar ultraviolet radiation (UVR) is important for the assessment of potential beneficial and adverse impacts on the biosphere, plants, animals, and humans. Excess solar UVR exposure in humans is associated with skin carcinogenesis and immunosuppression. Several factors influence solar UVR at the Earth's surface, such as latitude and cloud cover. Given the potential risks from solar UVR there is a need to measure solar UVR at different locations using effective instrumentation. Various instruments are available to measure solar UVR, but some are expensive and others are not portable, both restrictive variables for exposure assessments. Here, we compared solar UVR sensors commercialized at low or moderate cost to assess their performance and quality of measurements against a high-grade Bentham spectrometer. The inter-comparison campaign took place between March 2018 and February 2019 at Saint-Denis, La Réunion. Instruments evaluated included a Kipp&Zonen UVS-E-T radiometer, a Solar Light UV-Biometer, a SGLux UV-Cosine radiometer, and a Davis radiometer. Cloud fraction was considered using a SkyCamVision all-sky camera and the Tropospheric Ultraviolet Visible radiative transfer model was used to model clear-sky conditions. Overall, there was good reliability between the instruments over time, except for the Davis radiometer, which showed dependence on solar zenith angle. The Solar Light UV-Biometer and the Kipp&Zonen radiometer gave satisfactory results, while the low-cost SGLux radiometer performed better in clear sky conditions. Future studies should investigate temporal drift and stability over time.

Keywords: solar ultraviolet radiation; UV index; UV instruments; clear sky; La Réunion

1. Introduction

Solar ultraviolet radiation (UVR) is known today for its beneficial effects on the biosphere, plants, animals, and humans [1], but also for its negative effects, especially on humans [2]. Most skin diseases are related to UVR exposure [3]. The risk related to UV exposure increases with changes in human behavior, such as increased participation in outdoor activities [4]. UVR is divided into three wavebands: UVA—315–400 nm; UVB—280–315 nm; and UVC—100–280 nm [5]. Surface UVR depends on several atmospheric parameters such as ozone, aerosols, and cloud cover [6], and also geographic parameters, namely altitude and latitude. UV index (UVI) was defined in 1992 by the World Health Organization as a simple tool for public awareness and remains widely used today [7]. UVI starts from zero and increases with UVR intensity. Different thresholds have been defined as a function of risk for human health (i.e., 1–2: low, 3–5: moderate, 6–7: high, 8–10: very high, >11: extreme).

UV solar irradiance is usually measured using a spectro-radiometer and UVI is calculated via a standard formula [8]. Broadband UVR radiometers are also used with a spectral response that is adapted to the UV erythemal (sunburn) action spectrum. Many instrument uncertainties have to be considered [9]. Moreover, UVR instruments have to be regularly checked.

Reunion Island (55°E, 21°S) is a tropical island situated in the Western Indian Ocean (**Figure 1**) and is exposed to extreme UVR all year around. UVI is generally in the range of 0 to 16 and can exceed 20 under certain conditions, such as at high altitude or cloud diffusion [10]. Therefore, UVI measurement, public awareness, and prevention campaigns are very important for Reunion Island and in tropical regions in general. The Laboratoire de l'Atmosphère et des Cyclones (LACy) is located in Saint-Denis (**Figure 1**) at the University of Reunion, where a Bentham DTMc300 spectroradiometer has been in use since 2009. The uncertainty on UVI is about 5%, with a coverage factor of k = 2 [11]. The instrument is affiliated with the Network for the Detection of Atmospheric Composition Change (NDACC). There are other Bentham DTMc300 instruments in operation around the world. Two Bentham DTMc300 instruments have been in operation in metropolitan France at Villeneuve d'Ascq (in the North) and Observatoire de Haute-Provence (in the South) since 2009 with similar uncertainty [11]. In Italy, Aosta Valley, a Bentham DTMc300 has recorded spectral UV irradiance since 2006 with 5% bias to QASUME (Quality Assurance of Spectral Ultraviolet Measurements in Europe) through the Development of a Transportable Unit [12]. Similar results were found with DTMc300 instruments operating in Germany, Great Britain and New Zealand [13].

There are currently various instruments dedicated to the measurement of solar radiation in the ultraviolet (UV) band of 280 nm to 400 nm. These instruments are available at different price ranges; however, price does not guarantee quality of the measurement. The present study aimed to compare, at the same site with high level of UVR and under the same experimental conditions, a set of UVR sensors commercialized at low to moderate costs. The objective was to assess their individual performance and the quality of the respective measurements. To this end, we set up an inter-comparison campaign bringing together five instruments (including the Bentham DTMc300 spectrometer) for evaluation over a continuous 12-month period from March 2018 to February 2019. The datasets collected over the study period were evaluated, taking into account the cloud fraction data obtained by a co-localized all-sky camera.
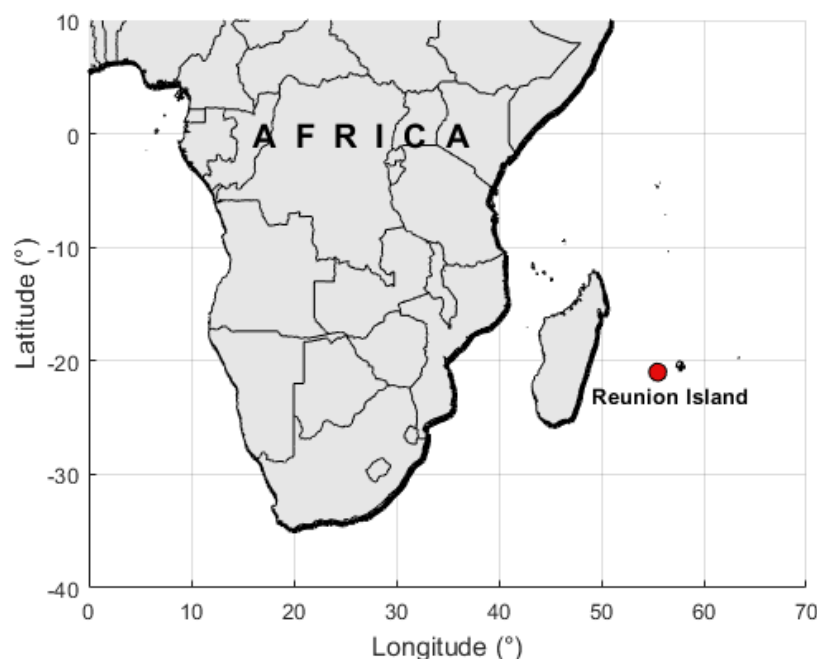
Figure 1. Geographical location of the study site, Sainte-Denis, La Réunion.

2. Materials and Methods

2.1. Materials

2.1.1. Spectroradiometer Bentham DTMc300

The reference instrument for this study was a high grade double monochromator Bentham DTMc300 (**Figure 2**) provided by Bentham Instrument Ltd. Co. (Reading, England, United Kingdom), hereafter referred to as BT, operated by the OPAR (Observatoire de Physique de l'Atmosphère de la Réunion) since January 2009. The BT is affiliated with the NDACC. The instrument is enclosed in a thermally-stabilized box and records global irradiance spectra in the 280–450 nm wavelength range every 15 min in its user configuration, with a wavelength scan duration of about five minutes. The BT is calibrated every 3 months with a 150W lamp and a 1000W quartz tungsten halogen lamp from the National Institute of Standards and Technology (NIST). Wavelength misalignment correction is done via a software developed at the Laboratoire d'Optique Atmosphérique [14] using a cosine correction function.

The erythemally-weighted UVR is obtained by integrating the global irradiance in the 280–400 nm wavelength range weighted by the erythemal action spectrum (Commission Internationale de l'Eclairage (CIE) S007-1998 [15]). The UVI is calculated following standard formulae. The instrument uncertainty of UVI is about ±5%, with a coverage factor of k = 2 [11].

In 2013, during a QASUME campaign [16], a BT/QASUME ratio of −5% to 0% was found [17]. A recent comparison between BT and UVI obtained by modelling showed ±5% difference [18]. However, since 2009, there have been some gaps in the data due to technical problems and prolonged maintenance delays.

The UVI data measured by BT are presented in **Figure 3.** There was satisfactory time-coverage data, as only 12% of data were missing for the period March 2018 to February 2019. The UVI range during the inter-comparison exercise was 0 to 16. The seasonal maximum appeared during mid-summer (January) with a UVI up to 16, while the UVI was around 8 during winter.

The BT cost is ~50.000 € and an estimation of the calibration cost is ~1000 €/year for seven full days of work (four calibrations per year). These costs do not take into account unexpected maintenance operation.
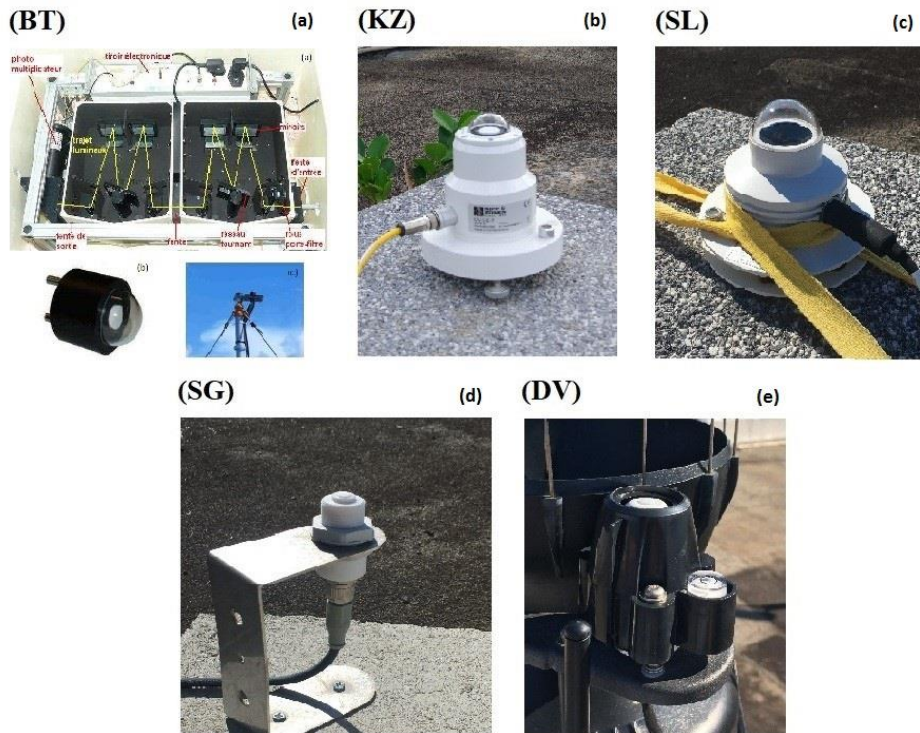
Figure 2. Images of the UV instruments evaluated during the inter-comparison campaign held at Reunion University. (a): Bentham DTMc300; (b): Kipp&Zonen UVS-E-T; (c): Solar Light UV-Biometer Model 501; (d): SGLux UV-Cosine; (e): Radiometer Davis;
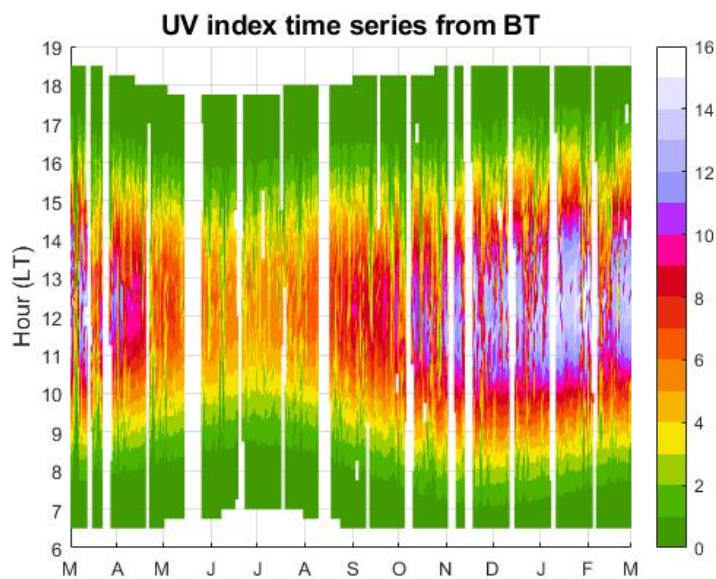
Figure 3. Time series UV index measured by Bentham spectro-radiometer (BT) during the period of comparison (March 2018 to February 2019).

2.1.2. Radiometer Kipp&Zonen UVS-E-T

A Kipp&Zonen UVS-E-T (**Figure 2**) was used for the inter-comparison campaign, referred to hereafter as KZ. It is a moderate-cost (~3000 €) broadband radiometer recording erythemal irradiance in the 280–400 nm wavelength range. The erythemal action spectra used for UVI calculation is defined by the CIE (CIE S007/E-1998). Erythemal irradiance is recorded every minute. However, final data are averaged using five erythemal irradiance records and are given every five minutes. According to Gröbner et al. [19] the KZ uncertainty is ±7%.

The radiometer was calibrated during the international UV filter Radiometer Comparison in summer 2017 by Physikalisch-Meteorologisches Observatorium Davos/World Radiation Center (PMOD/WRC) in Davos [20]. A calibration factor was given, with an ozone and zenith angle correction. Erythemal irradiance was calculated using Equation (1) below [21]:

$$E_{CIE} = (U - U_{dark}).C.f_n(\theta, TO_3).Coscor(\theta) , \tag{1}$$

where E_{CIE} is the erythemal weighted irradiance, U is the raw signal of the instrument, U_{dark} is the dark offset, C is the calibration factor, determined for the solar zenith angle $\theta = 40°$ and the total column of ozone $TO_3 = 300$ DU, f_n is a function of θ and TO_3, COSCOR is the cosine correction function. It is a dimensionless factor that rectifies the mismatch between the actual angular response of a radiometer and the ideal behaviour expected, given by the cosine law.

This radiometer is part of the UV-Indien UVR Observation Network in the Western Indian Ocean [22].

2.1.3. Radiometer Solar Light UV-Biometer Model 501

The SL501 UV-Biometer (**Figure 2**) is a moderate-cost (~5000 €) broadband radiometer manufactured by Solar Light Pty Ltd, referred to hereafter as SL. UVR is recorded between 280 to 340 nm with a 1-minute sampling rate. Since the SL wavelength range differs from the UVI standard, a spectral correction depending on total ozone and solar zenith angle is applied from a generic table for this specific instrument [23]. Data are recorded in [MED/h] units, where 1 MED (minimal erythemal dose) is 210 J·m^{-2}. UVI was calculated using Equation (2):

$$UV\ index = \ UVd[MED.h^{-1}].\frac{210[J.m^{-2}].40[m^2.W^{-1}]}{3600[s]} , \tag{2}$$

According to Gröbner et al. [19] the SL uncertainty is ±7%. The instrument is calibrated in intensity and corrected to solar zenith angle and total ozone. This calibration was done during the International UV Filter Radiometer Comparison in summer by PMOD/WRC at the World Calibration Centre in Davos [20] (See Section 2.1.2).

2.1.4. Radiometer SGLux UV-Cosine

The UV-Cosine sensor (hereafter referred to as SG) from SGLux Company is a low-cost (~250 €) broadband radiometer integrating erythemal UVR following the ISO 17166 erythema action spectra in the 280–400 nm wavelength range (**Figure 2**). The solar zenith angle correction and the calibration factor are provided by the manufacturer and applied by Reuniwatt. Data are recorded every minute.

2.1.5. Radiometer Davis

The DAVIS UV sensor referred to as DV (**Figure 2**) operates on the Vantage Pro 2 meteorological station from DAVIS Company. It is a low-cost (~200 €) radiometer recording UVR in the 280–360 nm wavelength range. UVI, dose, and cumulative dose are provided every second. The sensor was calibrated by the manufacturer.

2.1.6. Sky Camera

Reuniwatt's SkyCamVision (hereafter referred to as SCV) is an all-sky camera system acquiring hemispherical images of the sky vault in the visible range (380–440 nm) at 1-minute intervals. The system is equipped with a CMOS sensor (1600 × 1200 pixels resolution) mounted with a fisheye lens. More information about the system specifications is available at the website: http://www.reuniwatt.com/.

The cloud fraction calculation using this device involves a multi-step procedure [24]. A cloud segmentation algorithm is applied to classify the pixels as either: (1) clear sky; (2) thick cloud; (3) thin cloud; or (4) sun. The classifier is based on a Random Forest algorithm [25], which is programmed beforehand using as inputs a number of pixel features from manually annotated images using both the RGB and HSV colour spaces. Once the classification is achieved, the sun and clear sky indices (1–2) and the thick and thin cloud indices (2–3) are merged together into a binary cloud cover: single clear sky (0) and cloud (1) classes. The overall cloud fraction is then calculated from a geometrically calibrated image. The raw image is undistorted onto a flat plane of reference perpendicular to the zenith, and each pixel of the cloud cover is weighted by its solid angle view [26].

This camera is part of the UV-Indien UVR Observation Network in the Western Indian Ocean [22].

2.1.7. TUV Model

We used the Tropospheric Ultraviolet Visible (TUV) radiative transfer model version 5.3 [27] to obtain modelled clear-sky outputs. The radiative transfer scheme in TUV is used to solve the radiative transfer equation in pseudo-spherical 8-stream discrete ordinates [28]. The following parameters were modified in the model in order to reproduce the UVI measurements with site-specific climatology:
  –extraterrestrial spectrum (ETS),
  –solar zenith angle (SZA),
  –total ozone column amount (TO3),
  –total nitrogen dioxide (TNO2),
  –ozone profile (OP),
  –temperature profile (TP),
  –aerosol optical thickness (AOT) at 340 nm
  –aerosol Ångström exponent (α) between 340 and 440 nm,
  –single-scattering albedo (SSA) [29,30],
  –ground surface albedo (ALB) and
  –altitude (Z).

The ETS used was from Dobber et al. [31]. Similar to McPeters et al. [32], a monthly climatology of ozone and temperature profiles was derived from local ozone soundings and Microwave Limb Sounder (MLS) satellite measurements. TO3 and TNO2 used are from a Système d'Analyse par Observation Zénitale (SAOZ) instrument. AOT and α data used were from the Aerosol Robotic Network (AERONET). As demonstrated by Dubovik et al. [33], single-scattering albedo (SSA) from the CIMEL sun photometer is not usable when the AOT is lower than 0.3, which was almost always the case here. As proposed by Takemura et al. [29] and Lacagnina et al. [30], a fixed SSA of 0.95 was set. As described by Corrëa et al. [34], UVI doses can be reduced by 10 to 30% for a lower SSA of about 0.70 which indicates the presence of strongly absorbing aerosols. These aerosols are observed for small areas, limited time periods, and during specific events, such as biomass burning emissions or fires with incomplete biomass burning episodes. As established by Koelemeijer et al. [35], surface albedo was taken to be constant at 0.08. According to Koepke et al. [36], the UVI modelling error is approximately 5% for a coverage factor of 2.

Figure 4 shows the monthly mean UVI captured by the TUV model compared to those of BT by using all data (**Figure 4**a; left panel) and clear sky data (**Figure 4**b; right panel). As expected,

comparisons are better with clear-sky filtered observation data (**Figure 4**b) as the model outputs are made without taking into account cloud cover. However, the differences on the left panel (**Figure 4**a) are greater during the summer months. This result and the method of filtering are discussed later.
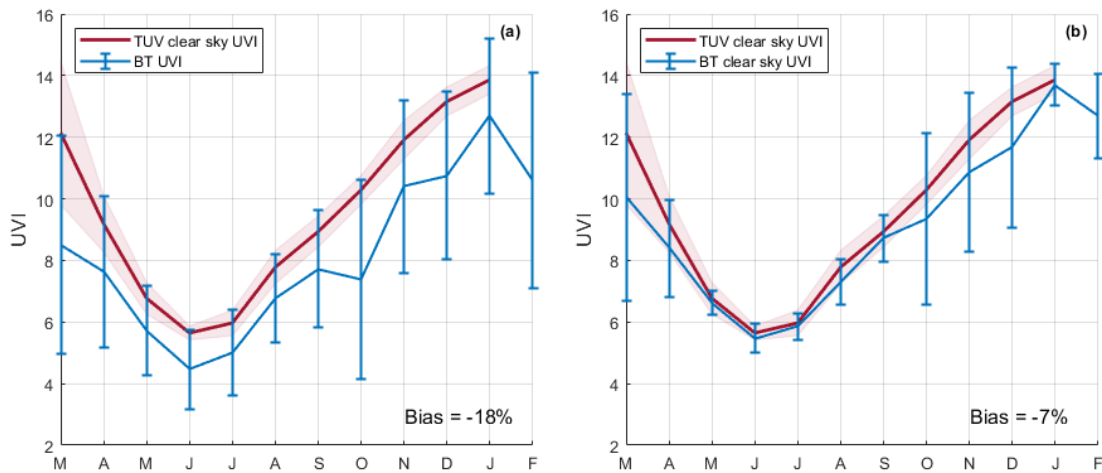
Figure 4. Comparison of UVI between the TUV model (red) and BT (blue). Standard deviation is represented by red shading for TUV data and by vertical bars for BT data. Plot **(a)** represents the comparison by using all data, while plot **(b)** represents clear sky data only.

2.2 Methods

The objective of the instrument comparison exercise was to evaluate their performance and quality of measurement. All of the instruments, i.e., BT, KZ, SL, SG, DV, and SCV, were co-localised on the Moufia Campus of Reunion University in Saint-Denis (20.9°S, 55.5°E, 85 m ASL), with the Bentham spectro-radiometer (BT) as the reference. Solar zenith angle range is from 0° to 90° during summer and from 45° to 90° during winter. The comparisons were performed during a one-year period, from 1 March 2018 to 28 February 2019. As the instruments evaluated during the inter-comparison campaign do not measure at the same time resolution, the corresponding recorded time-series were interpolated, according to the zenith angle, with a one-degree step.

Cloud fraction (CF) data calculated from the all-sky camera SCV were used. Yearly statistics are presented to describe the cloud cover conditions over Saint-Denis. The instrument inter-comparison was performed only for clear sky conditions. Cloud fraction data were analysed in two ways to determine a clear sky threshold:

1) Lamy et al. [18] showed that TUV clear sky outputs could be compared to Bentham clear sky outputs on the same site with differences of less than 5% when TUV was correctly set up. From this result we compared the TUV outputs with the appropriate setting and the Bentham over the reference period in order to determine the cloud fractions (as seen by the camera) corresponding to a difference in UVI of less than 5%. Associated cloud fraction was analysed to determine the cloud fraction clear-sky threshold;

2) Clear sky UVI was determined by using the filtering method developed by Bodeker and McKenzie [37] based on the geometrical form of the daily UVI curve. Three tests were done on BT UVI to determine clear-sky days: (a) a correlation test; (b) a monotonicity test between morning and afternoon UVI; and (c) a comparison of the daily maximum to the climatology. Associated cloud fraction was analysed to determine the cloud fraction clear-sky threshold.

The statistical analysis was initially carried out on the data measured over the entire study period, after which analyses were done per month. A statistical analysis was also done as a function of solar zenith angle. Statistical tools for the analysis were determination coefficient (r^2), relative difference (RD), relative standard deviation (RSD), root mean square error (RMSE), as shown in Equations (4) to (7), and box diagrams.

$$DIFF_{[X],i} = \frac{UVI_{[X],i} - UVI_{[BT],i}}{UVI_{[BT],i}}, \tag{3}$$

$$r^2 = \frac{\left(\sum_{i=1}^{n}\left(UVI_{[BT],i} - \overline{UVI_{[BT]}}\right)\left(UVI_{[X],i} - \overline{UVI_{[X]}}\right)\right)^2}{\left(\sum_{i=1}^{n}\left(UVI_{[BT],i} - \overline{UVI_{[BT]}}\right)^2\right)\left(\sum_{i=1}^{n}\left(UVI_{[X],i} - \overline{UVI_{[X]}}\right)^2\right)}, \tag{4}$$

$$RD = 100 * \frac{1}{n}\sum_{i=1}^{n} DIFF_{[X],i}, \tag{5}$$

$$RSD = 100 * \frac{\sqrt{\frac{1}{n-1}\sum_{i=1}^{n}\left(DIFF_{[X],i} - \overline{DIFF}\right)^2}}{\overline{DIFF}}, \tag{6}$$

$$RMSE = \sqrt{\frac{1}{n-1}\sum_{i=1}^{n}\left(UVI_{[X],i} - UVI_{[BT],i}\right)^2}, \tag{7}$$

where n is the number of observations and [X] the instruments compared (KZ, SL, SG and DV).

3. Results and Discussion

3.1 Cloud Cover Conditions over Saint-Denis

Cloud cover and its daily cycle contribute to the variability of solar surface UV radiation at different timescales. As previously mentioned, in order to understand this variability an all-sky camera was installed in the vicinity of UV instruments over the roof of the Physics Department, Moufia Campus. The all-sky camera has been operating continuously and allows retrieval of cloud fraction values on a daily basis. **Figure 5a** shows the daytime statistics obtained (hourly median values) of cloud fraction as derived from one year of sky imaging over the study site. Overall, the values of cloud fractions remained relatively low in the morning (below 30%, until 11 am), while they exceeded 50% from 1 pm, with the maximum (68%) around 4 pm. This was consistent with the prevailing meteorological conditions and the geographical location of the study site. Indeed, as shown in **Figure 5b**, Reunion is an island located in the southwestern Indian Ocean. It is characterized by mountainous terrain (the highest peak, Piton des Neiges, is 3069 m) and is subjected to the southeast trade winds, which implies cloud developments on the windward side, with an overflow of clouds in the early afternoon on the opposite side, where the study site is located. Such cloud development is typically characteristic of isolated islands in the tropics [38]. There is also a difference in cloud cover between summer and winter months. Reunion Island is located in a tropical region, which implies that there is a strong cloud cover during the summer months [39,40]. The strong cloud cover which occurs during the wet season (from November to March) introduces more bias, as can be seen in **Figure 4b**. However, the bias in clear-sky conditions remains a factor within the BT uncertainties. These results are consistent with findings from Lamy et al. [18] for the time period 2009–2018.
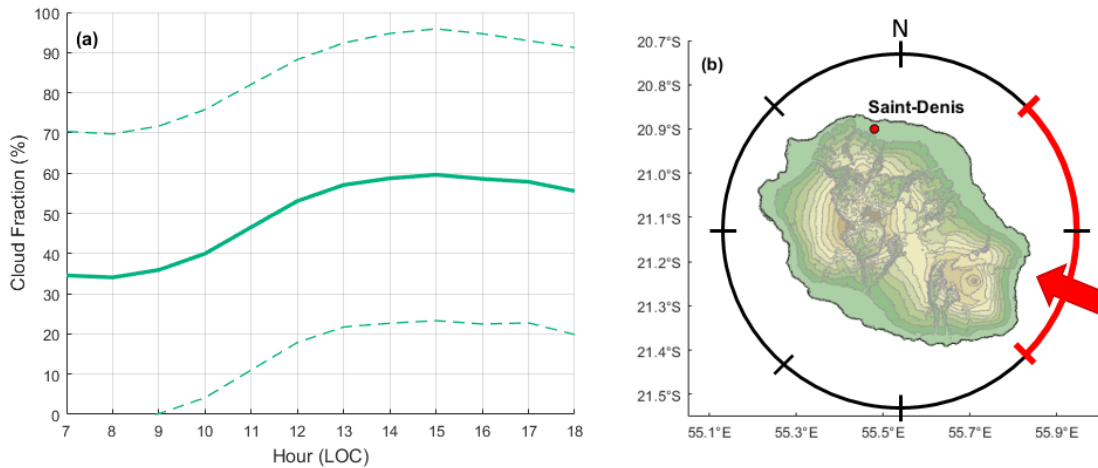
Figure 5. (a) Cloud fraction statistics over Saint-Denis. The green solid line shows the mean cloud fraction per hour, and the dashed lines represent one standard deviation. **(b)** Reunion island map and the dominant trade winds. The red arrow shows the main direction of the trade winds with a possible variation illustrated by the red arc. The study site (Saint-Denis) was located in the North and is indicated by a red dot.

3.2. Clear Sky Filtering

We applied a statistically determined threshold to select clear sky UVI measurements:

In the first method proposed, we compared UVI from BT and TUV model outputs, and detected cloud fractions (CFs) when the difference was less than 5%, as reported in Lamy et al. [18]. **Figure 6a** shows the distribution of the clear-sky CFs selected. The data range of selected CFs was from 2% to 100% and represented 24% of all data. There were no observations between 0 to 2% and an obvious concentration of observations between 2% to 6%, even though the median was 9%. The weighted mean was 19%.

For the second method proposed [37], the analysis of the clear-sky cloud fraction observations (**Figure 6b**) showed the same pattern as Figure 6a with a median at 15% and a wider dispersion, while the weighted mean was 29%. The disadvantage of using this method of filtering is that only full days of clear-sky are detected and therefore partial clear-sky periods during the day could not be taken into account. Therefore, this method was not used.

The dispersion of the observations in both cases from the median to the maximum represents the limit of the cloud fraction data. Indeed, cloud fraction data does not indicate whether the sun is hidden by clouds. The cloud cover can be important, but the UVR can be maximal if the sun is not hidden by clouds. The UVR can also be increased in the case of scattered cloud cover [10,41].

It was decided that the results from the first method, based on the difference between BT UVI and TUV clear sky UVI to determine clear sky measurement, would be used. A threshold of 20% of the cloud fraction measured by the all-sky camera was applied, which corresponded (approximately) with the statistical average shown above, and up to about 70% of the clear sky conditions detected. **Figure 7** shows the UVI as recorded by BT and CF, as recorded by SCV on 19/09/2018.
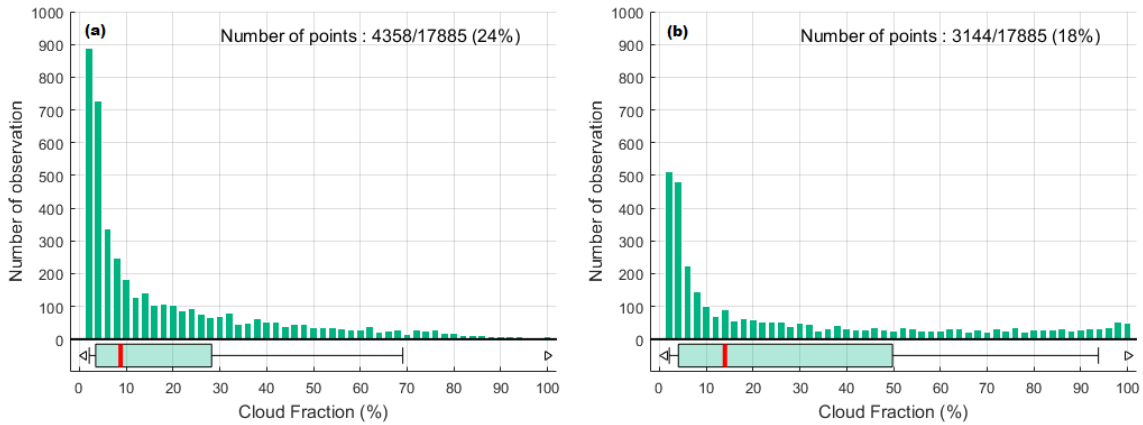
Figure 6. Distribution of clear sky cloud fraction (CF) data from the all sky camera. The green diagram boxes at the bottom represent the quantiles 0, 0.05, 0.25, 0.50, 0.75, 0.95, 1. **(a)** shows the clear-sky conditions in CF by using data selected when the difference between UVI from BT and clear sky UVI from TUV model are less than 5%. **(b)** shows the clear-sky conditions in CF by using the Bodeker and McKenzie [37] filtering method.
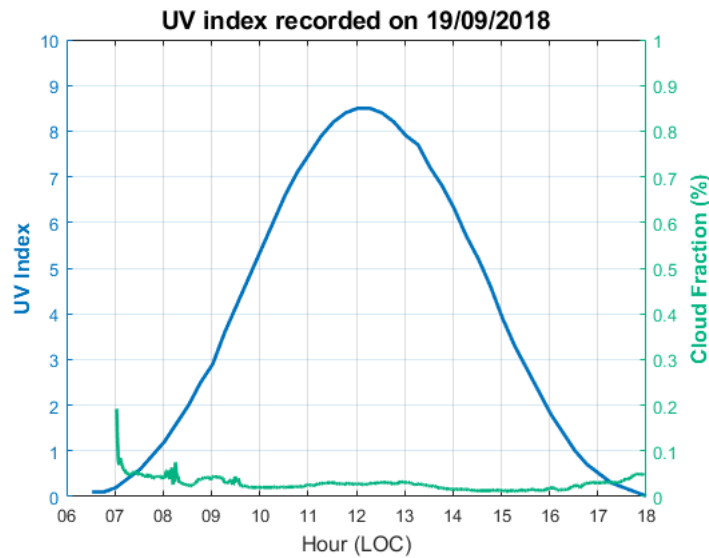
Figure 7. UVI (BT) and CF (SCV) distribution on 19/09/2018 at Saint-Denis. The blue line represents the UVI and the green line represents the CF.

3.3. Inter-Comparison

The present work aimed to assess the quality of a set of UV sensors selected as low- to moderate-cost instruments. This was achieved through a continuous one year inter-comparison campaign with a BT spectrometer selected as the reference instrument. The results of this comparison are statistically summarised below in **Table 1** and are shown in **Figure 8** and **Figure 9**. From the r^2 values (in the 3rd column of **Table 1**), the four UV instruments show a very good correlation with the BT (99%). It is expected that these correlations are very high because the same annual UVI course dominates the data sets and all instruments were co-located.

It can be seen from plots of **Figure 8a,b** that data from the KZ radiometer is very closely aligned with that of the BT spectrometer. Indeed, the RD between the two instruments is as low as 1.1%, with a median RD value of 2.6%. The scatter plot (**Figure 8a**) and the RD distribution (**Figure 8b**) show a low dispersion of the deviations. Furthermore, **Figure 9b** shows a low dependence of the KZ RD with respect to the zenith solar angle, i.e., averages for several solar zenith angle ranges show a decreasing

RD with increasing zenith angle within ±6%. As expected, and shown in plot of **Figure 9**a, this low zenith angle dependence results in low variations of the KZ RD over time (RD averages for several months), within ±4%. Nevertheless, this small but not negligible zenith angle dependence shows that the cosine correction introduced in the calibration could be improved.

With regard to UVI measurements from SL and SG radiometers, a very close alignment with BT is noted. They show similar narrow RD dispersions, with low RD values of 3.1% and 1.4%, and median values of the relative differences at 1.7% and 1.2%, respectively (see plots of **Figure 8**d,f). When one considers the evolvement of RD over months (**Figure 9**c,e) as a function of the solar zenith angle, by looking at the RD for several solar zenith angle ranges (**Figure 9**d,f), the mean RD remained almost constant for both instruments. However, the small positive RD obtained for the SL radiometer between June and October (around +5%), when there is virtually no dependence on the zenith angle, should be noted.

The Davis radiometer showed an RD of 14.2%, with a 13.3% median compared to BT. The RD dispersion is higher than the other instruments (**Figure 8**g,h). The DV was not corrected for ozone or solar zenith angle which may explain the RD.

Figure 9h clearly shows a dependence of the RD on the zenith solar angle, ranging from 0% at low solar zenith angles and increasing up to 30% at 70° solar zenith angle. It should be noted that the RD is very small at low solar zenith angles, when UV radiation is most intense. There is also a seasonal oscillation of the RD during the comparison period due to the dependence of the RD on SZA, in the order of ±4% around the mean RD, with a minimum in summer (DJF) and a maximum in winter (JJA). This is consistent with the annual evolution of mean SZA.

Overall, the panels on the left of **Figure 9** highlight the reliability of the instruments over time, despite a +14% shift for the DV. The right side of **Figure 9** shows a slight dependence on solar zenith angle except for the DV, which was not corrected for solar zenith angle.

No dependence on solar zenith angle was found for KZ, SL and SG. The same behaviour can be expected if these sensors are used in other latitude sites. However, RD depends on solar zenith angle for the DV. Therefore, the global RD depends on the solar zenith angle range of the site of use. At low latitude, the same RD behaviour as for the Reunion site is expected. However, with regard to latitudinal variation, the RD could increase with latitude, polewards from the equator.

Several Kipp&Zonen UVS-E-T and Solar Light SL501 have also been compared in other comparison campaigns in El Arelosillo, Spain [42] and Davos, Switzerland [19,20] using QASUME as reference. The results showed good compliance with the reference, with a RD less than ±10%, except in a few instances. The results shown here are fairly consistent with these previous studies, even though the UV levels reported here were much higher than those of the previous studies.

The SGLUX UV-Cosine and the Davis Radiometer are two new UV sensors. There is no comparison of high grade UV instruments in the literature as yet.

Table 1. Summary of comparison statistics between BT and all instruments. RD, relative difference; RSD, relative standard deviation; RMSE, root mean square error; KZ, Kipp&Zonen UVS-E-T; SL, SL501 UV-Biometer; SG, SGLux UV-Cosine sensor; DV, DAVIS UV sensor.

	Number of Points	r² (%)	RD (%)	RSD (%)	RMSE	Quantile (%)				
						0.05	0.25	Median	0.75	0.95
KZ	19220	99	1.1	10.2	0.5	−17.9	−2.9	2.6	6.3	14
SL	18878	99	3.1	10.6	0.4	−8.6	−0.5	1.7	4.9	20.1
SG	18967	99	1.4	9.4	0.4	−11.6	−1	1.2	3.8	13.7
DV	16675	99	14.2	14.5	0.7	−3.5	6.2	13.3	21.9	35.4
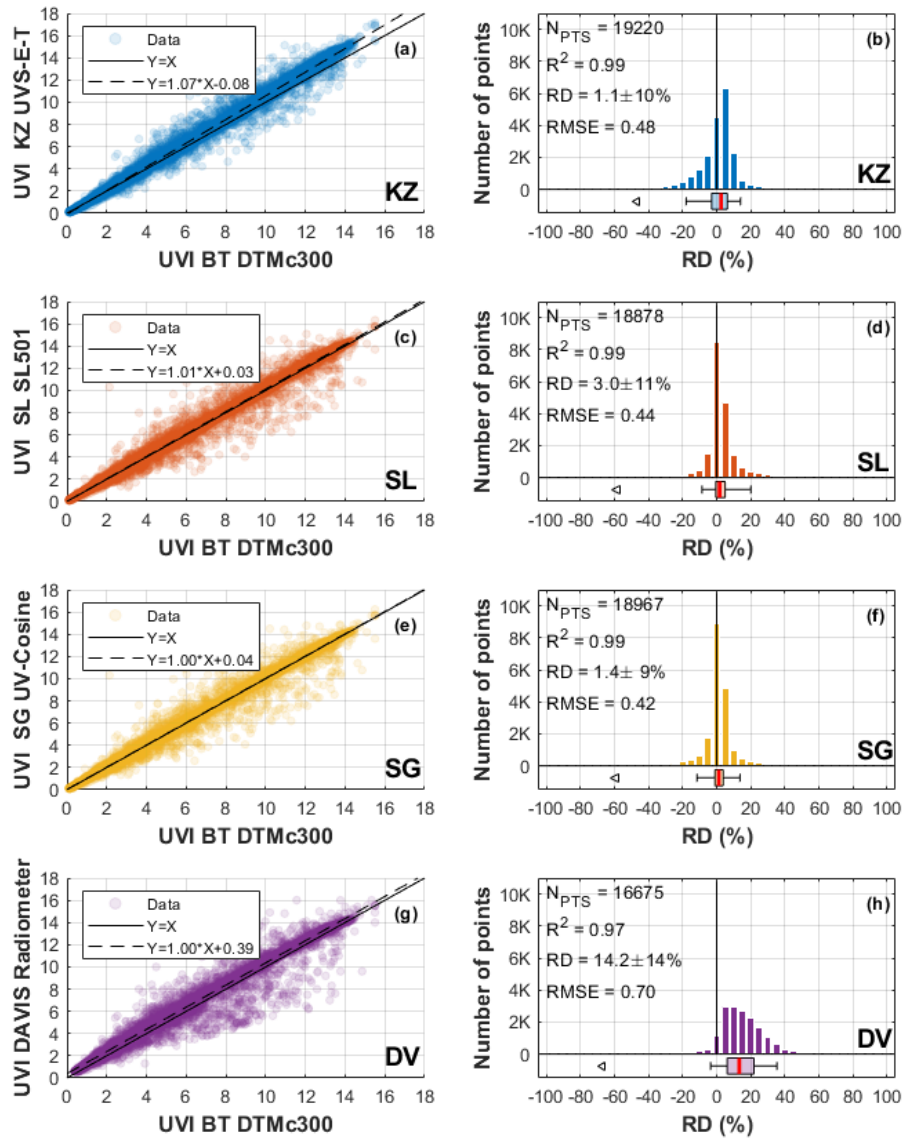
Figure 8. Comparison between BT and all of the instruments under evaluation. The left column (a, c, e and g) shows a scatterplot specific for each instrument with a linear fit; the right column (b, d, f and h) shows the RD distribution with statistics. The box diagram shows the 5e, 25e, 50e, 75e, 95e percentile and the arrows show the minimum and the maximum when they appear in the X-axis range.
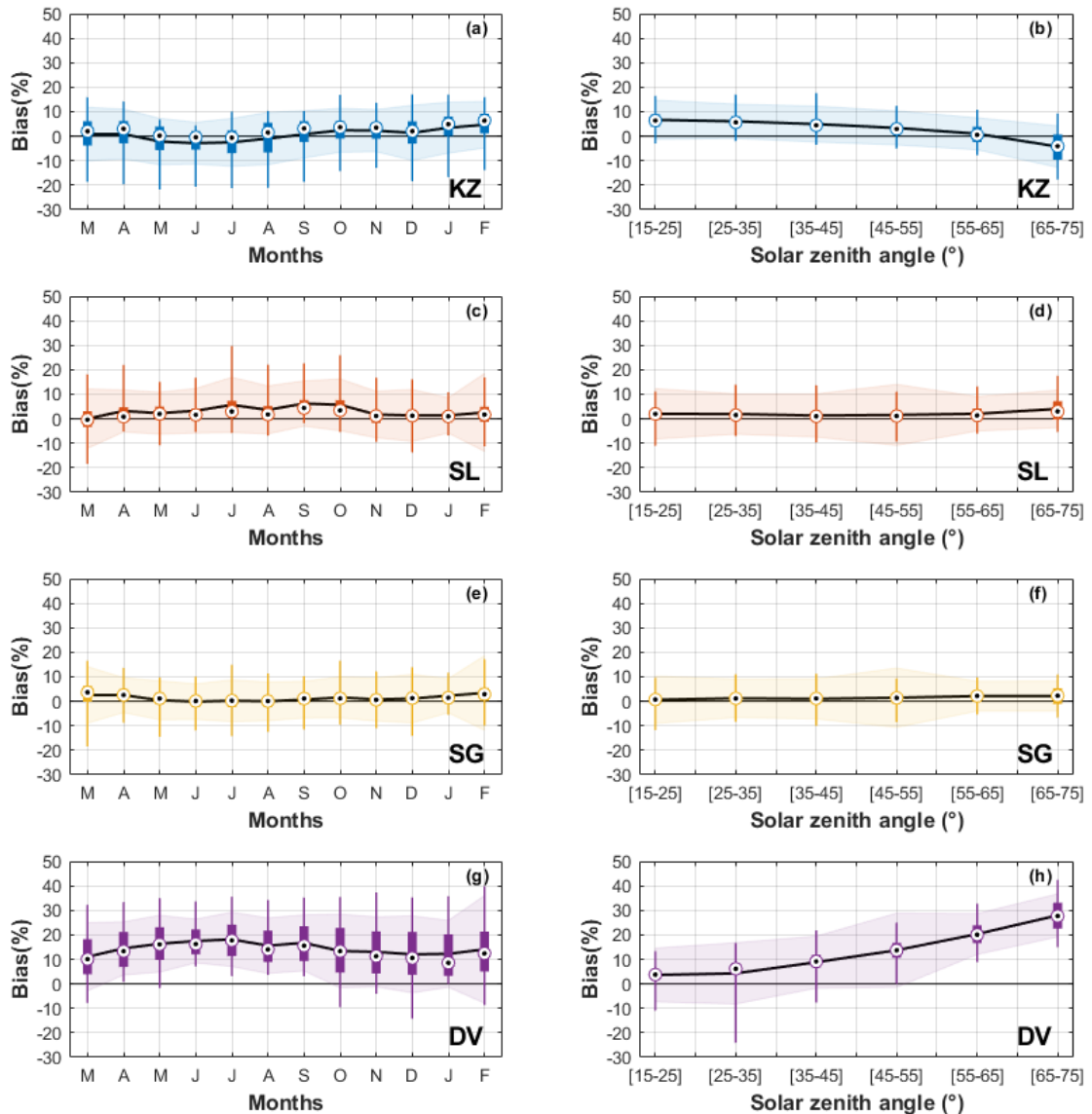
Figure 9. The left column (a, c, e and g) shows the evolvement of the RD as a function of time, and the right column (b, d, f and h) shows the evolvement of the RD as function of solar zenith angle. The black solid line represents the mean RD and the shaded surface one RSD. The box diagram shows the 5e, 25e, 50e, 75e, 95e percentile.

4. Conclusions

In conclusion, an inter-comparison of four radiometers to a spectroradiometer Bentham DTMc300 (as reference) was performed. Bentham DTMc300 is a high-grade instrument, affiliated WITH NDACC. Comparison with TUV model showED less than 5% difference. All of these instruments were installed on the same instrumental platform at the University of Reunion and operated simultaneously between February 2018 and March 2019. The purpose of such a study was to qualify these UV sensors under high irradiances, such as those observed in the tropics and on Reunion Island in particular. Of the instruments compared, some were moderately costly (3000–5000 €) while others were fairly inexpensive (a few hundred euros).

The clear sky filtering was carried out using an original method implemented at LACy, based on the measurement of the cloud fraction from an all-sky imaging camera. Clear sky time was characterised by a maximum threshold of 20% cloud fraction. Typical tropical cloud conditions are

illustrated by cloud fraction data: clear sky mainly in the morning, with an increase of cloud fraction in the afternoon. Similar daily cloud cover conditions may be found at different tropical sites.

The results show that two medium-cost instruments (KZ and SL) give very satisfactory results with regards to the RD in comparison with the BT. Nevertheless, a small zenith angle dependence remains with KZ and the cosine correction introduced in the calibration could be improved.

A clear dependence on solar zenith angle was found for the DV, with a 14% RD. A specific calibration should be done before using this instrument with a solar zenith angle correction.

It was also found that the low-cost SGLux UV cosine instrument performed quality measurements with an average clear sky RD of less than 1.5% compared to our reference measurement and a low dispersion (max. 10%).

In the future, it will be interesting to investigate the temporal drift of these instruments after different lengths of operating time, as well as in different geographical locations, and to check whether even low-cost instruments like SGLux UV Cosine remain reliable over time.

In addition, it would be interesting to develop integrated low-cost measurement solutions based on the SGLux UV cosine in order to increase the number of observation sites on Reunion Island and in neighbouring Indian Ocean countries.

References

1. Holick, M.F. Chapter 2—A perspective on the beneficial effects of moderate exposure to sunlight: Bone health, cancer prevention, mental health and well-being. *Compr. Series Photosciences* **2001**, *3*, 13–37, doi:10.1016/S1568-461X(01)80037-5.
2. Gallagher, R.P.; Lee, T.K. Adverse effects of ultraviolet radiation: A brief review. *Biophys. Mol. Biol.* **2016**, *92*, 119–131, doi:10.1016/j.pbiomolbio.2006.02.011.
3. Armstrong, B.K.; Kricker, A. How much melanoma is caused by sun exposure? *Melanoma Res.* **1993**, *3*, 395–401.
4. Albert, M.; Ostheimer, K. The evolution of current medical and popular attitudes toward ultraviolet light exposure: Part 3. *J. Am. Acad. Dermatol.* **2003**, 3, 1096–1106.
5. International Commission on Non-Ionizing Radiation Protection. Guidelines on limits of exposure to ultraviolet radiation of wavelengths between 180 nm and 400 nm. *Health Phys.* **2004**, *86*, 171–186.
6. Kerr, J.B.; Fioletov, V.E. Surface ultraviolet radiation. *Atmos. Ocean* **2008**, *46*, 159–184, doi:10.3137/ao.460108.
7. Fioletov, V.; Kerr, J.B.; Fergusson, A. The UV Index: Definition, Distribution and Factors Affecting it. *Can. J. Public Health* **2010**, *101*, 15–19, doi:10.17269/cjph.101.1905.
8. OMS. L'indice Universel de Rayonnement UV Solaire. Available online: http://www.who.int/uv/publications/French_final.pdf (accessed on 17 April 2020).

9. Bernhard, G.; Seckmeyer, G. Uncertainty of measurements of spectral solar UV irradiance. *J. Geophys. Res. Atmos.* **1999**, *104*, 14321–14345, doi:10.1029/1999JD900180.

10. Cadet, J.-M.; Bencherif, H.; Du Preez, D.J.; Portafaix, T.; Sultant-Bichat, N.; Belus, M.; Brogniez, C.; Auriol, F.; Metzger, J.-M.; Ncongwane, K.; et al. Solar UV radiation in Saint-Denis, La Réunion and Cape Town, South Africa: 10 years Climatology and Human Exposure Assessment at Altitude. *Atmosphere* **2019**, *10*, 589, doi:10.3390/atmos10100589.

11. Brogniez, C.; Auriol, F.; Deroo, C.; Arola, A.; Kujanpää, J.; Sauvage, B.; Kalakoski, N.; Pitkänen, N.R.A.; Catalfamo, M.; Metzger, J.-M.; et al. Validation of satellite-based noontime UVI with NDACC ground-based instruments: Influence of topography, environment and satellite overpass time. *Atmos. Chem. Phys.* **2016**, *16*, 15049–15074, doi:10.5194/acp-16-15049-2016.

12. Fountoulakis, I.; Diémoz, H. *Monitoring of Spectral UV Irradiance in Aosta, Saint-Christophe, Italy: From Measurements to Data Analysis;* VII Convegno Nazionale Agenti Fisici: Stresa, Italy, 2019.

13. Bais, A.F.; Gardiner, B.G.; Slaper, H.; Blumthaler, M.; Bernhard, G.; McKenzie, R.L. SUSPEN inter-comparison of ultraviolet spectroradiometers. *J. Geophys. Res. Atmos.* **2001**, *106*, 12509–12525, doi:10.1029/2000JD900561.

14. Houët, M. *Spectroradiométrie du Rayonnement Solaire UV au Sol: Améliorations Apportées à L'instrumentation et au Traitement des Mesures, Analyse pour L'évaluation du Contenu Atmosphérique en Ozone et en Aérosols;* Université de Lille: Lille, France, 2003.

15. Joint, I.S.O. *CIE Standard 17166: 1999/CIE S007-1998 Erythema Reference Action Spectrum and Standard Erythema Dose;* ISO: Vienna, Austria, 1999.

16. Bais, A.F.; Blumthaler, M.; Gröbner, J.; Seckmeyer, G.; Webb, A.R.; Gorts, P. Quality Assurance of spectral ultraviolet measurements in Europe through the development of a transportable unit (QASUME). *Ultrav. Ground- Space-Based Meas. Models Effects II* **2003**, *4896*, 232–238, doi:10.1117/12.468641.

17. Hülsen, G.; Gröbner, J. Protocol of the Inter-Comparison at Université de La Réunion, Saint-Denis, France on April 08 to 17, 2013 with the Travelling Reference Spectroradiometer QASUME. PMOD/WRC. Davos, Switzerland: PMOD/WRC, 2014 Available online: http://www-old.pmodwrc.ch/wcc_uv/qasume_audit/reports/2013_04_StDenis_LaReunion.pdf (accessed on 17 April 2020).

18. Lamy, K.; Portafaix, T.; Brogniez, C.; Godin-Beekmann, S.; Bencherif, H.; Morel, B. Ultraviolet radiation modelling from ground-based and satellite measurements on Reunion Island, southern tropics. *Atmos. Chem. Phys.* **2018**, *18*, 227–246, doi: 10.5194/acp-18-227-2018.

19. Gröbner, J.; Hülsen, G.; Vuilleumier, L.; Blumthaler, M.; Vilaplana, J.M.; Walker, D.; Gil, J.E. Report of the PMOD/WRC-COST Calibration and Inter-Comparison of Erythemal radiometers. PMOD/WRC-COST: Davos, Switzerland, 2006 available online: Ftp://ftp.pmodwrc.ch/pub/publications/PMOD_COST726_BBreport.pdf (accessed on 17 April 2020).

20. Hülsen, G.; Gröbner, J. 2nd International UV filter Radiometer comparison UVC-II. PMOD/WRC: Davos, Switzerland, 2017. Available online: http://projects.pmodwrc.ch/bb2017/media/UVC-II_report.pdf (accessed on 17 April 2020).

21. Webb, A.; Gröbner, J.; Blumthaler, M. *A Practical Guide to Operating Broadband Instruments Measuring Erythemally Weighted Irradiance;* Office for Official Publication of the European Communities: Luxembourg, Luxembourg, 2006, EUR 22595, ISBN 92-898-0032-1.

22. Lamy, K.; Portafaix, T.; Forestier, J.-B.; Rakotoniaina, S.; Amélie, V. *Réseau UV-Indien—Premiers Résultats. Meeting Geosciences, Resources;* Risques, Technologies: Antananarivo, Madagascar, 2019.

23. Seckmeyer, G.; Bernhard, A.; Blumthaler, M.; Booth, C.; Lantz, K.; Webb, A. *Instruments to Measure Solar Ultraviolet Radiation. Part 2: Broadband Instruments Measuring Erythemally Weighted Solar Irradiance;* World Meteorological Organization (WMO): Geneva, Switzerland, 2005.

24. Liandrat, O.; Cros, S.; Braun, A.; Saint-Antonin, L.; Decroix, J.; Schmutz, N. Cloud cover forecast from a ground-based all sky infrared thermal camera. *Remote Sens. Clouds Atmos. XXII* **2017**, *10424*, 104240B, doi:10.1117/12.2278636.

25. Breiman, L. Random forests. *Mach. Learn.* **2001**, *45*, 5–32, doi: 10.1023/A:1010933404324.

26. Long, C.; Sabburg, J.; Calbo, J.; Pages, D. Retrieving cloud characteristics from ground-based daytime colour all-sky images. *J. Atmos. Ocean. Technol.* **2006**, *23*, 633–652, doi:10.1175/JTECH1875.1.

27. Madronich, S. *UV Radiation in the Natural and Perturbed Atmosphere*; Lewis Publisher: Boca Raton, FL, USA, 1993.

28. Stamnes, K.; Tsay, S.-C.; Wiscombe, W.; Jayaweera, K. Numerically stable algorithm for discrete-ordinate-method radiative transfer in multiple scattering and emitting layered media. *Appl. Opt.* **1988**, *27*, 2502–2509, doi:10.1364/AO.27.002502.

29. Takemura, T.; Nakajima, T.; Dubovik, O.; Holben, B.N.; Kinne, S. Single-scattering albedo and radiative forcing of various aerosol species with a global three-dimensional model. *J. Clim.* **2002**, *15*, 333–352, doi:10.1175/1520-0442015<0333:SSAARF>2.0.CO;2.

30. Lacagnina, C.; Hasekamp, O.P.; Bian, H.; Curci, G.; Myhre, G.; van Noije, T. Aerosol single-scattering albedo over the global oceans: Comparing PARASOL retrievals with AERONET, OMI, and AeroCom models estimates. *J. Geophys. Res. Atmos.* **2015**, *120*, 9814–9836, doi: 10.1002/2015JD023501.

31. Dobber, M.R.; Voors, R.; Dirksen, R.J.; Kleipool, Q.; Levelt, P.F. The high-resolution solar reference spectrum between 250 and 550 nm and its application to measurements with the ozone monitoring instrument. *Solar Phys.* **2008**, *249*, 281–291, doi: 10.1007/s11207-008-9187-7.

32. McPeters, R.D.; Labow, G.J. Climatology 2011: An MLS and sonde-derived ozone climatology for satellite retrieval algorithms. *J. Geophys. Res. Atmos.* **2012**, *117*, D10303, doi: 10.1029/2011JD017006.

33. Dubovik, O.; Smirnov, A.; Holben, B.N.; King, M.D.; Kaufman, Y.J.; Eck, T.F.; Slutsker, I. Accuracy assessments of aerosol optical properties retrieved from Aerosol Robotic Network (AERONET) Sun and sky radiance measurements. *J. Geophys. Res. Atmos.* **2000**, *105*, 9791−9806, doi: 10.1029/2000jd900040.

34. Corrëa, M.d.; Godin-Beekmann, S.; Haeffelin, M.; Bekki, S.; Saiag, P.; Badosa, J. Projected changes in clear-sky erythemal and vitamin D effective UV doses for Europe over the period 2006 to 2100. *Photochem. Photobiol. Sci.* **2013**, *12*, 1053–1064, doi: 10.1039/C3PP50024A.

35. Koelemeijer, R.B.; De Haan, J.F.; Stammes, P. A database of spectral surface reflectivity in the range 335–772 nm derived from 5.5 years of GOME observations. *J. Geophys. Res. Atmos.* **2003**, *108*, 4070, doi: 10.1029/2002jd002429.

36. Koepke, P.; Bais, A.; Balis, D.; Buchwitz, M.; De Backer, H.; de Cabo, X. Comparison of models used for UV index calculations. *Photochem. Photobiol.* **1998**, *67*, 657–662, doi:10.1111/j.1751-1097.1998.tb09109.x.

37. Bodeker, G.E.; McKenzie, R.L. An Algorithm for Inferring Surface UV Irradiance Including Cloud Effects. *J. Appl. Meteorol.* **1996**, *35*, 1860–1877, doi:10.1175/1520-0450035<1860:AAFISU>2.0.CO;2.

38. Barnes, M.L.; Miura, T.; Giambelluca, T.W. An assessment of Diurnal and seasonal Cloud Cover Changes over the Hawaiian Islands Using Terra and Aqua MODIS. *J. Clim.* **2016**, *29*, 77–90, doi:10.1175/JCLI-D-15-0088.1.

39. Jumeaux, G.; Quetelard, H.; Roy, G. *Atlas Climatique de La Réunion*; Météo-France Direction interrégionale de la Réunion: Sainte-Clotilde, La Réunion, 2002.

40. Cadet, B.; Goldfarb, L.; Faduilhe, D.; Baldy, S.; Réchou, A.; Giraud, V.; Keckhut, P. A sub-tropical cirrus clouds climatology from Reunion Island (21S, 55E) lidar data set. *Geophys. Res. Lett.* **2003**, *30*, 1130.

41. Cede, A.; Blumthaler, M.; Luccini, E.; Piacentini, R.D.; Nuñez, L. Effects of clouds on erythemal and total irradiance as derived from data of the Argentine network. *Geophys. Res. Lett.* **2002**, *29*, 76-1, doi: 10.1029/2002GL015708.

42. Vilaplana, J.M.; Serrano, A.; Anton, M.; Cancillo, M.L.; Parias, M.; Gröbner, J. *Report of the "El Arenosillo"/INTA-COST Calibration and Inter-Comparison Campaign of UVER Broadband Radiometers*; El Arenosillo: Huelva, Spain, 2007.

International Journal of
Environmental Research and Public Health

an Open Access Journal by MDPI

Indexed in: **PubMed**

CITESCORE 2.81 SCOPUS

IMPACT FACTOR 2.468

CERTIFICATE OF PUBLICATION

Certificate of publication for the article titled:

Inter-Comparison Campaign of Solar UVR Instruments under Clear Sky Conditions at Reunion Island (21°S, 55°E)

Authored by:

Jean-Maurice Cadet; Thierry Portafaix; Hassan Bencherif; Kévin Lamy; Colette Brogniez; Frédérique Auriol;

Jean-Marc Metzger; Louis-Etienne Boudreault; Caradee Yael Wright

Published in:

Int. J. Environ. Res. Public Health **2020**, Volume 17, Issue 8, 2867

MDPI

Academic Open Access Publishing
since 1996

Basel, April 2020

Chapitre 3 COMPARAISON SATELLITALE

3.1   ARTICLE : RESUME

La mesure précise du rayonnement ultraviolet est importante notamment à cause des enjeux liés à la biosphère terrestre. L'objectif de cette étude exploratoire est de comparer les données UV mesurées par un réseau d'instruments au sol à des mesures UV faites par satellite.

Le South African Weather Service (SAWS) possède un réseau de 6 radiomètres UV répartis sur tout le territoire Sud-Africain : Cape Point, Cape Town, De Aar, Durban, Port Elizabeth et Pretoria. Ce réseau, en fonctionnant depuis 1994 pour les 3 plus anciennes stations, est destinés à la prévention publique sur le risque UV.

Les instruments sont des radiomètres UV large bande manufacturés par la société Solar Light Pty Ltd : UV-biometer model 501. Le rayonnement UV erythemal est intégré sur une bande de 280 nm à 340 nm par une photodiode GaAsP protégée par un dôme de quartz. Les données sont enregistrées une fois par heure sous la forme de MED/h où 1 MED=210 J.m^{-2}. Les données sont corrigées de la longueur d'onde en utilisant une table standard. L'incertitude est évaluée à $\pm 7\%$.

Les données UV mesurées par les UV-Biometer sont comparées aux données UV mesurées par le capteur OMI (Ozone Monitoring Instrument) embarqué sur le satellite Aura. L'indice UV (erythemal) est obtenu à partir de la mesure d'ozone issue de l'analyse du rayonnement solaire UV rétrodiffusé. La version des données utilisées prend en compte des données d'aérosols issus du réseau AERONET. Les données utilisées sont obtenues sur une grille de 1° x 1° et avec une incertitude estimée à $\pm 5\%$.

Dans un premier temps, les données ont été examinées afin de retirer et corriger des erreurs. Ensuite, les climatologies ont été calculées et analysées. Enfin, la comparaison a été effectuée. La comparaison entre les instruments au sol et satellite ont été effectuées à l'heure du passage du satellite Aura et par ciel clair. Les données de réflectivité (Lambertian Equivalent Reflectivity LER) ont été utilisées avec un seuil de 10% pour le filtrage de la nébulosité.

Les climatologies journalières montrent un comportement similaire pour les 4 stations situées au niveau de la mer : Durban, Port Elizabeth, Cape Town et Cape Point, avec une médiane

situé en 4 et 5 d'indice UV. Il est à noter que les stations de mesure de Cape Town et Cape Point, situées à environ 50 km l'une de l'autre, présentent une différence d'intensité. Cette différence est très certainement liée à une différence de conditions atmosphériques, la station de Cape Town est située sur un aéroport à proximité de la ville, alors que la station de Cape Point est isolé. Les stations en altitude, Pretoria et De Aar, présentent des niveaux d'UV plus élevés. Cependant, le niveau d'ultraviolet est plus fort à De Aar due à son atmosphère propre, contrairement à Pretoria où le niveau d'aérosols est plus important, entrainant une plus grande absorption. Les climatologies mensuelles montrent les mêmes résultats.

La climatologie issue des données satellites sont similaires, avec un indice UV médian autour de 12 durant l'été austral. De Aar présente toutefois un niveau UV plus fort, 14.

La comparaison globale entre les données mesurées au sol et par satellite montrent des différences notables. La corrélation entre les 2 jeux de données est positive, >70%, étant donné que le cycle annuel est dominant dans le signal temporel d'indice UV. Le MAPE est de 22% à 28% pour les différentes stations, 46% pour la station de De Aar.

Le suivi annuel de la comparaison met en évidence une particularité pour De Aar et Pretoria, tandis que pour les autres stations, le biais est stable autour de 20%. Le MAPE est très variable pour les données de De Aar : 40% de 2005 à 2008, puis 25% de 2009 à 2011 et 50% de 2012 à 2014. Dans le cas de Pretoria, nous avons une augmentation soudaine en 2013, due à un changement d'albédo autour de l'instrument.

L'utilisation de données satellites présente cependant quelques limitations. L'empreinte spatiale trop large, 1° x 1°, est problématique lorsque la variabilité de paramètres déterminants au sol est grande. Les sites de Cape Town et Cape Point présentent une atmosphère différente, ce qui n'est pas visible par satellite. De même, le site de De Aar présente une atmosphère très claire et bien que les données UV OMI prennent en compte les aérosols, un site ponctuel très isolé n'est pas visible.

Il est à noter que les biomètres model 501 ne sont pas destinés à la mesure à long terme, mais plutôt pour la prévention publique. Le suivi temporel des différences ne montre pas de régularité, par exemple le site de De Aar, entrainant l'impossibilité de détecter d'éventuelles tendances. En revanche, il a été possible de calculer la variabilité saisonnière en fonction de la position géographique des différents sites. En l'état, nous ne pouvons pas statuer sur la

qualité des données sol utilisées sans données supplémentaires, telles que les données de radiomètres ou spectromètres de meilleures stabilités.

Pour conclure, cette étude exploratoire a permis de mettre en évidence des irrégularités dans les bases de données ne permettant pas l'évaluation précise de la qualité de ces données ni la détection de tendance. L'écart trouvé entre les données du réseau de mesure Sud-africain et les données OMI montre un écart allant de 0% à 45%, dépendant des différents sites ou variable dans le temps. Dans l'ensemble, les écarts les plus importants apparaissent durant les périodes d'hiver austral.

3.2 ARTICLE : CADET ET AL., 2017 (IJERPH)

Article ci-dessous publié le 14 novembre 2017 dans IJERPH disponible sur :

https://www.mdpi.com/237702

International Journal of
**Environmental Research
and Public Health**

MDPI

Article

Comparison of Ground-Based and Satellite-Derived Solar UV Index Levels at Six South African Sites

Jean-Maurice Cadet [1,*], Hassan Bencherif [1,2], Thierry Portafaix [1], Kévin Lamy [1], Katlego Ncongwane [3], Gerrie J. R. Coetzee [3] and Caradee Y. Wright [4,5]

1 LACy, Laboratoire de l'Atmosphère et des Cyclones (UMR 8105 CNRS, Université de La Réunion, Météo-France), Saint-Denis de La Réunion 97744, France; hassan.bencherif@univ-reunion.fr (H.B.); thierry.portafaix@univ-reunion.fr (T.P.); kevin.lamy@univ-reunion.fr (K.L.)
2 School of Chemistry and Physics, University of KwaZulu-Natal, Durban 4041, South Africa
3 South African Weather Service, Private Bag X097, Pretoria 0001, South Africa; katlego.ncongwane@weathersa.co.za (K.N.); gerrie.coetzee@weathersa.co.za (G.J.R.C.)
4 Environment and Health Research Unit, South African Medical Research Council, Pretoria 0001, South Africa; Caradee.Wright@mrc.ac.za
5 Department of Geography, Geoinformatics and Meteorology, University of Pretoria, Pretoria 0002, South Africa
* Correspondence: jean.cadet@univ-reunion.fr; Tel.: +262-692-93-82-97

Abstract: South Africa has been measuring the ground-based solar UV index for more than two decades at six sites to raise awareness about the impacts of the solar UV index on human health. This paper is an exploratory study based on comparison with satellite UV index measurements from the OMI/AURA experiment. Relative UV index differences between ground-based and satellite-derived data ranged from 0 to 45% depending on the site and year. Most of time, these differences appear in winter. Some ground-based stations' data had closer agreement with satellite-derived data. While the ground-based instruments are not intended for long-term trend analysis, they provide UV index information for public awareness instead, with some weak signs suggesting such long-term trends may exist in the ground-based data. The annual cycle, altitude, and latitude effects clearly appear in the UV index data measured in South Africa. This variability must be taken into account for the development of an excess solar UV exposure prevention strategy.

Keywords: solar ultraviolet radiation; UV index; ground-based measurements; satellite-derived data; OMI/AURA; South Africa

1. Introduction

Solar ultraviolet radiation (UVR) is known to have biological effects on ecosystems, plants, animals, and humans [1]. Solar UVR is usually divided into three wavebands [2]: UVA: 315–400 nm; UVB: 280–315 nm; and UVC: 100–280 nm. All UVC, potentially the most dangerous UVR band, is absorbed by ozone and oxygen in the atmosphere and, therefore, does not reach the Earth's surface, while UVA is weakly absorbed by ozone, and only a fraction of UVB reaches the surface with the majority being absorbed by ozone. The important implications of UVA and UVB on human health are translated via the application of an action spectrum, here, specifically, for erythema (sunburn) which occurs due to excess UVA and UVB exposure [3]. The Ultraviolet Index is a standard unitless measure of UVR used to describe an erythemal dose rate where 1 UV index unit is equivalent to 25

mW·m−2 [4]. The UV index is recommended as a public communication tool to convey solar UVR levels and appropriate sun protection advice [4]. Several countries around the world monitor ground-based solar UVR and/or forecast a predicted UV index reading for the general public on a daily basis.

South Africa, located in the mid-latitudes between 22° S and 35° S, has been measuring ground-based UV index levels since 1990. The network was originally initiated due to concerns regarding the possible adverse health impacts of excess personal solar UVR exposure on the South African population. Environmental monitoring was deemed an important approach to provide observational evidence for the typical levels of solar UV index across the country. These data would help to understand the results of studies showing relatively high UV index patterns [5], as well as high incidence of skin cancers, especially among Caucasian groups [6]. Furthermore, ozone depletion has been an international concern from the late 1970s. Therefore, there was a need for local ground-based UV index data across South Africa to consider health impacts relative to changing stratospheric ozone levels and possible human health impacts. Thus, the network was initiated comprising four sites, initially, with two additional sites being added later.

Several studies were conducted during the 1990s and early 2000s to consider both ground-based and satellite-derived UV index levels at South African sites. Past (1978–1994) and future (1998–2007) UV index trends were assessed using data from the satellite-borne TOMS (Total Ozone Mapping Spectrophotometer) instruments for Johannesburg, Bloemfontein, Durban, Cape Town, and Port Elizabeth [7]. Small increases in the UV index levels were predicted for the early 2000s. The UV index measured with a pyranometer in Durban between 1996 and 1998 showed good agreement with satellite data of annual erythema irradiance curves [8]. While the period was too short to test for long-term trends, a positive anti-correlation was found between UV index and total column ozone.

To date, the full dataset measured by the ground-based UV index network instruments has not been analysed or compared to satellite-derived UV index data for the same sites. A process of data verification or qualification is necessary should these data be used for long-term trend analysis, or for the monitoring of solar UVR exposure risk and possible impacts on human health. Studies have shown the complexities of applying satellite-derived UV index estimates for surface UV index levels, where relative differences between the two UV index measures range from 0 to 20% [9-17]. Satellite-derived UV index data is largely affected by spatial and temporal cloud modification effects, among other factors, such as total column ozone, aerosols, albedo, etc. [18], that cannot be accurately incorporated in the algorithm or model-calculated UV index levels.

Given these complexities, the aim of the study reported here is to compare the available ground-based and satellite-derived solar UV indices at six South African sites. Two objectives were identified: (1) to compare ground-based and satellite-derived solar UV index levels at the six sites; and (2) to provide an estimate of the quality of the ground-based solar UV index data. No attempts were made to correct the ground-based solar UV index data; the findings are discussed in terms of the challenges of using ground-based and satellite-derived solar UV index datasets to, in the most accurate manner, determine the surface solar UV index.

For the first time, data and methods of comparison will be presented. Afterward, the result of the comparison will be shown and discussed, before gathering our findings and reporting our conclusion.

2. Data and Methods

2.1. Ground-Based Solar UVR Data

In 1994, the South African Weather Service (SAWS) implemented a network of three UV biometers at Cape Town, Durban, and Pretoria (**Figure 1**). The Cape Point station was added to the network in 1997, and two other stations were added later, namely Port Elizabeth station in 2000 and De Aar station in 2002. All geographical information is presented in **Table 1**.
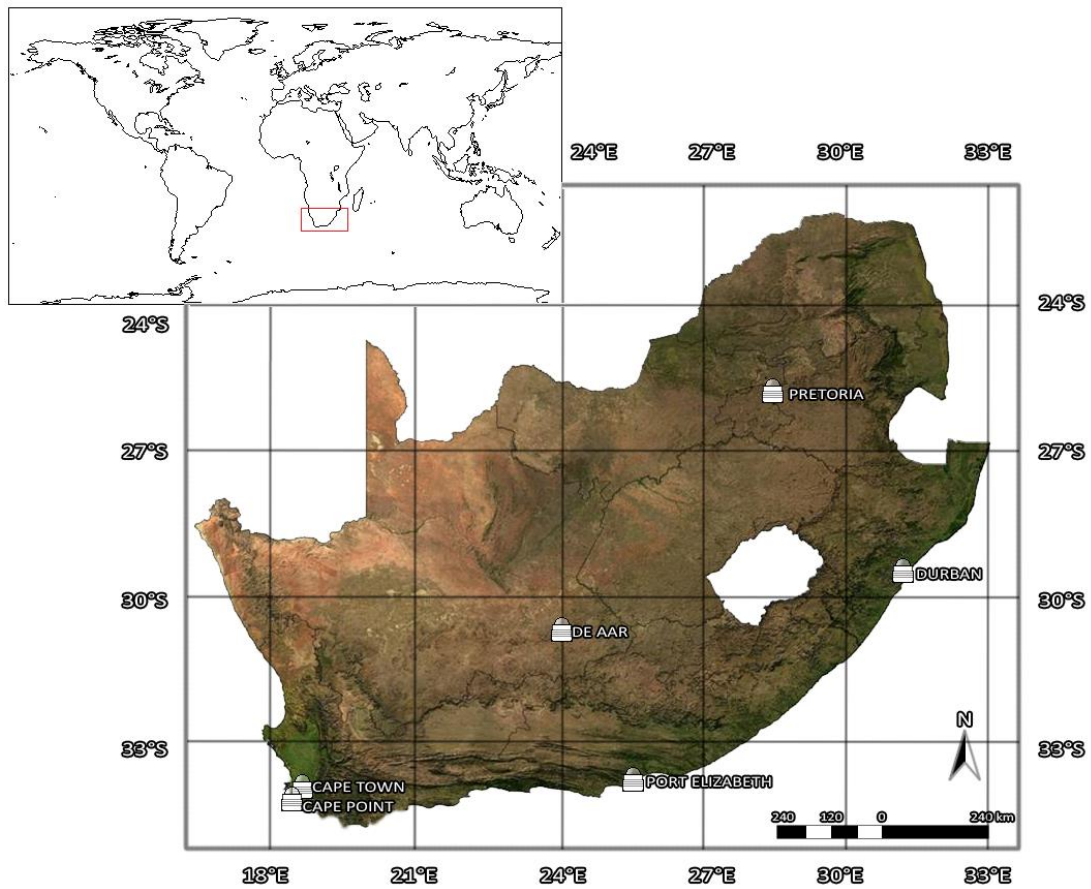
Figure 1. Geographical locations of the six South African Weather Service ground-based solar UVR measurement sites in South Africa.

Table 1. Geographical information of the six South African Weather Service ground-based UV index measurement sites.

Station	Geographical Position	Coordinates	Altitude	Time Series
Pretoria	1—FORUM Building	25.73° S, 28.18° E	1330 m	1994 to May 2003
	2—Erasmusrand	25.81° S, 28.49° E	1228 m	May 2003 to present
Durban	1—Louis Botha Airport	29.97° S, 31.00° E	9 m	1994 to May 2010
	2—King Shaka Airport	29.61° S, 31.11° E	103 m	May 2010 to present
De Aar	1—SAWS Building	30.67° S, 23.99° E	1286 m	2002 to present
Port Elisabeth	1—Port Elizabeth Airport	33.97° S, 25.61° E	63 m	2000 to present
Cape Town	1—Cape Town Intl Airport	33.98° S, 18.60° E	42 m	1994 to present
Cape Point	1—GAW station	34.35° S, 18.48° E	228 m	1997 to present

Solar UVR (280–340 nm) is recorded using a broadband instrument: a model 501 UV-biometer manufactured by Solar Light Pty Ltd. (Glenside, Pennsylvania, USA). A GaAsP diode, protected by a quartz dome, collects the solar UV radiation, and the electrical intensity is converted into a minimum erythemal dose per hour (MED), where 1 MED is equivalent to 210 J·m^{-2}. Measurements are made hourly to determine a MED/h. For the purpose of this study, MED/h readings from the UV biometers were converted to a UV index using Equation (1). A correction of the spectral response depending on total ozone and solar zenith angle was applied by using a generic table for the model 501 UV biometer to convert the instrument-weighted UVR to the erythemally-weighted UVR [19].

$$UV\ index = UVd[MED \cdot \text{h}^{-1}].\frac{210[\text{J} \cdot \text{m}^{-2}] \cdot 40[\text{m}^2 \cdot \text{W}^{-1}]}{3600[\text{s}]} \tag{1}$$

where UV index is the hourly UV index and *UVd* is the hourly erythemally-weighted exposure [20].

The accuracy of the UV biometer used is ±5% of the daily total. Taking into consideration the installation, the maintenance, and the temperature control, the uncertainty can reach up to ±8%. The biometer at Cape Point station was calibrated in 2012 at the Meteorological Observatory Service Deutscher Wetterdienst by using the spectrometer SPECTRO 320D NO 15 (Instrument Systems GmbH, Munich, Germany). The calibration was done by using the sun as the source and by comparison of the two instruments.

2.2. Satellite-Derived Solar UVR Levels

Launched in late 2004, the Aura satellite is dedicated to measuring ozone, aerosols, and other key gases in the atmosphere. The OMI (Ozone Monitoring Instrument) sensor aboard Aura measures ozone total quantities by analysing the backscattered solar radiation. The erythemally-weighted irradiance (290–400 nm) is computed by using an enhanced version of the TOMS (Total Ozone Mapping Spectrometer) surface UV-B flux algorithm [11,21]. A recent version of OMI datasets taking better consideration of aerosol optical depth and single scattering albedo obtained by modelling and ground-based observations from the AERONET network was used [22]. Data from OMI/Aura for the UV index given at overpass are available on the GIOVANNI platform for download [23].

We applied the 'all-sky UV index' data and not the 'clear-sky UV index' data in this study, since the ground-based solar UV index data included the effects of clouds, where clouds are known factors influencing ambient solar UVR levels [1]. We did not have cloud data at the ground sites, therefore, we were unable to identify clear sky only days. The OMI data are gridded at 1° × 1° [24]. Satellite data from 2005 to 2015 (i.e., 10 years) overpass time UVI measurements are used in these analyses. The uncertainty is 2% to 5% for small to large solar zenith angles.

2.3. Methods and Statistical Analysis

Both datasets were prepared separately and scrutinised for obvious errors. Erroneous night-time UV index values were removed. The ground-based dataset for Durban exhibited a 2-h time shift in instrument timing between 2009 and 2012 and this timing error was corrected. Ground-based data were analysed for diurnal, monthly, and annual trends and satellite-derived data for monthly and annual trends since one value (overpass satellite time) of the UV index was available per day. Both datasets were compared at satellite overpass time (around 1:45 p.m. for South Africa). To only keep clear sky days for the comparison, OMI Lambertian equivalent reflectivity (LER) was used. The days with an LER higher than 10% were removed [25].

A comparison of ground-based and satellite-derived solar UV index values were made in two ways: (1) computation of a daily correlation year-by-year to see if ground-based and satellite data evolve in the same way; and (2) computation of a daily bias year-over-year to provide an estimate of the relative difference between the two datasets.

To compare the ground-based data with satellite data, we calculated the bias, median, standard deviation, and root mean square error (RMSE). Bias is defined as the ground-based observation subtracted by the satellite observation and can be interpreted as the difference between the two datasets. The median separates the data in two equal parts. Standard deviation is defined as the dispersion of the previous bias. RMSE is defined as a measure of the differences between calculated values (here, OMI data) and observed values, i.e., ground-based observations. Lower RMSE values indicate less residual variance.

The equation (Equation (2)) for the R-squared correlation is given below:

$$r = \frac{\sum_{i=1}^{n}\left(S_{GND,i} - \overline{S_{GND}}\right)\left(S_{OMI,i} - \overline{S_{OMI}}\right)}{\sqrt{\left(\sum_{i=1}^{n}\left(S_{GND,i} - \overline{S_{GND}}\right)^2\right)\left(\sum_{i=1}^{n}\left(S_{OMI,i} - \overline{S_{OMI}}\right)^2\right)}} \tag{2}$$

where S is the UV index, $\bar{S}$ is mean UV index, GND is the ground-based observation, OMI is the satellite observation, and n the number of observation.

We computed a bias (Equation (3)) and mean absolute percentage error (MAPE) (Equation (4)), a standard deviation (Equation (5)), and an RMSE (Equation (6)) as given below:

$$Bias = \frac{1}{n}\sum_{i=1}^{n}\left(S_{OMI,i} - S_{GND,i}\right) \tag{3}$$

$$MAPE = \frac{1}{n}\sum_{i=1}^{n}\left(100 * \frac{|S_{OMI,i} - S_{GND,i}|}{S_{GND,i}}\right) \tag{4}$$

$$Std = \sqrt{\frac{1}{n-1}\sum_{i=1}^{n}\left(\left(S_{OMI,i} - S_{GND,i}\right) - Bias\right)^2} \tag{5}$$

$$RMSE = \sqrt{\frac{1}{n-1}\sum_{i=1}^{n}\left(S_{OMI,i} - S_{GND,i}\right)^2} \tag{6}$$

where S is the UV index, GND is the ground-based observation, OMI is the satellite observation, and n is the number of observations. These calculations were made for the full period of comparison, i.e., 2005 to 2015, as well as year-over-year in order to quantify the temporal evolution of change in solar UVR data from ground-based sites and satellite-derived observations.

3. Results

3.1. Ground-Based Solar UVR Observations

All solar UVR results are given in UV index units. Hourly data from the six ground-based solar UVR measurements sites were analysed for the period 1994–2015 where data were available for each site. Raw data are provided in **Figure 2**. Four stations initiated observations in 1994, while De Aar and Port Elizabeth observations begun later, in 2000 and 2002, respectively. Several data gaps are also evident, with the longest being at De Aar between 2010 and 2012. The typical diurnal solar UVR pattern is evident with UV index levels increasing during the day, reaching a peak at solar noon and decreasing during the afternoon as solar zenith angles increase again. Annual variability, modulated by the seasonal cycle, is also evident in **Figure 2**, with summer UV index values regularly exceeding 11 UV index units at De Aar. De Aar presents a clear atmosphere because of its isolated geographical position and its relatively low industrial activity [26]. Similar results on these time series have been found previously [27,28].

The effects of latitude and altitude on solar UV index levels are apparent in **Figure 3** where South African sites situated closer to the equator and at higher altitude tend to experience higher mean solar UV index levels, i.e., De Aar (mean: 8) and Pretoria (mean: 6) compared to other sites.

Figure 4 shows the monthly climatological median ground-based solar UV index levels for all six South African sites for all available years between 1994 and 2015 shown as a function of time of day and month in the year. Annual variability and change in UV index levels by season are emphasized. Solar UV index levels are the highest during the austral summer and lowest during the winter. It is apparent that the hour of maximum intensity (i.e., daily peak UV index) depends on the longitude of the site. Cape Town had the latest mean hour of maximum UV index followed by De Aar, Port Elizabeth, Pretoria, and Durban.

Since the satellite-derived solar UVR data were only available for the period of 2005 to 2015, the ground-based solar UVR dataset was reduced, for comparison purposes and further analysis (see Section 3.3. below), to only include the UV index at satellite overpass time readings from 2005 to 2015 (**Figure 5**).

If we do not consider De Aar, which is the second highest and the clearest site, Cape Town shows the more exposed site to UVR around noon. Cape Town and Cape Point show similar UVR levels; they are two geographically-close sites (about 50 km apart).
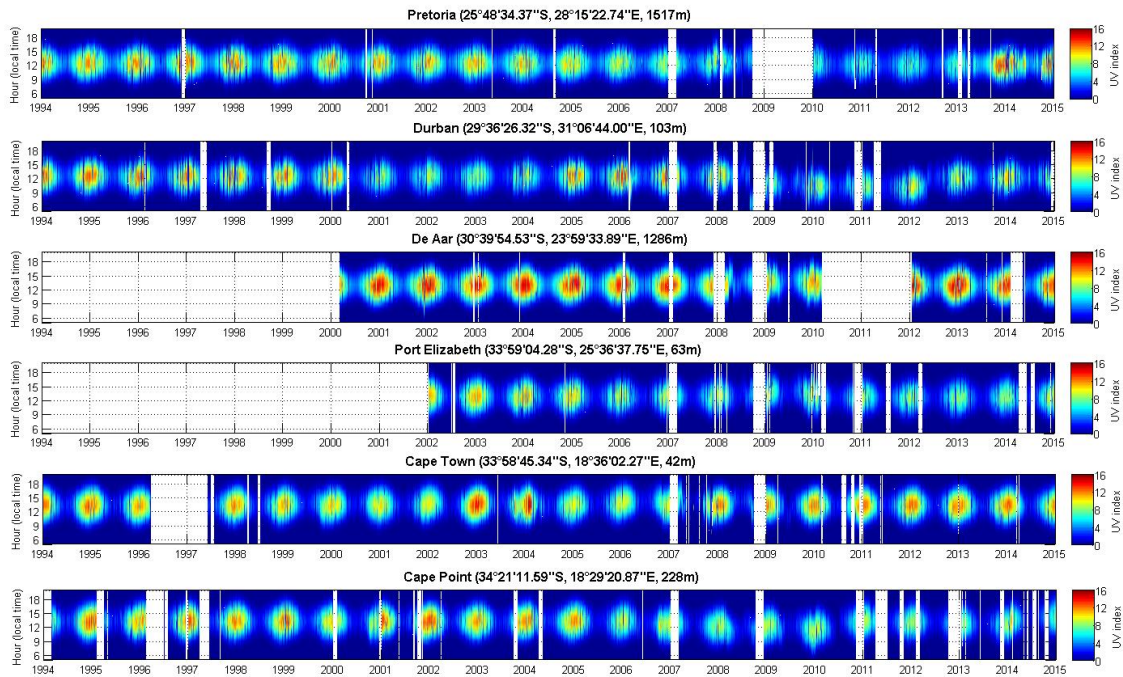
Figure 2. UV index observations as a function of day and hour per day for Cape Point, Cape Town, Durban, De Aar, Port Elisabeth, and Pretoria from 1994 to 2015.
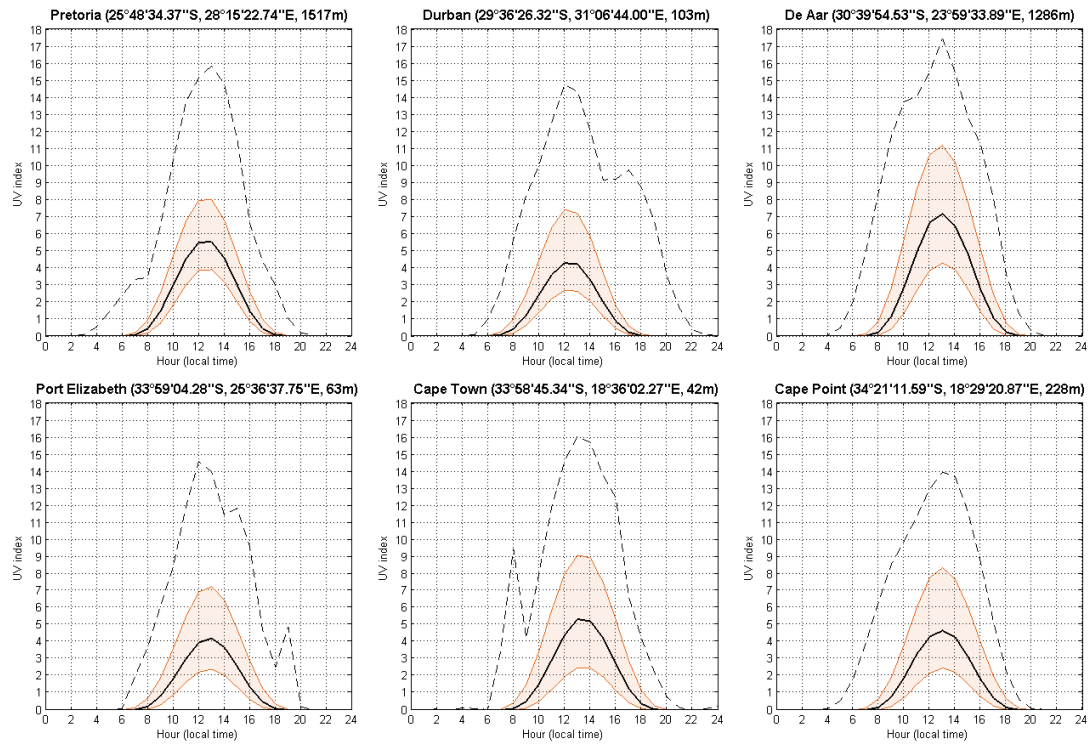
Figure 3. Daily climatological median (black line) of the solar UVI for the six South African sites, for all years of observation (i.e., 1994–2015). Quantile 25 and 75 (filled orange lines) and minimum and maximum (black dash line) are also represented.
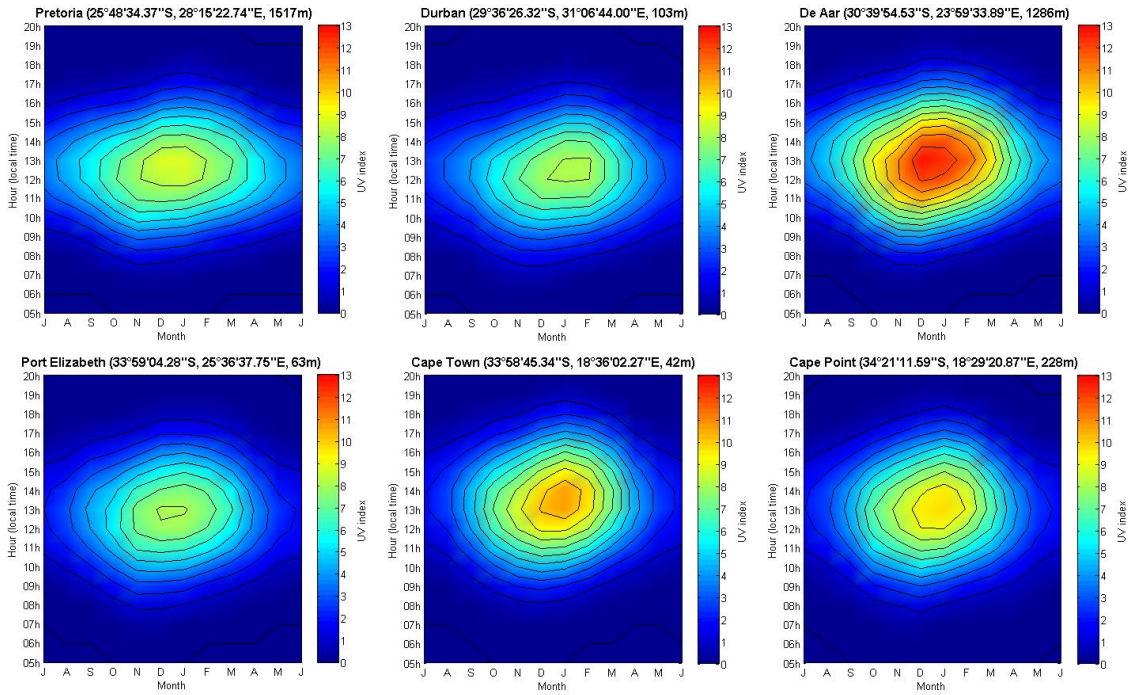
Figure 4. The monthly climatological median ground-based solar UV index levels for all six South African sites for all available years between 1994 and 2015 shown as a function of time of day and month of the year. For seasons to be shown more easily, the plots show the first month on the *X*-axis as July through to December, followed by January through to June. Therefore, summer months are in the middle of the plot.
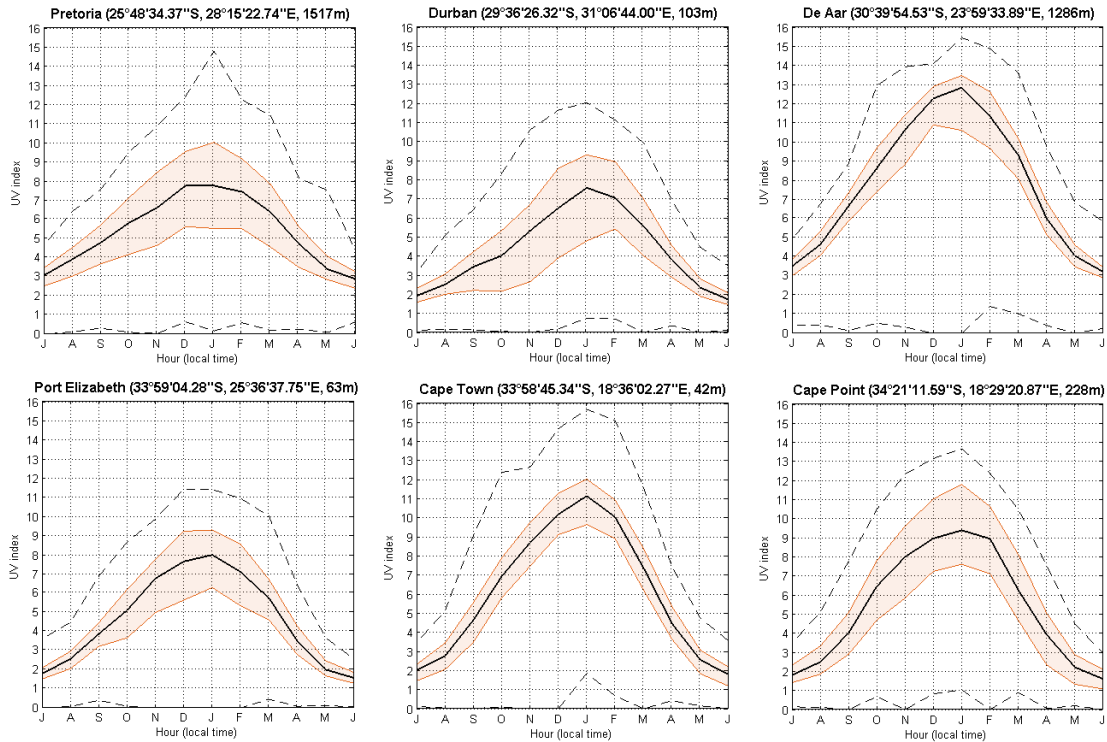
Figure 5. Monthly climatological median (black line) of the solar UVI for the six South African sites at satellite overpass time, for all years of observation (i.e., 1994–2015). Quantile 25 and 75 (filled orange lines) and minimum and maximum (black dash line) are also represented.

3.2. Satellite-Derived Solar UVR Measurements

Satellite-derived UV index values at overpass time above all sites were similar with maximum UV index levels of ~15 and low levels of ~2. For all sites, scatter about the mean is mostly tight with the most scatter evident at the coastal site of Durban. The yearly UV index median was highest at De Aar, followed by Pretoria and lowest at Port Elizabeth (see **Figure 6**). The UV index profiles at Cape Town and Cape Point are similar because of the proximity of the two measurements' sites, as they are separated by ~50 km.
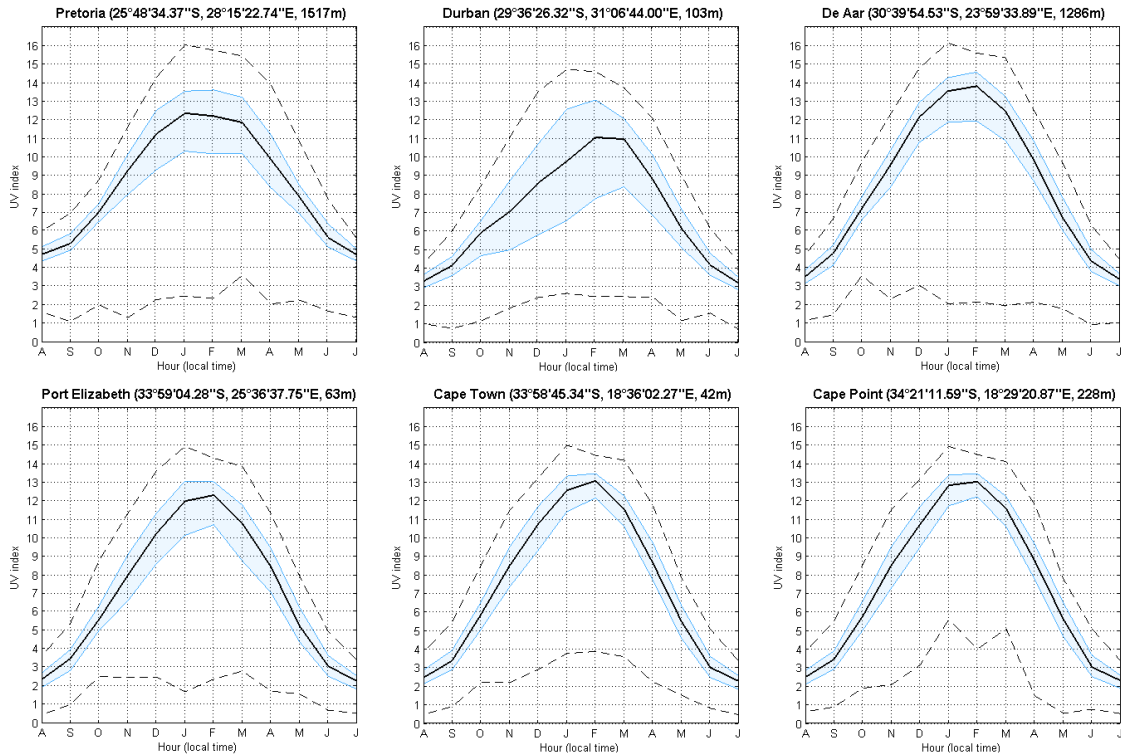
Figure 6. Monthly climatological median (black line) of solar UVI for the six South African sites at satellite overpass time, for all years of observation (i.e., 1994–2015). Quantile 25 and 75 (filled blue lines) and minimum and maximum (black dash line) are also represented.

3.3. Comparison of Ground-Based and Satellite-Derived Solar UVR Data

Ground-based UV index measurements at satellite overpass time were compared with those derived from the satellite OMI measurements for the six South African sites and for the period 2005–2015 (**Figure 7**). A similarity in the timing patterns of seasonal peaks is apparent in the two datasets.

A visual comparison shows large differences for certain periods of time between the instruments. For example, at Cape Town in 2007, a new logger was used. At De Aar, in February 2007 the logger was changed because of lightning damage. At Pretoria, in 2013, the amplitude increases suddenly because of the roof was painted silver, although the sinusoidal pattern is preserved.

Correlation analysis confirmed a positive correlation between the two datasets (**Figure 8**) where R^2 values ranged from a moderate correlation co-efficient of 0.71 for Pretoria, to a strong correlation co-efficient of 0.88 for Durban (**Table 2**). These high correlations are due to the dominating annual course of the two datasets. The MAPE between the two datasets tended to be between 22% and 28%, 46% for De Aar. Hence, the ground-based UV index observations are in good agreement with satellite measurement, except for De Aar where ground-based observations are higher (**Figure 9**).
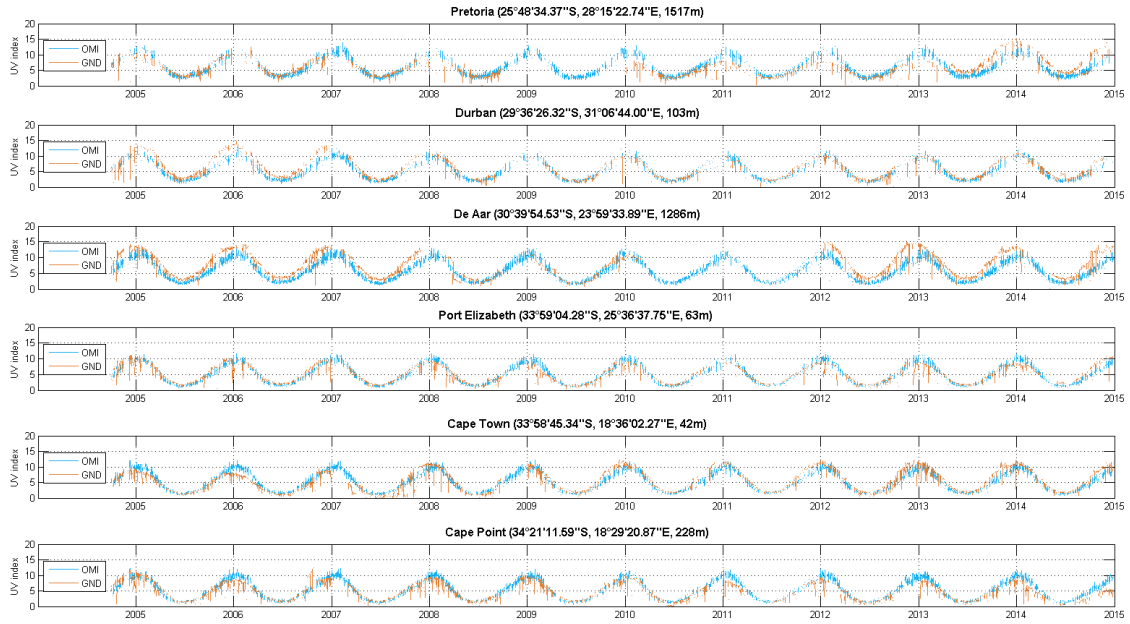
Figure 7. Time series comparing ground-based versus satellite-derived solar UV index data for 2005 to 2015 at satellite overpass time (the comparison was performed at the satellite overpass time and only clear sky days are selected with LER).
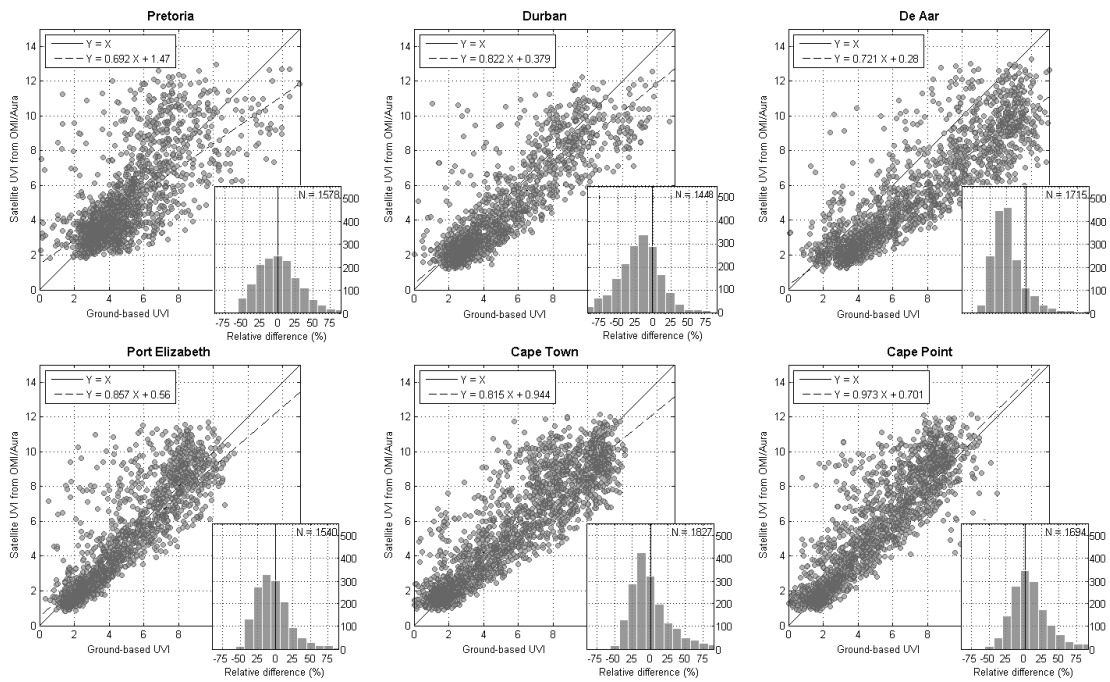
Figure 8. Correlation between the ground-based UV index and satellite-derived UV index data for 2005 to 2015 at the six South African sites at satellite overpass time. The six inserted histograms show the relative difference between the two datasets by the number of observations for each respective site (the comparison was performed at the satellite overpass time and only clear sky days are selected with LER).

Variability is evident in the year-over-year analyses of MAPE, standard deviation, and RMSE. The yearly MAPE range from 15% to 30%, except for De Aar, where a 60% MAPE can be reached. A relatively constant bias is observed at Port Elizabeth around 15%. At the Pretoria station, the bias

decreases significantly in 2013 because of a change of surface albedo (this effect is considered to have reduced since 2015 with fading of the roof paint). The daily percentage RMSE values by year also varied across years and sites, but generally stayed within the 30% range (**Figure 9c**). The largest change in correlation percentage (25%) is obtained for Pretoria from 2007 onwards.

Table 2. Summary validation statistics for overpass UV index values (all available years) including bias, RMSE, and R^2 values for the comparison of ground-based solar UVR and satellite-derived solar UVR (statistics computed only for clear sky day selected with LER).

Site	Number of Observation	Bias	MAPE	Median	SD [#1]	RMSE	R² Value	p Value [#2]
	n	UVI	%	UVI	UVI	UVI	%	p
Pretoria	1578	−0.15	27.3	0.15	1.93	1.93	71.0	<0.001
Durban	1448	−0.59	28.8	0.59	1.48	1.57	88.5	<0.001
De Aar	1715	−1.73	46.5	1.67	1.85	2.57	87.9	<0.001
Port Elizabeth	1540	−0.19	23.1	0.34	1.46	1.46	84.9	<0.001
Cape Town	1827	−0.12	24.6	0.18	1.57	1.58	88.4	<0.001
Cape Point	1694	0.57	22.2	−0.28	1.51	1.62	87.4	<0.001

Note: #1: Standard deviation; #2: A *p*-value provides an indication of the level of statistical significance, $p < 0.001$ shows there is less than a 1 in a 1000 chance of the statistics computed in Table 2 being incorrect based on observed error.

4. Discussion

The aim of this study is to compare ground-based and satellite-derived UV index measurements at six South African sites. Two objectives were identified. When comparing the solar UV index measurements made by the ground-based stations versus the satellite-derived estimates, the correlation analyses showed that the two datasets were in good agreement with each other for most sites and time periods with an annual systematic bias (noted to be low at times). It is well known that satellite-derived solar UVR data have limitations, particularly for sites that are cloudy, polluted, and/or loaded with aerosols. In our study this was evident at the De Aar station. Additional data on factors influencing solar UVR are needed to compute the true ground-based solar UV index levels, to detail the comparison for sites with high bias, or improve the comparison for others. For example, if high resolution and quality cloud data were available at the ground-based stations, one could detect clear-sky days and compare clear-sky ground-based data with clear-sky satellite-derived data for solar UVR. However, cloud data are not routinely collected at the ground-based stations, hence, this subset of ground-based clear-sky solar UVR data cannot be determined.

Otherwise, we used the TUV model as another method of comparison. Ozone from the OMI satellite and the aerosol optical depth from MODIS were used as input parameters. The comparison between the UV index from the TUV model and the UV index from the OMI shows less than 5% of MAPE. The UV index from modelling does not provide more information for our study.

The UV biometers are not manufactured with an intention of use for long-term trend analysis [29]. They are ideally suited to provide an indication of the UV index for public exposure assessment, risk awareness, and excess sun exposure prevention messaging. Hence, the intention here is not to detect long-term trends, but rather to compare our time-series to satellite observations and determine seasonal variability at different locations depending on longitude and altitude. However, there are subtle signs that the solar UV index levels at ground-based stations in South Africa have changed over the network measurement period. The raw data suggests that the intensity of the solar UV index is not consistent year-over-year; however, the pattern of change is irregular and it is impossible to make a definitive statement about any clear trend over time. This is shown by the monthly mean of the ground-based UV index (**Figure 10**) where one can identify an irregular pattern.
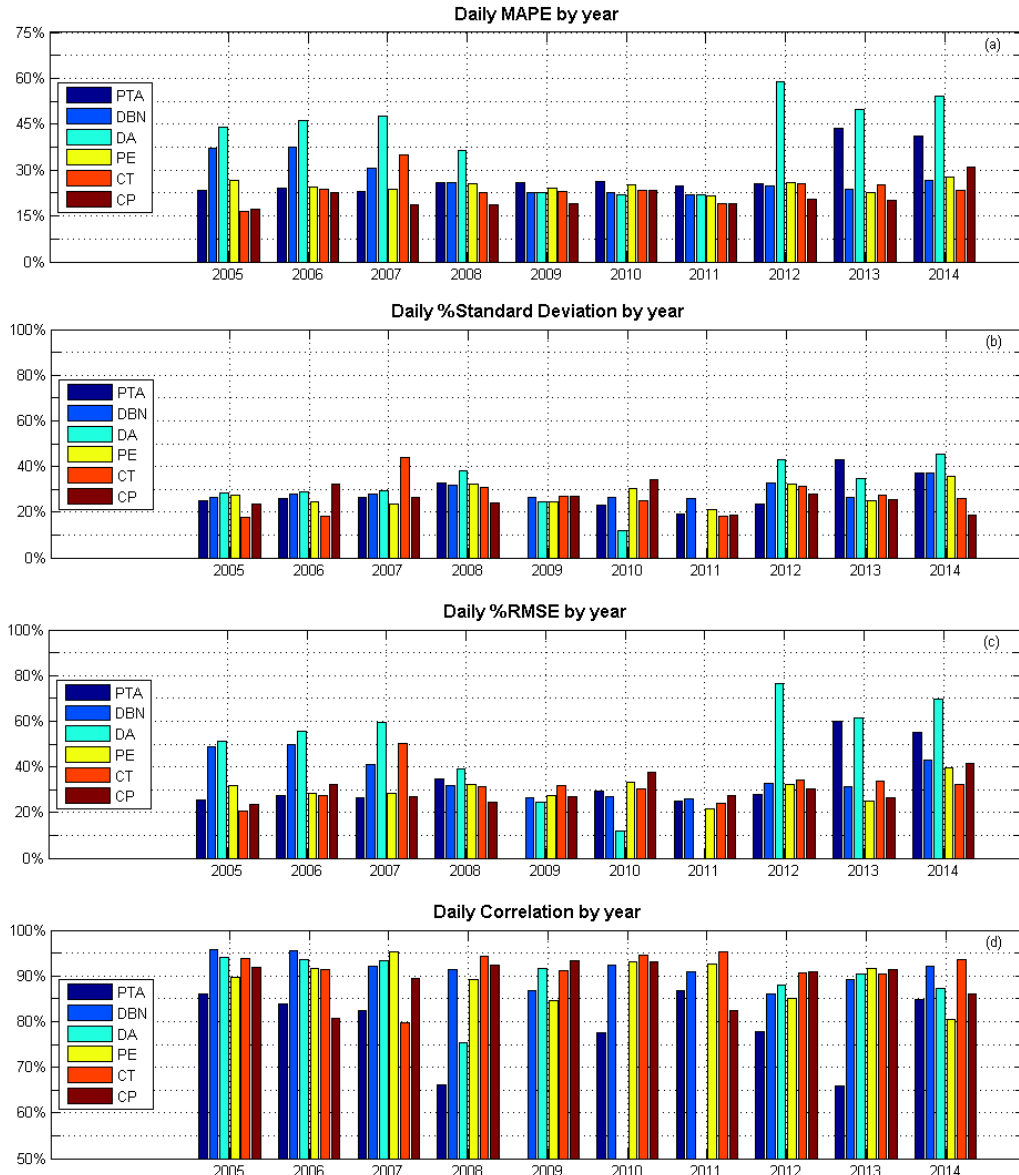
Figure 9. Year-on-year validation statistics for daily clear sky satellite overpass time UV index values at each of the six sites: Cape Point (CP), Cape Town (CT), Durban (DBN), De Aar (DA), Port Elizabeth (PE), and Pretoria (PTA), where (a) shows the daily MAPE by year; (b) the daily percentage standard deviation by year; (c) daily percentage RMSE; and (d) daily percentage correlation by year.

This relative difference may be explained by several factors including:

- OMI resolution can be a factor of this difference. Indeed, OMI data are integrated on a pixel of $1° × 1°$ (square of 110 km). In a region where cloud cover changes widely, it can quickly appear as a large difference with local data. A $1° × 1°$ pixel can also include a mountain and it is not taking into consideration the surface albedo, which may also have an effect [10,21,30,31]. This is evident at Cape Town and Cape Point stations. Ground-based observations show an evident difference, but this difference is transparent to the satellite.
- Ozone measured by OMI is an important factor of UVR variation. However, a recent study shows that the OMI satellite evaluates the total ozone at less than 5% accuracy in the South African region [32,33].

- Aerosols play an important part in the UVR response [30]. Global climatological aerosol datasets are used in OMI processing, but this is likely not relevant for an isolated, relatively clear site, like De Aar station, although wind-blown dust may be a factor.

We cannot prove which one, between ground-based and satellite datasets, is responsible for the large difference without additional high-grade solar UVR measurements, for example using Kipp and Zonen UVS-AB-T UV radiometers [28], being made alongside the UV biometers. Recently, the South African Weather Service, together with its partners, installed UVA/UVB radiometers at several sites as part of a solar radiation network. These instruments provide reliable data at high resolution and are strictly calibrated and maintained. It is anticipated that they will provide good quality data for future analyses.
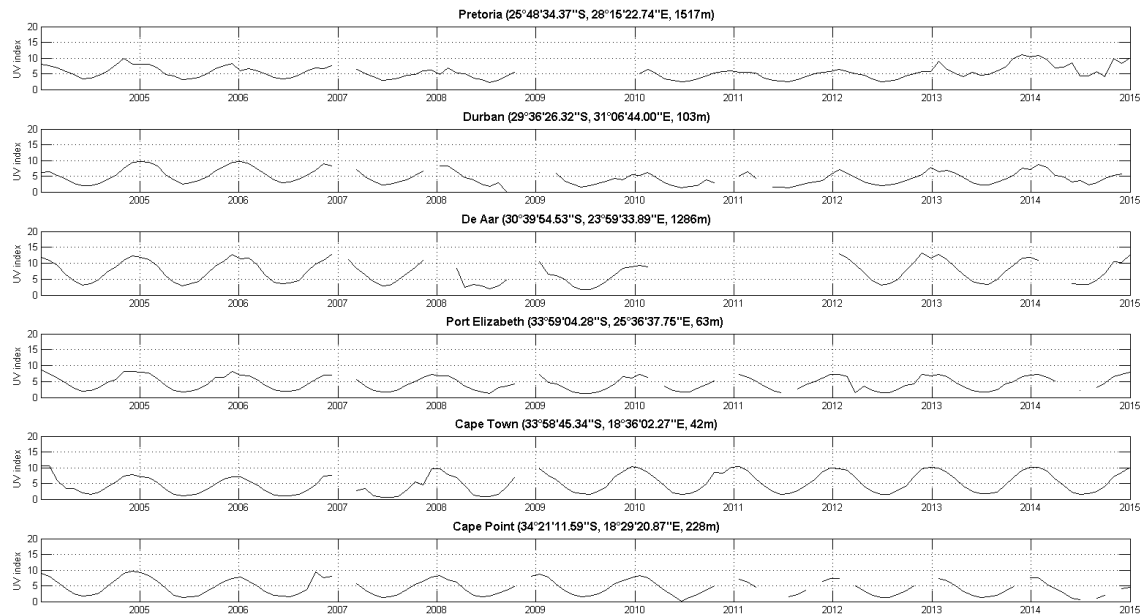
Figure 10. Ground-based monthly mean UV indices from 2004 to 2015 for the six South African sites.

5. Conclusions

In this paper we analysed ground-based UV indices recorded during the 1994–2015 period (more than two decades) by the SAWS (South African Weather Service) at six sites at different latitudes. In fact, South Africa has been measuring solar UVR to raise awareness about the impacts of the solar UV index on human health.

The SAWS UV index observations are based on the use of UV-biometers and the six datasets are not homogeneous in terms of time coverage and observations (Table 1). However, the present work is an exploratory study. It is based on the comparison with satellite UV index measurements from the OMI/AURA experiment. We found that relative UV index differences between ground-based and satellite-derived data range from 0% to 45%, depending on the site and year. Overall, there was a good agreement (absolute difference within ±25%) between South African ground-based station solar UV measurements and satellite-derived data from OMI/Aura, except for one station where an important bias is found. Most of the time, these differences appear in the winter, which emphasizes the importance of the annual cycle, in conjunction with altitude and latitude effects clearly underlined in our study on the UV index in South Africa.

Some of our ground-based stations' data showed close agreement with satellite-derived UV index values. However, it should be noted that previous works showed that satellite-derived data can be overestimated by 11% [10], while free cloud filtering can also be improved by using different methods based on UV irradiance [15,34,35].

The ground-based instruments are not intended for long-term trend analysis; instead, they provide UV index information for public awareness, and some weak signs suggest such long-term trends may exist in our ground-based data. In future works we will study the variability and trends of the UV index in South Africa.

Author Contributions: "K.N. (Katlego Ncongwane) and G.J.R.C. (Gerrie J.R. Coetzee) provided data and expertise; J.C. (Jean-Maurice Cadet) and K.L. (Kévin Lamy) performed data processing; All authors analyzed the data; J.C. (Jean-Maurice Cadet), H.B. (Hassan Bencherif), T.P. (Thierry Portafaix) and C.Y.W. (Caradee Y. Wright) wrote the paper."

Conflicts of Interest: The authors declare no conflict of interest.

References

1. Diffey, B.L. Solar ultraviolet radiation effects on biological systems. *Phys. Med. Biol.* **1991**, *36*, 299–328.
2. International Commission on Non-Ionizing Radiation Protection. Guidelines on limits of exposure to ultraviolet radiation of wavelengths between 180 nm and 400 nm. *Health Phys.* **2004**, *87*, 171–186.
3. McKinlay, A.F.; Diffey, B.L. A reference action spectrum for ultraviolet induced erythema in human skin. *CIE J.* **1989**, *6*, 17–22.
4. WHO Report. *Global Solar UV Index*; *A Practical Guide;* World Health Organization: Geneva, Switzerland, 2002. Available online: http://www.who.int/uv/publications/en/UVIGuide.pdf (accessed on 25/10/2017).
5. Von Schirnding, Y.; Strauss, N.; Mathee, A.; Robertson, P.; Blignaut, R. Sunscreen use and environmental awareness among beach-goers in Cape Town, South African. *Public Health Rev.* **1991–1992**, *19*, 209–217.
6. Sitas, F. Histologically diagnosed cancers in South Africa, 1988. *S. Afr. Med. J.* **1994**, *84*, 344–348.
7. Bodeker, G.E.; Scourfield, M.W.J. Estimated past and future variability in UV radiation in South Africa based on trends in total column ozone. *S. Afr. J. Sci.* **1998**, *94*, 24–33.
8. Prause, A.R.; Scourfield, M.W.J. Surface erythema irradiance and total column ozone above Durban, South Africa, for the period 1996–1998. *S. Afr. J. Sci.* **2002**, *98*, 186–188.
9. Brogniez, C.; Auriol, F.; Deroo, C.; Arola, A.; Kujanpää, J.; Sauvage, B.; Kalakoski, N.; Pitkänen, M.R.A.; Catalfamo, M.; Metzger, J.-M.; et al. Validation of satellite-based noontime UVI with NDACC ground-based instruments: Influence of topography, environment and satellite overpass time. *Atmos. Chem. Phys.* **2016**, *16*, 15049–15074.
10. Bernhard, G.; Arola, A.; Dahlback, A.; Fioletov, V.; Heikkilä, A.; Johnsen, B.; Koskela, T.; Lakkala, K.; Svendby, T.; Tamminen, J. Comparison of OMI UV observations with ground-based measurements at high northern latitudes. *Atmos. Chem. Phys.* **2015**, *15*, 7391–7412.
11. Jégou, F.; Godin-Beekman, S.; Corrrea, M.P.; Brogniez, C.; Auriol, F.; Peuch, V.H.; Haefffelin, M.; Pazmino, A.; Saiag, P.; Goutail, F.; et al. Validity of satellite measurements used for the monitoring of UV radiation risk on health. *Atmos. Chem. Phys.* **2011**, *11*, 13377–13394.
12. Kazadzis, S.; Bais, A.; Arola, A.; Krotkov, N.; Kouremeti, N.; Meleti, C. Ozone Monitoring Instrument spectral UV irradiance products: Comparison with ground based measurements at an urban environment. *Atmos. Chem. Phys.* **2009**, *9*, 585–594.
13. Madronich, S.; Mayer, B.; Fischer, C.A. *A Climatology of Erythemal Ultraviolet Radiation, 1979–1992*; NATO Advanced Study Institute (ASI), Chemistry and Radiation Changes in the Ozone Layer: Lokympari, Crete, Greece, 1999.
14. Varotsos, C. Solar ultraviolet radiation and total ozone, as derived from satellite and ground-based instrumentation. *Geophys. Res. Lett.* **1994**, *21*, 1787–1790.
15. Zempila, M.M.; Koukouli, M.E.; Bais, A.; Fountoulakis, I.; Arola, A.; Kouremeti, N.; Balis, D. OMI/Aura UV product validation using NILU-UV ground-based measurements in Thessaloniki, Greece. *Atmos. Environ.* **2016**, *140*, 283–297.

16. Janjai, S.; Wisitsirikun, S.; Buntoung, S.; Pattarapanitchai, S.; Wattan, R.; Masiri, I.; Bhattarai, B.K. Comparison of UV index from Ozone Monitoring Instrument (OMI) with multi-channel filter radiometers at four sites in the tropics: Effects of aerosols and clouds. *Int. J. Climatol.* **2014**, *34*, 453–461.

17. Fan, L.; Li, W.; Dahlback, A.; Stamnes, J.J.; Stamnes, S.; Stamnes, K. Long-term comparisons of UV index values derived from a NILU-UV instrument, NWS, and OMI in the New York area. *Appl. Opt.* **2015**, *54*, 1945–1951.

18. Kerr, J.B.; Seckmeyer, G.; Bais, A.F.; Bernhard, G.; Blumthaler, M.; Diaz, S.B.; Krotkov, N.; Lubin, D.; McKenzie, R.L.; Sabziparvar, A.A.; et al. Surface ultraviolet radiation: Past and future, Chapter 5. In *Scientific Assessment of Ozone Depletion*; 2002. Available online: https://acd-ext.gsfc.nasa.gov/Documents/O3_Assessments/Docs/WMO_2002/10_chapter5.pdf (accessed on 25/10/2017).

19. Seckmeyer, G.; Bais, A.; Bernhard, G.; Blumthaler, M.; Booth, C.R.; Lantz, K.; Webb, A. *Instruments to Measure Solar Ultraviolet Radiation. Part 2: Broadband Instruments Measuring Erythemally Weighted Solar Irradiance*; WOM-GAW Report; World Meteorological Organization (WMO): Geneva, Switzerland, 2005.

20. McKenzie, R.; Smale, D.; Kotkamp, M. Relationship between UVB and erythemally weighted radiation. *Photochem. Photobiol. Sci.* **2004**, *3*, 252–256.

21. Ozone Monitoring Instrument (OMI). *OMI Algorithm Theoretical Basis Document Version III*; Stammes, P., Noordhoek, R., Eds.; ATBD-OMI-03, Version 2.0, August 2002; Ozone Monitoring Instrument: Netherlands's Agency for Aerospace Programs (NIVR), Netherland, and Finnish Meteorological Institute (FMI), Finland, 2002. Available online: http://eospso.gsfc.nasa.gov/sites/default/files/atbd/ATBD-OMI-03.pdf (accessed on 25/10/2017).

22. Arola, A.; Kazadzis, S.; Lindfors, A.; Krotkov, N.; Kujanpää, N.; Tamminen, J.; Bais, A.; di Sarra, A.; Villaplana, J.M.; Brogniez, C.; et al. A new approach for absorbing aerosols in OMI UV. *Geophys. Res. Lett.* **2009**, *36*, L22805, doi:10.1029/2009GL041137.

23. Giovanni platform, NASA Earth Data, Available online :https://giovanni.gsfc.nasa.gov/giovanni/ (accessed on 08/11/2017)

24. Ozone Monitoring Instrument (OMI) team. *Data User's Guide*; Ozone Monitoring Instrument (OMI): Netherlands's Agency for Aerospace Programs (NIVR), Netherland, and Finnish Meteorological Institute (FMI), Finland, 2012.

25. Antón, M.; Cachorro, V.E.; Vilaplana, J.M.; Toledano, C.; Krotkov, N.A.; Arola, A.; Serrano, A.; de la Morena, B. Comparison of UV irradiances from Aura/Ozone Monitoring Instrument (OMI) with Brewer measurements at El Arenosillo (Spain)—Part 1: Analysis of parameter influence. *Atmos. Chem. Phys.* **2010**, *10*, 5979–5989.

26. Wright, C.Y.; Coetzee, G.; Ncongwane, K. Ambient solar UV radiation and seasonal trends in potential sunburn risk among schoolchildren in South Africa. *S. Afr. J. Child Health* **2011**, *5*, 33–38.

27. Ncongwane, K.P. Erythemally-Weighted UV Radiation Measurements at Six South African Sites. Master Thesis, University of KwaZulu-Natal, Durban, South Africa, 2015.

28. Ncongwane, K.; Coetzee, G. A quantitative analysis of the SAWS GAW UV network and data since 1994. In Proceedings of the South African Society for Atmospheric Sciences Conference (SASAS), Gariep Dam, South Africa, 20-22 September 2010; pp. 20–22.

29. McKenzie, R.; Kotkamp, M.; Seckmeyer, G.; Erb, R.; Roy, C.R.; Gies, H.P.; Toomey, S.J. First southern hemisphere intercomparison of measured solar UV spectra. *Geophys. Res. Lett.* **1993**, *20*, 2223–2226.

30. Kazadzis, S.; Bais, A.; Kouremeti, N.; Zemplila, M.; Arola, A.; Giannakaki, E.; Amiridis, V.; Kazantzidis, A. Spatial and temporal UV irradiance and aerosol variability within the area of an OMI Satellite pixel. *Atmos. Chem. Phys.* **2009**, *9*, 4593–4601.

31. Weihs, P.; Blumthaler, M.; Rieder, H.E.; Kreuter, A.; Simic, S.; Laube, W.; Schmalwieser, A.W.; Wagner, J.E.; Tanskanen, A. Measurements of UV irradiance within the area of one satellite pixel. *Atmos. Chem. Phys.* **2008**, *8*, 5615–5626.

32. Toihir, A.M.; Bencherif, H.; Sivakumar, V.; Amraoui, L.E.; Portafaix, T.; Mbatha, N. Comparison of total column ozone obtained by the IASI-MetOp satellite with ground-based and OMI satellite observations in the southern tropics subtropics. *Ann. Geophys.* **2015**, *33*, 1135–1146.

33. Buchard, V.; Brogniez, C.; Auriol, F.; Bonnel, B.; Lenoble, J.; Tanskanen, A.; Bojkov, B.; Veefkind, P. Comparison of OMI ozone and UV irradiance data with ground-based measurements at two French sites. *Atmos. Chem. Phys.* **2008**, *8*, 4517–4528.

34. Zempila, M.M.; Giannaros, T.M.; Bais, A.; Melas, D.; Kazantzidis, A. Evaluation of WRF shortwave radiation parameterizations in predicting Global Horizontal Irradiance in Greece. *Renew. Energy* **2016**, *86*, 831–840.

35. Vasaras, A.; Bais, A.F.; Feister, U.; Zerefos, C.S. Comparison of two methods for cloud flagging of spectral UV measurements. *Atmos. Res.* **2001**, *57*, 31–42.

International Journal of
Environmental Research and Public Health

an Open Access Journal by MDPI

Indexed in: **PubMed**

CITESCORE **2.81** SCOPUS

IMPACT FACTOR 2.468

CERTIFICATE OF PUBLICATION

Certificate of publication for the article titled:

Comparison of Ground-Based and Satellite-Derived Solar UV Index Levels at Six South African Sites

Authored by:

Jean-Maurice Cadet; Hassan Bencherif; Thierry Portafaix; Kévin Lamy; Katlego Ncongwane; Gerrie J. R. Coetzee; Caradee Y. Wright

Published in:

Int. J. Environ. Res. Public Health **2017**, Volume 14, Issue 11, 1384

MDPI
Academic Open Access Publishing
since 1996

Basel, April 2020

Chapitre 4 CLIMATOLOGIE DU RAYONNEMENT UV

4.1 ARTICLE : RESUME

Le suivi du rayonnement ultraviolet est très important. En effet, celui-ci dépend de nombreux paramètres atmosphériques et par ailleurs, influe directement sur la biosphère terrestre, en particulier sur la santé humaine. Le rayonnement ultraviolet n'agit pas de la même manière en fonction des individus, dépendant de leur phototype. Le phototype caractérise la sensibilité de la peau lors d'une exposition au rayonnement solaire. Par définition, on trouve 6 phototypes. Le phototype 1 est extrêmement sensible au rayonnement UV solaire, alors que le phototype 6 est le moins sensible.

Cette étude présente les résultats d'un calcul de moyennes climatologiques sur une période de 10 ans, ainsi qu'une étude de tendance à Saint-Denis, La Réunion et au Cape, Afrique du Sud. Les données d'un spectromètre Bentham DTMc300 ont été utilisées pour Saint-Denis, et ceux d'un Solar Light SL501 pour Le Cape. Parallèlement, des mesures d'exposition ont été réalisées à La Réunion et au Cape dans des sites touristiques fréquentés, où la population est susceptible d'être très exposée.

L'étude climatologie pour ces 2 sites, Saint-Denis et le Cape, a révélé des niveaux d'exposition extrêmes. En effet, les doses cumulées peuvent atteindre 30 et 15 SED respectivement en hivers, et peuvent aller jusqu'à 80 SED en été. Dans le cas de Saint-Denis, le rayonnement UV est au moins modéré (WHO (World Health Organization), 2002) toute l'année et est extrême 80% du temps entre novembre et mars. Pour Le Cape, les niveaux d'UV sont faibles en hivers et 80% du temps en été, entre décembre et janvier. On note une plus grand dispersion des doses UV, principalement due à la nébulosité qui très variable à la Réunion.

L'analyse des tendances pour ces 2 sites a révélé des comportements : une augmentation de 3.7% et une diminution de 3.6%, respectivement. Cependant, l'analyse de ces résultats doit prendre en compte le fait que pour Saint-Denis, il y a 38% de données manquantes. Aussi, la différence en longueurs d'onde entre les 2 instruments peut induire des erreurs. En effet, le Solar Light SL501 ne mesurant le rayonnement qu'entre 280 et 340 nm, des coefficients de correction doivent être appliqués. Ces coefficients ne dépendent que de l'ozone total et de l'angle solaire zénithal. Un changement de paramètre atmosphérique tel que les aérosols ou la couverture nuageuse peut donc engendre un biais dans le calcul de tendance. Une étude

récente (Toihir, et al., 2018) montre qu'il n'y a pas de changement significatif de l'ozone au-dessus de La Réunion. Un changement de nébulosité liée à l'augmentation de la température des océans est cependant une explication possible de la tendance obtenue à Saint-Denis. La tendance au Cape peut être expliquée par l'augmentation du niveau d'aérosols lié à l'activité anthropogénique et aux feux de biomasse.

Des mesures d'exposition au rayonnement ultraviolet dans des sites touristiques en altitude ont été effectuées. A la Réunion, les mesures ont été faites sur la randonnée Maïdo-Grand Bénare (2168m – 2898m d'altitude) et en Afrique du Sud, sur la randonnée de Table Mountain (380m – 1035m d'altitude). Il a été trouvé un cumul de 64 SED et 40 SED respectivement. Ces doses correspondent à de multiples fois la dose minimale érythémale pour chaque phototype (par exemple : 30 fois la dose minimale érythémale pour un phototype 1). Ces résultats soulignent l'extrême importance de la sensibilisation de la population face au risque UV, ce risque étant accru en altitude. A la Réunion, il n'existe aucun message d'alerte face au danger du rayonnement ultraviolet pour des activités en extérieur. La Réunion étant une île montagneuse réputée pour ces circuits de randonnées, un grand nombre d'activités se font en altitude.

4.2 ARTICLE : CADET ET AL., 2019 (ATMOS.)

Article ci-dessous publié le 1er octobre 2019 dans Atmosphere disponible sur :

https://www.mdpi.com/545770

atmosphere

MDPI

Article

Solar UV Radiation in Saint-Denis, La Réunion and Cape Town, South Africa: 10 years Climatology and Human Exposure Assessment at Altitude

Jean-Maurice Cadet [1,*], Hassan Bencherif [1,2], David J. du Preez [3], Thierry Portafaix [1], Nathalie Sultan-Bichat [4], Matthias Belus [5], Colette Brogniez [6], Frederique Auriol [6], Jean-Marc Metzger [7], Katlego Ncongwane [8], Gerrie J. R. Coetzee [8] and Caradee Y. Wright [3,9]

[1] LACy, Laboratoire de l'Atmosphère et des Cyclones (UMR 8105 CNRS, Université de La Réunion, Météo-France), Saint-Denis de La Réunion 97744, France; jean.cadet@univ-reunion.fr (J.M.C.); hassan.bencherif@univ-reunion.fr (H.B.); thierry.portafaix@uiv-reunion.fr (T.P.);

[2] School of Chemistry and Physics, University of KwaZulu-Natal, Durban 4041, South Africa

[3] Department of Geography, Geoinformatics and Meteorology, University of Pretoria, Pretoria 0002, South Africa; dupreez.jd@gmail.com (D.J.D.P.); caradee.wright@mrc.ac.za (C.Y.W.);

[4] Centre Hospitalier Ouest Réunion, Service Dermatologie, 5 impasse Plaine Chabier, Le grand pourpier sud, 97460, Saint-Paul, Réunion, France; sultanbichat.n@ch-gmartin.fr (N.S.B.);

[5] Conseil Régional de la Réunion, 5 Avenue René Cassin, Sainte-Clotilde, 97490, La Réunion, France ; matthias.belus@cr-reunion.fr (M.B.);

[6] Université Lille, CNRS, UMR 8518, Laboratoire d'Optique Atmosphérique, F-59000 Lille, France; colette.brogniez@univ-lille.fr (C.B.); frederique.auriol@univ-lille.fr (F.A.);

[7] Observatoire des Sciences de l'Univers de la Réunion, UMS3365, 97744 Saint-Denis de la Réunion, France; jean-marc.metzger@univ-reunion.fr (J.M.M.)

[8] SAWS, South African Weather Service, Private Bag X097, Pretoria 0001, South Africa; katlego.ncongwane@weather.co.za (K.N.); gerrie.coetzee@weathersa.co.za (G.J.R.C.);

[9] Environment and Health Research Unit, South African Medical Research Council, Pretoria 0001, South Africa; caradee.wright@mrc.ac.za (C.Y.W.);

* Correspondence: jean.cadet@univ-reunion.fr; Tel.: +262-692-93-82-97

Abstract: Solar ultraviolet radiation (UVR) monitoring is important since it depends on several atmospheric parameters which are associated with climate change and since excess solar UVR exposure and has significant impacts on human health and wellbeing. The objective of this study was to investigate the trends in solar UVR during a decade (2009–2018) in Saint-Denis, Reunion Island (20.9°S, 55.5°E, 85 m ASL) and Cape Town, South Africa (33.97°S, 18.6°E, 42 m ASL). This comparison was done using total daily erythema exposure as derived from UVR sensors continuously at both sites. Climatology over the 10-year period showed extreme UVR exposure for both sites. Slight changes with opposite trends were found, +3.6% at Saint-Denis and −3.7% at Cape Town. However, these two sites often experience extreme weather conditions thereby making the trend evaluation difficult. Human exposure assessment was performed for hiking activities at two popular high-altitude hiking trails on the Maïdo–Grand Bénare (Reunion) and Table Mountain (Cape Town) with a handheld radiometer. Extreme exposure doses of 64 SED and 40 SED (Standard Erythemal Dose, 1 SED = 100 J.m^{-2}) were recorded, respectively. These high exposure doses highlight the importance of raising public awareness on the risk related to excess UVR exposure at tourist sites, especially those at high altitude.

1. Introduction

The effects of ultraviolet radiation (UVR) on humans are well known today and depend on several factors including atmospheric variables influencing the amount of surface solar UVR such as cloud cover and altitude, as well as skin phototype which determines the individual risk to excess solar UVR [1]. The Fitzpatrick Skin Phototype classification (**Table 1**) [2] is commonly used and classifies skin phototypes as a function of their characteristics and sunburn susceptibility. The harmful effects of excess ultraviolet (UV) exposure include sunburn, skin cancer, cataracts, and ocular melanoma [3,4]. About 90% of skin-related health impacts are related to UVR exposure [5]. In South Africa, the melanoma rate is stable at 5 and 3 cases per 100,000 persons (computed for a world standard population) for males and females, respectively [6]. Even though statistics are not deemed comprehensive, a possible increasing trend is evident for invasive melanoma from 2006 to 2015 for La Reunion [7]. For 2006 to 2015, in a male standard population, the increase was 2.7 to 7.1 cases per 100,000 persons and 3.0 to 6.1 cases per 100,000 persons in a female standard population [8]. Human behaviour change is another important factor influencing solar UVR exposure and subsequent ill health effects [9]. In a social context in which people spend time outdoors and expose themselves to the sun, public awareness and skin cancer prevention campaigns are crucial.

This study focused on understanding total daily UVR exposure doses in Saint-Denis, Reunion Island and in Cape Town, South Africa. Firstly, UVR exposure dose was analyzed from a climatological point of view and then, by focusing on the trend over a 10-year period from 2009 to 2018. Secondly, results from two case studies that measured ambient solar UVR exposure at points along popular hiking sites located at altitude are presented.

Table 1. Skin phototype classification [1].

Phototype	Characteristics	History of Sunburn	Minimal Dose to Elicit Sunburn (SED)
I	Ivory white skin, light eyes	Burns easily	2-3
II	White skin, hazel/brown eyes	Burns easily	2.5-3
III	White skin, brown eyes	Burns moderately	3-5
IV	Lightly skin, dark eyes	Burns minimally	4.5-6
V	Moderate brown skin, dark eyes	Rarely Burns	6-20
VI	Strong brown/black skin, dark eyes	Never burns	6-20

2. Experiments

2.1. UV Instruments

2.1.1. Ground-Based UVR Instrument at Saint-Denis

UVR is recorded at Saint-Denis on the roof of the Laboratoire de l'Atmosphère et des Cyclones (20.9°S, 55.5°E, 85 m ASL, **Figure 1**). The instrument is a double-monochromator Bentham DTMc300 provided by Bentham Instrument Ltd. Co. (United Kingdom). Since February 2009, UV irradiance between 280 nm and 400 nm is sampled in 0.5 nm increments every 15-minutes. The instrument is calibrated every three months, a 150 W and a 1000 W tungsten-halogen lamp are used for spectral calibration and a software tool developed at Laboratoire d'Optique Atmosphérique is used for the

wavelength misalignment correction [10]. These lamps are traceable to the National Institute of Standards and Technology (NIST). The UV Index (UVI) is calculated following standard formula and standard erythemal action spectrum [11]. The UVR doses are extracted from UVI using Equation 1:

$$UVd = \sum_i \frac{\Delta t \times UVindex}{40 \times 100},$$ (1)

where UVd is the daily dose and Δt the interval time between two measurements. The UVI uncertainty has recently been estimated to be 5% [10]. This instrument is affiliated with the Network for the Detection of Atmospheric Composition Change (NDACC). A parametric and sensitivity study has been done by Lamy et al., 2018 [12] on Tropospheric Ultraviolet and Visible Model (TUV) at Saint-Denis. Ground-based and satellite data was used for clear sky UVI modelling and a relative difference of 0.5% was found with UVI from the Bentham DTMc300 (Bentham Instruments Ltd, Berkshire, UK).

2.1.2. Ground-based UVR instrument at Cape Town

The South African Weather Service (SAWS) maintains a network of six broadband radiometers (280–340 nm) in South Africa. The Cape Town station is located at the Cape Town International Airport (33.97°S, 18.6°E, 42 m ASL, **Figure 1**).
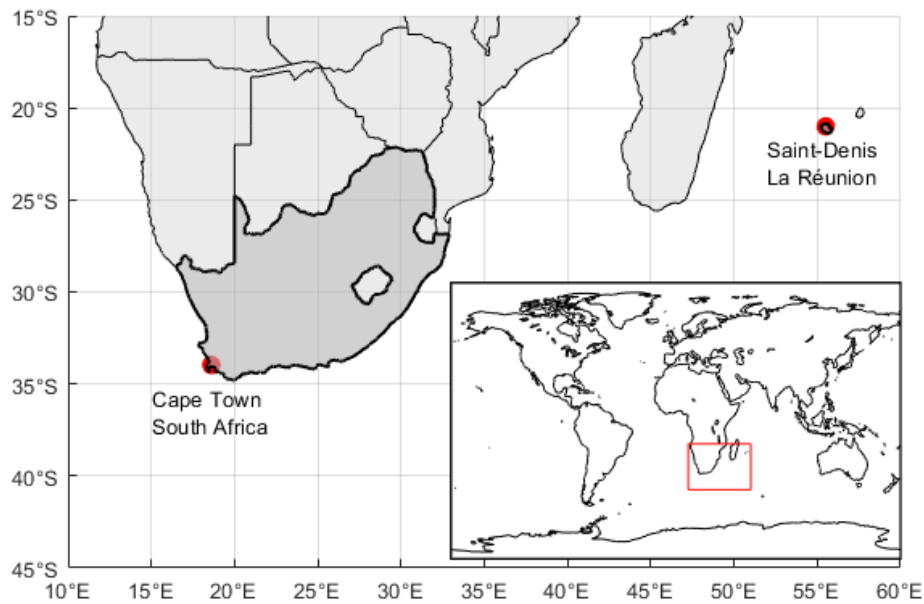
Figure 1. Geographical locations of Saint-Denis and Cape Town ground-based solar ultraviolet radiation (UVR) measurement sites.

The instrument is a UV-biometer model 501 (SN#10414) manufactured by Solar Light Company, Inc. (Glenside, PA, United States). Erythemal UVR is recorded hourly in Minimal Erythemal Dose (MED) unit by a GaAsP diode, where 1 MED is set to 210 J.m^{-2} [-]. UVR doses are calculated following Equation 2:

$$UVd = \sum_i UVm \times \frac{210}{100},$$ (2)

where UVd is the daily dose and UVm the one-hour cumulative dose in MED.

A generic table is used to correct the spectral response of the instrument, depending on total ozone and solar zenith angle [14,15]. In 2012, an inter-comparison was conducted with the SAWS

Solar Light SL-501 travelling standard instrument (SN#12010). This travelling standard instrument was calibrated at the Deutscher Wetterdienst (DWD, Germany) with spectroradiometer SPECTRO 320D NO 15 (Instrument Systems GmbH, Munich, Germany) and had traceability to the International Bureau of Weights and Measures (BIPM). The Cape Town biometer accuracy was estimated to be 8% [13].

2.1.3. Field UVR Instrument

The UVR instrument used for field measurements was the Solarmeter Model 6.5 UV Index Meter (SN#03692) from Solarmeter® (Glenside, PA, USA), a trademark of Solar Light Company Inc. This handheld instrument records erythemal weighted UV irradiance from 280 to 400 nm via a silicon carbide photodiode. UVI is provided with 10% manufacturer accuracy traceable to NIST. A previous inter-comparison campaign showed that this instrument has long-term stability and good agreement with a reference instrument (~ 5% bias) [16].

2.2. Methods and Statistical Analysis

The analyses were conducted using two variables: the daily cumulative UVR doses and the UVI, as the former provides an indication of human exposure and the latter provides UVR intensity.

2.2.1. Climatology Analysis

The climatological monthly mean of the total daily UVR dose was computed. Since daily total cumulative UVR dose in SED units was used, days with incomplete data were removed from the datasets. The monthly climatology mean, standard deviation, and box diagrams were computed. Then, the UVR intensity was analyzed by investigating the UVI threshold frequency using the UVI categories of low, moderate, high, very high, and extreme over the 10-year study period. In addition, the half-month maximum was used, following the World Health Organization (WHO) UVR exposure categories [17].

2.2.2. Trend Analysis

The second objective was to estimate the trend in UVR dose over the period of one decade. This was performed in two steps. The first year (2009) and the last year (2018) of the decade were compared. Correlation, bias, and standard deviation were computed using Equations 3, 4 and 5, respectively:

$$r = \frac{\sum_{i=1}^{n}\left(UVd_{2009,i} - \overline{UVd_{2009}}\right)\left(UVd_{2018,i} - \overline{UVd_{2018}}\right)}{\sqrt{\left(\sum_{i=1}^{n}\left(UVd_{2009,i} - \overline{UVd_{2009}}\right)^2\right)\left(\sum_{i=1}^{n}\left(UVd_{2018,i} - \overline{UVd_{2018}}\right)^2\right)}}, \tag{3}$$

$$Bias = \frac{1}{n}\sum_{i=1}^{n}\left(\frac{UVd_{2018,i} - UVd_{2009,i}}{UVd_{2009,i}}\right), \tag{4}$$

$$Std = \sqrt{\frac{1}{n-1}\sum_{i=1}^{n}\left(\left(\frac{UVd_{2018,i} - UVd_{2009,i}}{UVd_{2009,i}}\right) - Bias\right)^2}, \tag{5}$$

where *UVd* is the daily dose in SED unit, *r* the correlation coefficient, *n* the number of days.
Secondly, the evolution of UVR doses was analyzed for the decade using monthly mean values to reduce dispersion due to the influence of clouds. The trend was estimated from the difference between the monthly mean of daily doses and the climatological monthly mean of daily doses. Months without data were replaced using the monthly climatology mean. The trend analysis was

performed for the whole period and by season. Based on the least-squares method, the linear trend, and a 90% confidence interval were computed.

2.2.3. Case Study

Ambient erythemal UVR measurements were made at two popular hiking sites at relatively high altitude, namely, Maïdo–Grand Bénare (GB) hike in La Reunion and Table Mountain (TM) via Platteklip Gorge hike in Cape Town. TM in Cape Town is annually visited by approximately 800,000 people. The UVI was recorded by volunteers with the handheld Solarmeter Model 6.5 every 10 min while hiking on the mountains, following the supplier measurement recommendations, and UVR doses were calculated using Equation 1 (above). This instrument and method have been used in a previous study [18]. While many environmental parameters can affect the direct and diffuse UVR here only the presence of cloud and topography [19,20] occulting the direct sun were visually recorded, even though the diffuse UV irradiance is an important part of the global irradiance [21].

The GB hike took place on the 2 December 2018 and the TM hike took place a week later on the 10 December 2018. Topographic maps and photos of the two study sites are shown in **Figure 2**. The two mountain hikes environments have short (<2 m height) or very little vegetation and therefore the presence of vegetation did not interfere with the measured UVR levels. At both sites, there was the direct sun for the full duration of the hikes. The diffuse UVR was likely reduced in the Platteklip gorge on the TM hike due to the proximity of the cliff in the gorge.
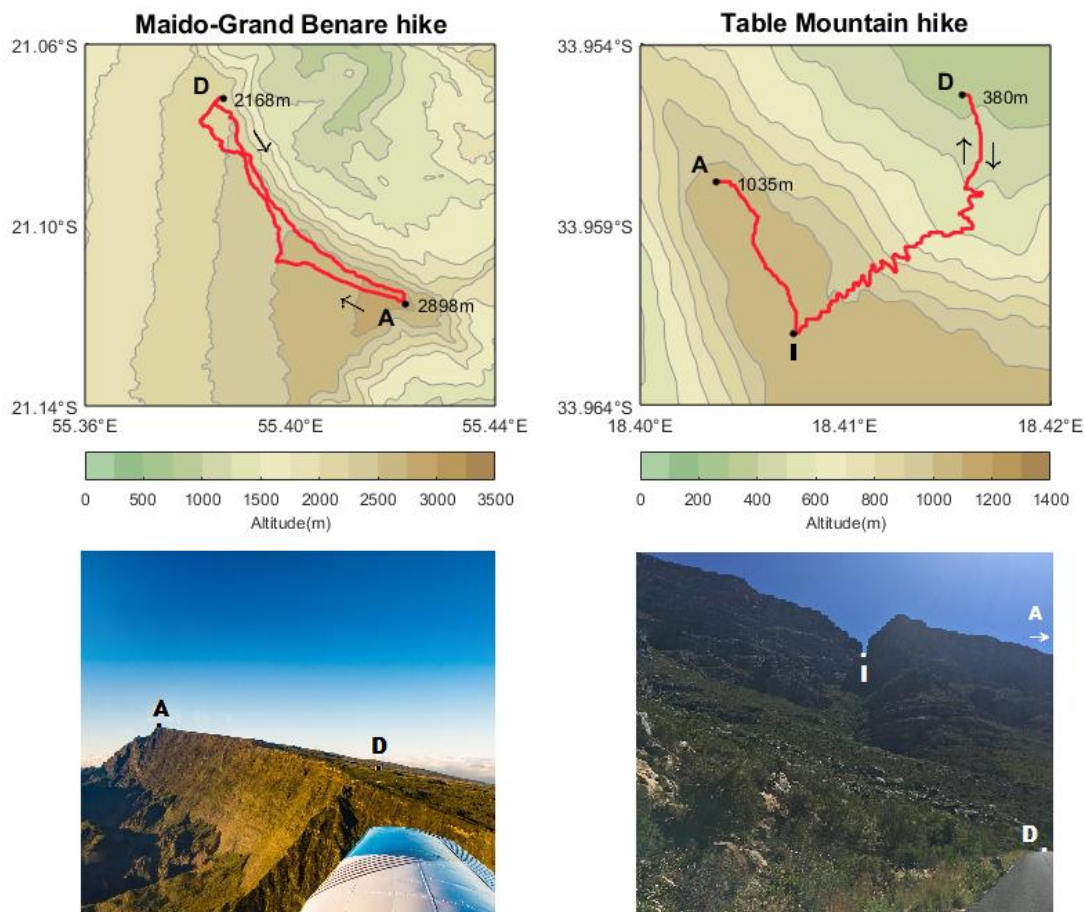
Figure 2. On the top panels, the red lines show the route of the Maïdo–Grand Bénare hike (left side) and Table Mountain hike (right side). The departure (D), intermediate (I), and arrival (A) locations

are indicated as well, in addition to the direction of the hike. The lower panels present photos of the 2 sites on the days of the hikes.

Results and Discussion

3.1. Climatology

The monthly climatology of total daily erythemal UVR doses for both locations over the period of study (2009–2018) is presented in **Figure 3**. The black boxplots provide the UVI median, interquartile range and absolute extreme values, while the orange lines illustrate the mean values framed with ±1 standard deviation. As expected, the most important forcing that drives the annual course of UVR doses is the annual oscillation, with maximum UVR doses during austral summer for both sites but showing a greater amplitude for Cape Town. In fact, for Reunion and Cape Town the total daily dose is at a maximum during austral summer (December, January, February) and at a minimum during austral winter (June, July, August). By focusing on the monthly mean (solid orange line), the seasonal minimum is lower at Cape Town than at Saint-Denis. This could be due to latitude effect. However, the maximum seasonal dose is higher at Cape Town than at Saint-Denis (≈ 63 SED and 55 SED, respectively). This likely depends on the seasonal variability of cloud cover at each site. In fact, the Reunion site of Saint-Denis, located 13° latitude to the north of the Cape Town site, is dominated by a tropical climate which is characterized by strong cloud cover during austral summer [22,23]. This may explain the lower amplitude of surface UVR recorded in Reunion in comparison with Cape Town. Moreover, as indicated by the SED standard-deviations (superimposed with orange lines in **Figure 3**), Saint-Denis shows more variability (larger standard-deviations). This seems to reflect the intermittent aspect of the cloud cover over the site. Also, the monthly maximum dose, presented by the top of the vertical black thin lines reveals a higher austral summer total daily doses in Saint-Denis than in Cape Town. Outliers are present, but only for days when the total daily doses are very low due to cloud cover.

The UVR climatology at Cape Town can be compared to the Cape Point UVR station as these stations are located within a short geographical distance one from each other (~50km). However, the UVR behaviour is different due to different atmospheric conditions—Cape Town is in the airport area, near the city center, and Cape Point station is on the Cape Point peninsula which is an isolated site protruding into the ocean. A previous study on the total daily UVR dose during 2009 showed a lower dose during the austral summer at Cape Point compared to Cape Town [24].

With a special focus on user-oriented presentations, the relative frequency of the WHO UVI exposure categories (low, moderate, high, very high, extreme) [25] was calculated for half-month means of UVI (**Figure 4**). Regarding the Reunion site (Figure 4a), the pattern of UVI distribution is dominated by "High", "Very-High", and "Extreme" UVI values almost all-year-round. However, we can differentiate two dominant seasons in Reunion: wet/summer (October to March) and dry/winter (April to September) seasons. During summer, UVI levels reach "Extreme" thresholds and represent more than 80% of the total number of observations, while during the winter season, UVI frequencies are distributed between "Moderate" and "High" categories. In addition, for the Reunion site, the "Low" UVI category remains infrequent regardless of the month and season, with an average frequency less than 5%. For Cape Town site (**Figure 4b**), the relative frequency distribution shows that "Low" and "Moderate" UVI categories dominate (about 100%) during winter, while during summer there was a preponderance of "High", "Very-High", and "Extreme" UVI thresholds, almost at 100% of the total number of observations. Overall, UVI is extreme during summer for both sites, but for a longer period at Saint-Denis. During winter, UVI is "Low" at Cape Town and "Moderate" to "High" at Saint-Denis. During summer, one can see that UVI shows "Extreme" values with relative frequencies from 60% up to 80% per fortnightly.

Considering the high UVI levels calculated for the two studied sites, and considering the high exposure of populations to solar UVR due to outdoor activities for leisure or professional reasons,

our results raise an important question: are the UVI thresholds, as defined by WHO classification [25], relevant for tropical and subtropical regions? Historically, the UVI scale was defined in Canada and it is indeed not adapted for the tropical and sub-tropical region [26,27]. While seeking an answer to the question above was not part of this work, specific studies on solar UVR and health impacts are necessary, and the concerned populations must be informed of the associated health risks using the most meaningful metrics.
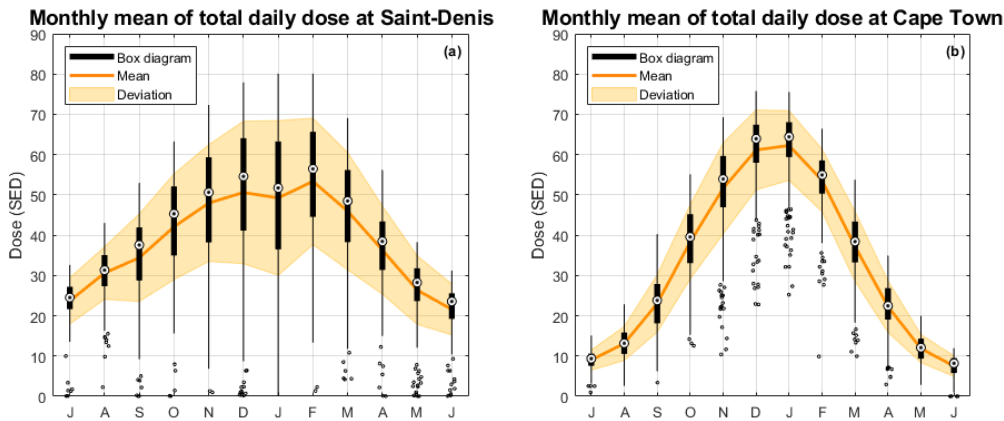
Figure 3. Monthly climatology of total daily erythemal dose at Saint-Denis (**a**) and at Cape Town (**b**). Box diagrams are represented in black for each month (the central value is the median, the box edge is set at 25th and 75th percentiles, the whiskers show the extreme values, excluding outliers, which is represented by single black dots). The orange line shows the monthly mean and the orange shading shows one standard deviation. Months on the X-axis have been reorganized to highlight the austral summer, which appears in the middle of the plot.
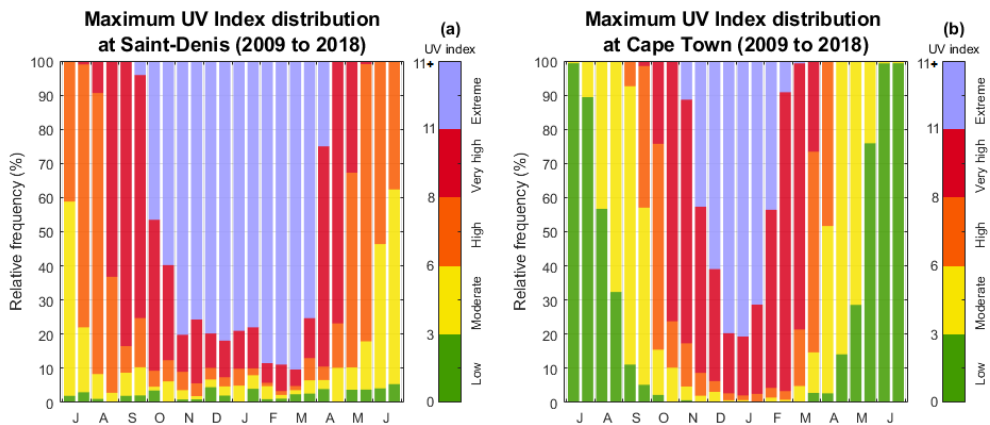
Figure 4. Relative frequency of ultraviolet (UV) index thresholds (WHO) based on the half-month maximum UV Index (UVI) over the decade (2009 to 2018), (**a**) for Saint-Denis UV station and (**b**) for Cape Town UV station. Months on the X-axis have been reorganized to highlight the austral summer, which appears in the middle of the plot.

3.2. Trend Analysis

Although the observation period is rather short (i.e., 2009–2018), we used ground-based UVR data from the two study sites to investigate changes and trends over a decade. Trend analyses were performed based on daily and monthly values obtained from observations at Saint-Denis and Cape Town sites. All UVR data were integrated into daily erythemal doses (**Figure 5**). There is a larger

dispersion of UVR doses at Saint-Denis (**Figure 5a**) in comparison with Cape Town distributions (**Figure 5b**). There was a moderate correlation at Saint-Denis, 63% (220/365 points), and a high correlation of 90% (289/365 points) at Cape Town. For both study sites, by comparing UVR doses recorded in 2009 and 2018, positive differences are evident. A bias of +15 ± 90% at Saint-Denis and +4 ± 50% at Cape Town was found by comparing 2009 and 2018. There was no significant difference in the total daily UVR doses between 2009 and 2018 for both sites. Overall, total daily doses were very high during austral summer, reaching 80 SED for both sites, and decreased as low as 30 SED and 10 SED during austral winter for Saint-Denis and Cape Town, respectively. Even though winter doses are lower than summer doses, they are still higher than the threshold for potential sunburn for almost all sun phototypes (**Table 2**) represented by the horizontal lines in **Figure 5**, except for sun phototypes V and VI at Cape Town. Similar high ambient UVR exposures were reported in a previous study [24].

We applied the least-squares method to the monthly mean UVR values derived for the two sites to estimate linear trends over a decade (2009–2018). For both sites, UVR trends were investigated in two ways: on a global and a seasonal basis. For each site, total daily erythemal doses (in SED unit) were averaged monthly and used from January 2009 to December 2018. The trend analyses are shown in **Figure 6a,b**. The relevance of this analysis depends on the total number of daily observations applied. The histograms at the bottom of each plot show the number of days with available data. The two sites had a rate of observational measurement higher than 60%: 62% for Saint-Denis and 92% for Cape Town over the studied period. **Figure 6** shows two opposed global daily erythemal UVR trends for the two sites: an increasing trend at Reunion Island (+3.6%) and a decreasing trend at Cape Town (−3.7%). Fountoulakis et al., 2018 found an increase in UVR of about 3% per decade over Europe, Canada and Japan, by using a 25-year ground-based database while zonal trend analysis (20 years) from Total Ozone Mapping Spectrometer (TOMS) also showed an increase of 3% per decade for latitudes similar to our study sites [28,29]. The two opposite trends may be explained by the wavelength range of the UV-biometer (280-340nm). Since the spectral response is corrected by coefficient depending only on ozone and solar zenith angle, differences on atmospheric conditions (aerosols, clouds, …) can induce bias in dataset. Moreover, the trend estimates for Saint-Denis site should be interpreted with care since 38% of daily observations were missing, while 8% of daily observations were missing for Cape Town.

As UVR depends on seasonal variability and on changes in the forcings that modulate UVR fluxes at the surface, we broke down the trend analysis by season (DJF: December-January-February, MAM: March-April-May, JJA: June-July-August, and SON: September-October-November), as shown in Table 2. The seasonal decomposition showed two positive trends in Saint-Denis, about +5.4% for summer (DJF) and autumn (MAM), and +1.8% for winter (JJA) and spring (SON), while it shows opposite trends for Cape Town site: negative trends from spring, summer and autumn, with about −5% in average, and a slightly positive trend (+1%) during winter.

In addition to aerosols and cloud cover, stratospheric ozone is an important atmospheric parameter affecting surface UVR [30]. A recent study by Ball et al. [31] using satellite data showed a continuous decrease in ozone in the lower stratosphere from 1998. However, the reasons for the continued reduction of lower stratospheric ozone are still unclear. This decrease appeared despite positive trends in total ozone following the Montreal protocol [32]. Models are not able to reproduce this decreasing trend of ozone in the lower stratosphere. The latter may be due to dynamical changes in the Brewer-Dobson circulation, which is a large-scale circulation that takes place in the winter stratosphere and depends on planetary waves propagation in the middle atmosphere [33–35]. Moreover, by analyzing radiosonde and satellite datasets, Toihir et al. [32] found no significant change in stratospheric ozone in the southern tropics over the period 1998–2013. Indeed, the positive change obtained for surface solar UVR in Reunion could not be attributed to the change in stratospheric ozone. It may be associated with a possible change in the troposphere. Climate models predict that the geographic distribution of cloud changes in response to anthropogenic warming, and the expected forced changes are likely to appear in the upper troposphere [36].

The change in solar UVR levels at the surface may also be due to a change in aerosol loading [37] or in tropospheric ozone formation. The two study sites are famous tourist sites and increasing anthropogenic activities may have resulted in an increase in air pollution. A positive trend in tropospheric ozone over Cape Town has been found by using ground-based, satellite-based, and modeling datasets for past decades [38]. This change in tropospheric ozone content can explain the change in surface UVR. However, the effect of aerosols is different for our study sites. Indeed, Saint-Denis is continuously affected by the trade winds that result in a short residence time of aerosols. The retrieved UVR trends derived for Saint-Denis should be interpreted with caution mainly because 1) there is missing data in the time series and 2) it is a tropical site with extensive cloud cover, especially during the summer season, and because of the possible change in cloud cover. Reunion Island is in a tropical region where the inter-tropical convergence zone (ITCZ) has a large impact on cloud cover.

Furthermore, within the context of climate change, there is a direct link between increasing sea surface temperatures and the distribution of cloud cover in the tropics [39]. The negative trends obtained for the Cape Town site could result from a combination of many processes at different scales. Aerosols and air pollutant loading in the troposphere has a negative forcing on surface UVR [28]. Moreover, biomass burning is the most significant source of gases and particulate matter emissions to the atmosphere. Almost 90% of all biomass burning emissions are anthropogenic [40]. Pollutants associated with anthropogenic activities and biomass burning could lead to the formation of ozone and other photochemical oxidants, in addition to UVR reductions at the surface. According to the South African National Veldfire Risk Assessment, there is a marked increasing trend in fire incidence in South Africa [41]. This is consistent with a recent review on trends of tropospheric ozone by Cooper et al. [38]. They showed the seasonal variations in the tropospheric column of ozone over South Africa in accordance with the biomass burning season and found a significant positive trend in surface ozone time series at Cape Town (0.19 ± 0.05 ppbv/year) for the 1986–2011 period. Our findings support these observed changes in the troposphere composition.

Table 2. Annual and seasonal UV trend estimates (in percentages) computed from daily total doses (SED) as derived from UVI observations at Saint-Denis in Reunion Island and Cape Town in South Africa.

Sites		Seasonal Trends (%)				Annual Trend (%)
		DJF	MAM	JJA	SON	
Saint-Denis	20.9°S, 55.5°E, 85 m ASL	+4.5	+6.3	+1.7	+1.9	+3.7
Cape Town	33.9°S, 18.6°E, 42 m ASL	−5.0	−5.7	+1.0	−4.2	−3.6
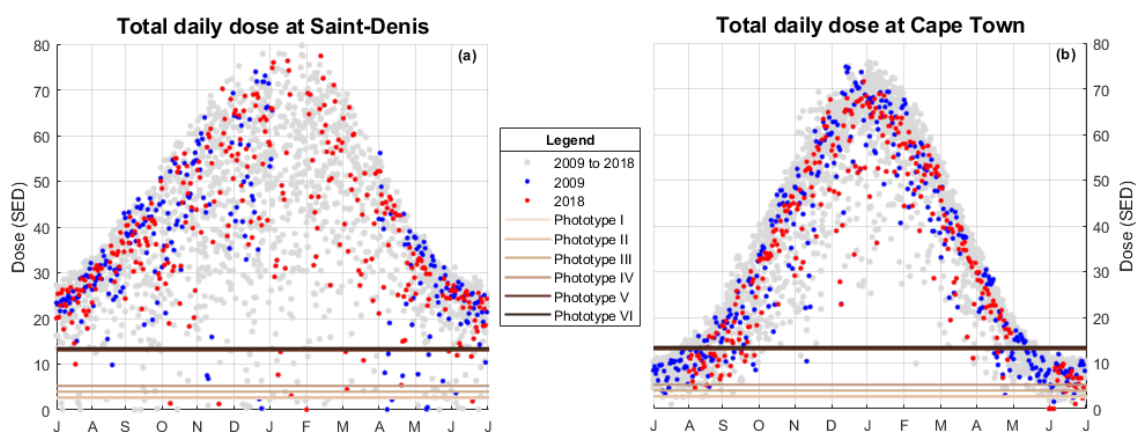
Figure 5. Total daily erythemal doses at Saint-Denis (**a**) and Cape Town (**b**). The grey dots represent all daily values recorded from 2009 to 2018. The blue and red dots highlight data from 2009 and 2018, respectively. The horizontal lines show the threshold for one dose to sunburn (Table 1) as a function

of skin phototype. Months on the X-axis have been reorganized to highlight the austral summer, which appears in the middle of the plot.
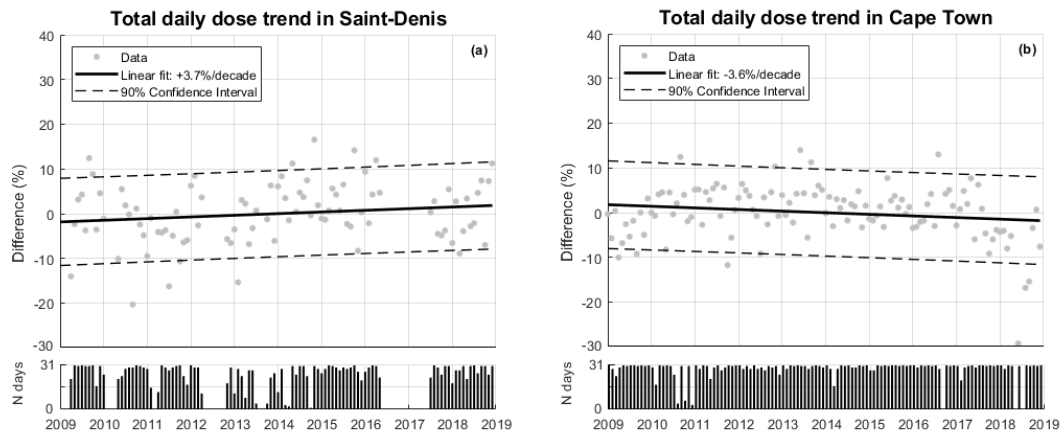
Figure 6. Total daily erythemal dose trend estimates in Saint-Denis (**a**) and Cape Town (**b**). The grey dots represent the relative difference from the monthly mean of daily doses to the climatological monthly mean of daily doses. The histogram shows the numbers of days with data available in each month. The black solid line represents a linear fit and the black dashed lines the 90% confidence interval.

3.3. Case Study

Reunion Island and Cape Town, South Africa are well-known tourist destinations due to their natural landscapes and varied terrains which are very popular for outdoor activities, almost all-year-round. Given the elevation at high altitude sites, such as Grand Bénare (GB, 2898 m) in Reunion Island and Table Mountain (TM, 1035 m) in Cape Town, intense UVR levels may be experienced by users such as tourists, trailers or hikers, as well as employees in the local national parks. In order to complete our comparative study between Reunion and Cape Town sites, we carried out two field experiments under quasi-similar conditions: measurements of UVI during ascent hikes of GB and TM with the same instrument and the same operational protocol (same time sampling and same sensor directional pointing, etc.). The recorded UVI and cumulative UVR doses for GB and TB hikes are shown in **Figure 7**. The GB hike started at 7:00 local time, while the TM hike started at 11:00. This is because the GB hike is more challenging to complete with steep ascents and lasts longer than the TM one. Moreover, we recorded some environmental parameters such as shading due to cloud cover or due to the topography (e.g., gorge passageway) during the two hikes. They are shown with grey boxes at the bottom of **Figure 7a,b**.
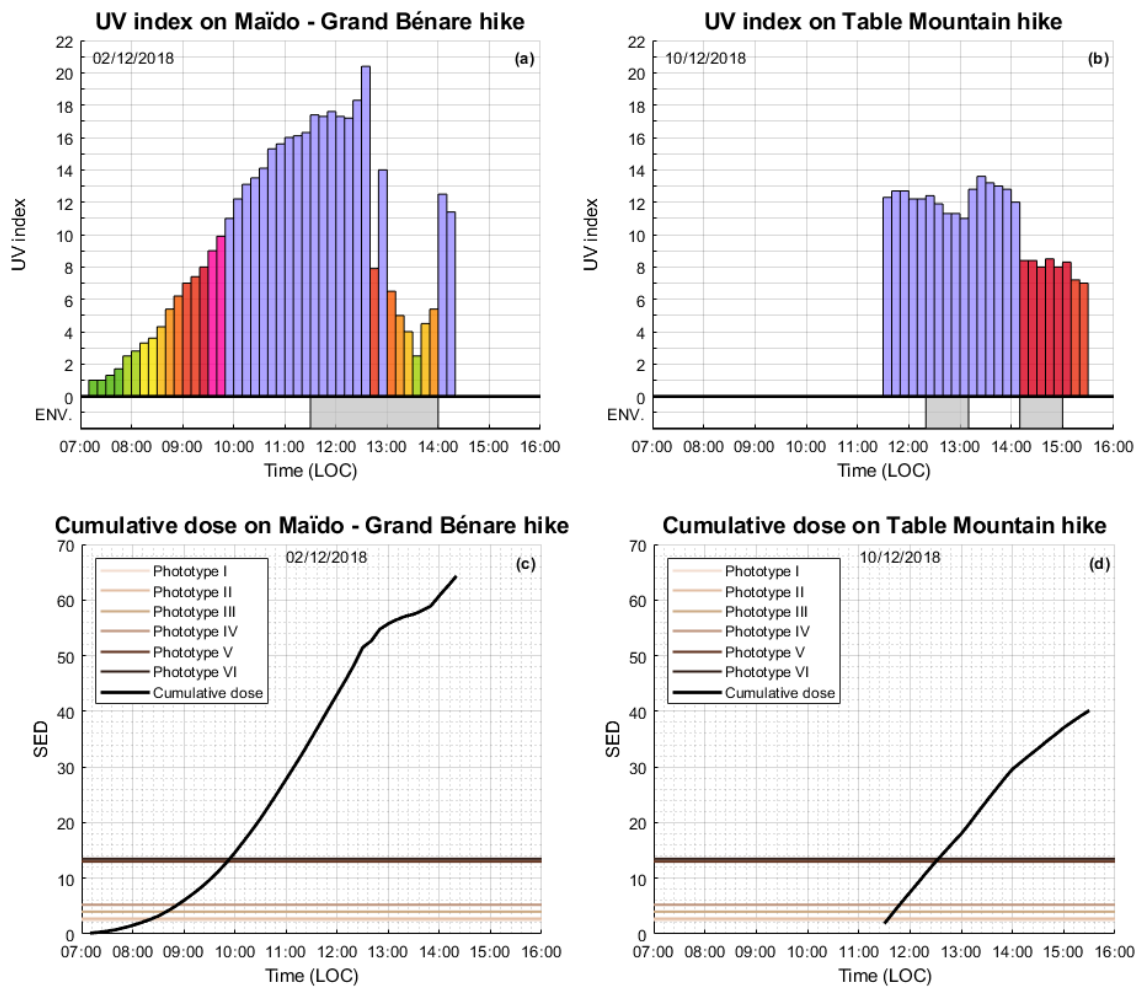
Figure 7. UV index recorded at Maïdo–Grand Bénare hike (**a**) and Table Mountain hike (**b**). The colors on the histogram represent also the UV index following the standard UV index color scale. The grey surface at the bottom of the figure shows environmental effects affecting UV radiation, mainly cloud cover or shade. The corresponding cumulative doses at Maïdo-Grand Bénare hike (**c**) and Table Mountain hike (**d**). The black line represents the cumulated dose. The horizontal lines show the threshold for 1 dose to sunburn (Table) as function of skin phototype.

For the GB hike (**Figure 7a**) some clouds (cumulus humilis) were recorded from 11:30 to 14:00, local time. During this time interval, as a result of the increase in cloud scattering, UVI increased to a high maximum value of 20.4 then progressively decreased and dropped as low as 2.5 due to the cloud spread and attenuation.

During the TM hike (**Figure 7b**) two environmental events occurred: the first one was the crossing upward of the Platteklip gorge (from 12:30 to 13:00). The gorge is a steeply sloping and shaded area. The second event was the crossing downward (from 14:10 to 14:40) of the gorge. One can observe from **Figure 7b** a decrease in UVI during the crossing of the gorge. The effect of the decrease in diffuse radiation by topography is noticeable where the UVI dropped by 4 units and went from 13 to about 8.

Figure 7c,d show the cumulative doses were extremely high during both GB and TM hikes, with total exposure doses of 64 SED and 40 SED, respectively. This corresponds to 3 to 25 times the minimal dose required to elicit a sunburn response for phototype I to phototype VI (see Table).

The likely difference in cumulative exposure doses between the two sites was in part due to the differences in the hike duration as well as the maximum altitude (i.e., 7h10 duration and 2898 m elevation for GB hike, and 4h and 1035m elevation for TM hike).

4. Conclusions

The aim of this study was to assess the level of UVR exposure doses in Saint-Denis, Reunion Island, France and Cape Town, South Africa. This evaluation was performed by analyzing 10 years of data (2009–2018) and by the assessment of UVR at two popular hiking sites located at high altitude. The trend analysis showed different levels of solar UVR at the two sites: an increase of 3.7% of total daily erythemal UVR dose in Saint-Denis and a decrease of 3.6% in Cape Town over the ten-year period. Environmental factors such as ozone, aerosols and cloud cover are sensitive to climate change and may be responsible for changes in UVR levels. Moreover, the evolution of UVR is difficult to evaluate in sites such as Reunion Island and Cape Town which are subject to many different forcings and atmospheric changes. The trends obtained must be interpreted carefully due to the relatively short time period (10 years) and the missing data.

The climatological analysis highlighted extreme UVR levels occur during the austral summer in Saint-Denis and Cape Town. Erythemal UVR levels are also high at Saint-Denis during the winter season at about 30 SED. These high erythemal UVR levels may lead to sunburn in people who spend extended periods of time outdoors without adequate sun protection. Similarly, in situ measurements showed potentially extreme UVR exposure doses for hikers walking the GB and TM hikes. These are two popular sites where UVR levels are very high due to latitude, altitude and environmental conditions. Acute exposure of this nature would likely result in sunburn and skin damage [42] while regular hiking at these sites would contribute to chronic exposure which is associated with harmful health effects such as skin cancer [43]. Hiking is therefore deemed a potentially high sun exposure activity and sun protection should be used. The results of this study highlight the importance of crafting appropriate public awareness campaigns on the UVR exposure-risks from excess sun exposure especially during outdoor recreational activities.

References

1.   Kerr, J.; Fioletov, V.; Fioletov, V. Surface ultraviolet radiation. *Atmos. Ocean* **2008**, *46*, 159–184.
2.   Fitzpatrick, T.B. Skin Phototypes. In Proceedings of the 20th World Congress of Dermatology, Paris, France, 1–5 July 2002.
3.   Gallagher, R.P.; Lee, T.K.; Adverse effects of ultraviolet radiation: A brief review. *Biophys. Mol. Biol.* **2016**, *92*, 119–131, doi:10.1016/j.pbiomolbio.2006.02.011.
4.   Tucker, M.A.; Shields, J.A.; Hartge, P.; Augsburger, J.; Hoover, R.N.; Fraumeni, J.F. Sunlight Exposure as Risk Factor for Intraocular Malignant Melanoma. *N. Engl. J. Med.* **1985**, *313*, 789–792.
5.   Armstrong, B.K.; Kricker, A. How much melanoma is caused by sun exposure? *Melanoma Res.* **1993**, *3*, 395–402.

6. National Institute for Communicable Diseases. Available online: http://www.nicd.ac.za/centres/national-cancer-registry/ (accessed on 5 July 2019).

7. Norval, M.; Kellett, P.; Wright, C.Y. The incidence and body site of skin cancers in the population groups of South Africa. *Photodermatol. Photoimmunol. Photomed.* **2013**, *30*, 262–265, doi:10.1111/phpp.12106.

8. Warocquier, J.; Miquel, J.; Chirpaz, E.; Beylot-Barry, M.; Sultan-Bichat, N. Groupe de travail des dermatologues et anatomopathologistes de l'île de la Réunion; Données épidémiologiques des mélanomes cutanés à la Réunion en 2015. *Ann. Dermatol. Vénéréologie* **2016**, *143*, S313–S314, doi:10.1016/j.annder.2016.09.476.

9. Albert, M.R.; Ostheimer, K.G. The evolution of current medical and popular attitudes toward ultraviolet light exposure: Part 3. *J. Am. Acad. Dermatol.* **2003**, *49*, 1096–1106.

10. Brogniez, C.; Auriol, F.; DeRoo, C.; Arola, A.; Kujanpää, J.; Sauvage, B.; Kalakoski, N.; Pitkänen, M.R.A.; Catalfamo, M.; Metzger, J.-M.; et al. Validation of satellite-based noontime UVI with NDACC ground-based instruments: Influence of topography, environment and satellite overpass time. *Atmos. Chem. Phys. Discuss.* **2016**, *16*, 15049–15074.

11. Joint, I.S.O. *CIE Standard 17166: 1999/CIE S007-1998 Erythema reference action spectrum and standard erythema dose*; ISO: Vienna, Austria, 1999.

12. Lamy, K.; Portafaix, T.; Brogniez, C.; Godin-Beekmann, S.; Bencherif, H.; Morel, B.; Pazmino, A.; Metzger, J.M.; Auriol, F.; DeRoo, C.; et al. Ultraviolet radiation modelling from ground-based and satellite measurements on Reunion Island, southern tropics. *Atmos. Chem. Phys. Discuss.* **2018**, *18*, 227–246.

13. Cadet, J.-M.; Bencherif, H.; Portafaix, T.; Lamy, K.; Ncongwane, K.; Coetzee, G.J.R.; Wright, C.Y. Comparison of Ground-Based and Satellite-Derived Solar UV Index Levels at Six South African Sites. *Int. J. Environ. Res. Public Health* **2017**, *14*, 1384.

14. Seckmeyer, G.; Bernhard, A.; Blumthaler, M.; Booth, C.; Lantz, K.; Webb, A. *Instruments to Measure Solar Ultraviolet Radiation. Part 2: Broadband Instruments Measuring Erythemally Weighted Solar Irradiance*; World Meteorological Organization (WMO): Geneva, Switzerland, 2005.

15. Blumthaler, M. UV Monitoring for Public Health. *Int. J. Environ. Res. Public Health* **2018**, *15*, 1723.

16. de Paula Corrêa, M.; Godin-Beekmann, S.; Haeffelin, M.; Brogniez, C.; Verschaeve, F.; Saiag, P.; Pazmiño, A.; Mahé, E.; Comparison between UV index measurements performed by research-grade. *Photochem. Photobiol. Sci.* **2010**, *9*, 459–463, doi:10.1039/B9PP00179D.

17. World Health Organization and International Commission on Non-Ionizing Radiation Protection. *Global Solar UV Index: A practical Guide*; World Health Organization: Geneva, Switzerland, 2002.

18. Mahé, E.; de Paula Corrêa, M.; Godin-Beekmann, S.; Haeffelin, M.; Jégou, F.; Saiag, P.; Beauchet, A.; Evaluation of tourists' UV exposure in Paris. *J. Eur. Acad. Dermatol. Venereol.* **2013**, *27*, e294–e304, doi:10.1111/j.1468-3083.2012.04637.x.

19. Cede, A. Effects of clouds on erythemal and total irradiance as derived from data of the Argentine Network. *Geophys. Res. Lett.* **2002**, *29*, doi:10.1029/2002GL015708.

20. Blumthaler, M.; Ambach, R.; Ellinger, R. Increase in solar UV radiation with altitude. *Photochem. Photobiol.* **1996**, *39*, 130–134, doi:10.1016/S1011-1344(96)00018-8.

21. Utrillas, M.P.; Marín, M.J.; Esteve, A.R.; Tena, F.; Cañada, J.; Estelles, V.; Martínez-Lozano, J.A.; Martínez-Lozano, J.A. Diffuse UV erythemal radiation experimental values. *J. Geophys. Res. Space Phys.* **2007**, *112*, 112.

22. Jumeaux, G.; Quetelard, H.; Roy, G. *Atlas climatique de La Réunion*; Météo-France Direction interrégionale de la Réunion: Sainte-Clotilde, La Réunion, 2002; ISBN: 978-2-11-128623-8.

23. Cadet, B.; Goldfarb, L.; Faduilhe, D.; Baldy, S.; Réchou, A.; Giraud, V.; Keckhut, P. A sub-tropical cirrus clouds climatology from Reunion Island (21° S, 55° E) lidar data set. *Geophys. Res. Lett.* **2003**, *30*, 1130.

24. Wright, C.Y.; Brogniez, C.; Ncongwane, K.P.; Sivakumar, V.; Coetzee, G.; Auriol, F.; DeRoo, C.; Sauvage, B.; Metzger, J.-M.; Metzger, J. Sunburn Risk Among Children and Outdoor Workers in South Africa and Reunion Island Coastal Sites. *Photochem. Photobiol.* **2013**, *89*, 1226–1233.

25. WMO (World Meteorological Organization) Assessment for Decision-Makers: Scientific Assessment of Ozone Depletion: 2014. In *Global Ozone Research and Monitoring Project – Report No. 56*; World Meteorological Organization: Geneva, Switzerland, 2014; pp. 88; ISBN: 978-9966-076-00-7.

26. Fioletov, V.; Kerr, J.B.; Fergusson, A. The UV Index: Definition, Distribution and Factors Affecting It. *Can. J. Public Health* **2010**, *101*, I5–I9.

27. Zaratti, F.; Piacentini, R.D.; Guillén, H.A.; Cabrera, S.H.; Ben Liley, J.; McKenzie, R.L. Proposal for a modification of the UVI risk scale. *Photochem. Photobiol. Sci.* **2014**, *13*, 980–985.

28. Tarasick, D.W.; Fioletov, V.E.; Wardle, D.I.; Kerr, J.B.; McArthur, L.J.B.; McLiden, C.A. Climatology and trends of surface UV radiation: Survey article. *Atmos. Ocean* **2010**, *42*, 121–138, doi:10.3137/ao.410202.

29. Fountoulakis, I.; Zerefos, C.S.; Bais, A.F.; Kapsomenakis, J.; Koukouli, M.-E.; Ohkawara, N.; Fioletov, V.; De Backer, H.; Lakkala, K.; Karppinen, T.; et al. Twenty-five years of spectral UV-B measurements over Canada, Europe and Japan: Trends and effects from changes in ozone, aerosols, clouds, and surface reflectivity. *Comptes Rendus Geosci.* **2018**, *350*, 393–402.

30. Bais, A.F.; Lucas, R.M.; Bornman, J.F.; Williamson, C.E.; Sulzberger, B.; Austin, A.T.; Wilson, S.R.; Andrady, A.L.; Bernhard, G.; McKenzie, R.L.; et al. Environmental effects of ozone depletion, UV radiation and interactions with climate change: UNEP Environmental Effects Assessment Panel, update 2017. *Photochem. Photobiol. Sci.* **2018**, *17*, 127–179.

31. Ball, W.T.; Staehelin, J.; Haigh, J.D.; Peter, T.; Tummon, F.; Stübi, R.; Stenke, A.; Anderson, J.; Bourassa, A.; Davis, S.M.; et al. Evidence for a continuous decline in lower stratospheric ozone offsetting ozone layer recovery. *Atmos. Chem. Phys.* **2016**, *18*, 1379–1394, doi:10.5194/acp-18-1379-2018.

32. Toihir, A.M.; Portafaix, T.; Sivakumar, V.; Bencherif, H.; Pazmino, A.; Bègue, N. Variability and trend in ozone over the southern tropics and subtropics. *Ann. Geophys.* **2018**, *36*, 381–404.

33. Leovy, C.; Sun, C.-R.; Hitchman, M.; Remsberg, E.; Russell, J.; Gordley, L.; Gille, J.; Lyjak, L. Transport of Ozone in the Middle Stratosphere: Evidence for Planetary Wave Breaking. *J. Atmos. Sci.* **1985**, *42*, 230–244.

34. Bencherif, H.; Portafaix, T.; Baray, J.-L.; Morel, B.; Baldy, S.; Leveau, J.; Hauchecorne, A.; Keckhut, P.; Moorgawa, A.; Michaelis, M.M.; et al. LIDAR observations of lower stratospheric aerosols over South Africa linked to large scale transport across the southern subtropical barrier. *J. Atmos. Sol. Terr. Phys.* **2001**, *65*, 707–715, doi:10.1016/S1364-6826(03)00006-3.

35. Bencherif, H.; Amraoui, L.E.; Kirgis, G.; Leclair de Bellevue, J.; Hauchecorne, A.; Mzé, N.; Portafaix, T.; Pazmiño, A.; Goutail, F. Analysis of a rapid increase of stratospheric ozone during late austral summer 2008 over Kerguelen (49.4° S, 70.3° E). *Atmos. Chem. Phys.* **2001**, *11*, 363–373, doi:10.5194/acp-11-363-2011.

36. Chepfer, H.; Noel, V.; Winker, D.; Chiriaco, M. Where and when will we observe cloud changes due to climate warming? *Geophys. Res. Lett.* **2014**, *41*, 8387–8395.

37. Fountoulakis, I.; Bais, A.F.; Fragkos, K.; Meleti, C.; Tourpali, K.; Zempila, M.M. Short and long-term variability of spectral solar UV irradiance at Thessaloniki, Greece: Effects of changes in aerosols, total ozone and clouds. *Atmos. Chem. Phys. Discuss.* **2016**, *16*, 2493–2505.

38. Cooper, O.R.; Parrish, D.D.; Ziemke, J.; Balashov, N.V.; Cupeiro, M.; Galbally, I.E.; Gilge, S.; Horowitz, L.; Jensen, N.R.; Lamarque, J.-F.; et al. Global distribution and trends of tropospheric ozone: An observation-based review. *Elem. Sci. Anth.* **2014**, *2*, 29.

39. Cesana, G.; Del Genio, A.D.; Ackerman, A.S.; Kelley, M.; Elsaesser, G.; Fridlind, A.M.; Cheng, Y.; Yao, M.-S. Evaluating models' response of tropical low clouds to SST forcings using CALIPSO observations. *Atmos. Chem. Phys. Discuss.* **2019**, *19*, 2813–2832.

40. Koppmann, R.; Von Czapiewski, K.; Reid, J.S. A review of biomass burning emissions, part I: Gaseous emissions of carbon monoxide, methane, volatile organic compounds, and nitrogen containing compounds. *Atmos. Chem. Phys. Discuss.* **2005**, *5*, 10455–10516.

41. Forsyth, G.G.; Kruger, F.J.; Le Maitre, D.C. *National Veldfire Risk Assessment: Analysis of Exposure of Social, Economic and Environmental Assets to Veldfire Hazards in South Africa*. CSIR Report No: CSIR/NRE/ECO/ER/2010/0023/C; National Resources and the Environment CSIR; Fred Kruger Consulting cc.: Stellenbosch, South Africa, March 2010.

42. Young, A.R. Acute effects of UVR on human eyes and skin. *Prog. Biophys. Mol. Boil.* **2006**, *92*, 80–85.

43. Marionnet, C.; Tricaud, C.; Bernerd, F. Exposure to Non-Extreme Solar UV Daylight: Spectral Characterization, Effects on Skin and Photoprotection. *Int. J. Mol. Sci.* **2015**, *16*, 68–90, doi:10.3390/ijms16010068.

atmosphere

an Open Access Journal by MDPI

IMPACT FACTOR 2.046

Indexed in: Ei Compendex

Indexed in: Scopus

CERTIFICATE OF PUBLICATION

Certificate of publication for the article titled:

Solar UV Radiation in Saint-Denis, La Réunion and Cape Town, South Africa: 10 years Climatology and Human Exposure Assessment at Altitude

Authored by:

Jean-Maurice Cadet; Hassan Bencherif; David J. du Preez; Thierry Portafaix; Nathalie Sultan-Bichat; Matthias Belus; Colette Brogniez; Frederique Auriol; Jean-Marc Metzger; Katlego Ncongwane; Gerrie J. R. Coetzee; Caradee Y. Wright

Published in:

Atmosphere **2019**, Volume 10, Issue 10, 589

MDPI
Academic Open Access Publishing
since 1996

Basel, April 2020

4.3 ARTICLE : CADET ET AL., 2020 (CONVERS.)

THE C**O**NVERSATION

Academic rigour, journalistic flair

We found high UV doses at high-altitude hiking trails in Reunion and Cape Town

May 11, 2020 4.13pm SAST

Authors

Jean-Maurice Cadet, PhD candidate, Université de la Réunion

Caradee Yael Wright, Specialist Scientist (Public Health), African Medical Research Council

Hassan Bencherif, Professor, Université de la Réunion

A couple taking in the view from Table Mountain, Cape Town. Getty Images

Ultraviolet (UV) radiation from the sun is important for life on earth and especially for humans.

In animals UV radiation is essential for biological functions like calcium metabolism. In vegetation it's necessary for photosynthesis. And in humans, UV plays an important role in synthesis of vitamin D, which makes for strong bones, joints and muscles.

But too much UV radiation is also very dangerous for human health. Excessive exposure can cause skin ageing and sunburn and can induce skin cancer such as melanoma, cataracts, ocular melanoma, and immunodeficiency.

The sun is the main natural source of ultraviolet radiation. The risk for human health also depends on UV intensity. The UV level is affected by several atmospheric factors, such as ozone, aerosol, cloud cover or altitude. This is one reason why changes to the ozone layer as a result of global pollutant emissions make a difference to human health. The UV intensity is higher at high altitudes because there is less atmosphere to absorb it. Tropical regions also experience high UV exposure because the sun shines there a lot of the time.

We tested the UV exposure in high-altitude sites in Cape Town and Reunion Island. We assessed human exposure for hiking activities at two popular high-altitude hiking trails on the Maïdo–Grand Bénare (Reunion) and Table Mountain (Cape Town) with a handheld radiometer. We recorded extreme exposure doses.

These high exposure doses highlight the importance of raising public awareness on the risk related to excess UVR exposure at tourist sites, especially those at high altitude. Our findings suggest a need for strong public awareness campaigns among visitors to sites like these to prevent skin diseases and cancers that could result from overexposure to UV radiation.

Our study

We chose our testing sites – Table Mountain (altitude of 1,035 metres) in Cape Town and Maïdo-Grand Bénare (2,898 metres) on Reunion Island – because they are popular tourist destinations for outdoor activities for most of the year. Yet their high risk for UV is not necessarily well known. Tourists, hikers and employees of the local national parks may be exposed to high UV levels. Every year, 1,000,000 people visit Table Mountain and 180,000 hike on Réunion Island mountain.

Two markers were used to quantify the UV exposure. One was the UV index, defined by the World Health Organisation (WHO) as a simple number for public awareness. UV index categories are low (1-2), moderate (3-5), high (6-7), very high (9-10), and extreme (11+).

The maximum UV index numbers recorded were 14 at Table Mountain and 20 at Maïdo-Grand Bénare, which is close to double the extreme UV index threshold defined by the WHO.

The study also measured cumulative standard erythemal dose (SED), a measure of UV exposure in terms of joules per square metre.

The field measurement indicated that people were exposed to 40 SED when hiking Table Mountain and 64 when hiking Maïdo-Grand Bénare. These doses correspond to 3 to 25 times the minimal dose required to elicit a sunburn response depending on skin type (lighter skin requires a smaller dose while darker skin requires a larger dose).

Information about the climate of the two sites shows that the total daily dose is extremely high during summer in Cape Town, and all year around in Reunion Island. Total daily dose is above the level where all skin types will experience sunburn, although people with deeply pigmented skin are less affected. These extreme exposures increase the risk of cataracts, immunodeficiency and melanoma – at least for people with white skin. The link between sunburn and these health risks is not known for people with dark skin.

Melanoma is a type of skin cancer. The mean melanoma rate worldwide in 2015 (male and female mixed) was five per 100,000. In South Africa, the melanoma rate for the total population, regardless of skin type, is five per 100,000 people for men and three per 100,000 for women. Among white South Africans, the melanoma rate is about 20 per 100,000 for men and 16 per 100,000 for women, which is similar to some of the rates recorded in Australia.

From 2006 to 2015, the male population of Reunion Island saw an increase in skin diseases from 2.7 to 7.1 cases per 100,000 people while cases in the female population surged from 3.0 to 6.1 per 100,000. These increasing rates may be due to an atmospheric change and a human behaviour change (such as the popularity of suntanning for aesthetic reasons).

Cover up

The results of our tests highlight the importance of public awareness and prevention of the risks related to UV, especially at exposed sites like Table Mountain and Maïdo-Grand Bénare. The WHO recommends that people avoid being outside in the middle of the day and wear long-sleeved shirts, hats, sunglasses and sunscreen.

This is particularly important in tropical regions, where there are several factors that can increase UV radiation: being relatively close to the Equator, low ozone, low aerosols, low solar zenith angle and clouds.

Public health Vitamin D Sunburn South Africa Ultraviolet radiation Table Mountain Reunion Island

Chapitre 5 IMPACT SUR LA SANTÉ

5.1 ARTICLE : RÉSUMÉ

L'île de la Réunion est une destination touristique connue pour ses plages de sables et son volcan actif, le Piton de la Fournaise, mais aussi pour ses montagnes. Chaque année, des milliers de personnes, population locale et touristes, empruntent le vaste réseau de sentiers de randonnées en montagne. Les nombreuses possibilités d'activités en plein air engendrent nécessairement une augmentation de l'exposition au soleil, et donc au rayonnement ultraviolet.

Le rayonnement ultraviolet a un impact conséquent sur la santé humaine. En effet, le rayonnement ultraviolet est un acteur majeur dans le processus de synthèse de vitamine D. En revanche, une surexposition à celui-ci peut entrainer des problèmes de peaux (coup de soleil, cancers, vieillissement prématuré…), oculaire ou encore des perturbations du système immunitaire.

L'objectif de cette étude est d'estimer le niveau d'exposition de la population dans des lieux où elle est le plus susceptible de s'exposer et où le rayonnement solaire ultraviolet est le plus intense. Trois sites ont été choisis : le volcan : le Piton de la Fournaise, le plus haut sommet : le Piton de Neiges et la plage de Saint-Leu. Ces mesures ont été effectuées en décembre 2019.

Les mesures d'exposition ont été réalisées à l'aide d'un radiomètre portatif, un Solarmeter Model 6.5 Index Meter. L'instrument mesure directement l'irradiance solaire érythémale et fournis l'indice UV. Les indices UV récoltés ont ensuite été convertis en doses standards erythemales. D'autres données ont également été utilisées : les données UV issues du spectro-radiomètre Bentham de l'OPAR situé à Saint-Denis et les données de prévisions UV de Météo-France.

Les doses cumulées mesurées ont été révélatrices d'expositions extrêmes aux UV : 57, 65 et 64 doses standards érythémales (SED) respectivement. Cela correspond à de multiple fois les seuils définis dans la classification de Fitzpatrick. Par ailleurs, les indices UV mesurés ont été également très élevés. Un indice UV de 22.5 a été mesuré au Piton des Neiges, le plus haut sommet, le seuil d'indice UV extrême étant fixé à 11 par l'OMS.

La climatologie (2009-2019) obtenue à l'aide du spectromètre Bentham à Saint-Denis (85m d'altitude) montre un niveau moyen d'indice UV en décembre de 11±4 et une dose journalière cumulée moyenne de 40±25 SED. Décembre 2019 est supérieur à la climatologie (non investigué dans cette étude).

Les prévisions d'indice UV de Météo-France donnent des indices UV inférieur de 10% au maximum des indices UV mesurés. Cette différence est principalement liée à la difficulté d'évaluer l'effet de la nébulosité sur le rayonnement ultraviolet, atténuation ou diminution, ainsi qu'à la topographie de l'île, où de très grandes variations d'altitude peuvent survenir dans un très court espace.

Cette étude a permis de quantifier le niveau d'exposition de la population dans des sites très fréquentés. D'autres campagnes de mesures peuvent être faites plus largement afin d'avoir une meilleure connaissance du risque et adapter les mesures de prévention.

5.2 ARTICLE : CADET ET AL., 2020 (IJERPH SUBMITTED)

Article ci-dessous soumis le 20 aout 2020 dans IJERPH.

International Journal of
Environmental Research and Public Health

MDPI

Article

Solar UV radiation in the tropics: human exposure at Reunion Island (21°S, 55°E) during summer outdoor activities

Jean-Maurice Cadet [1,*], Hassan Bencherif [1,2], Nicolas Cadet [3], Kévin Lamy [1], Thierry Portafaix [1], Matthias Belus [4] and Caradee Y. Wright [5,6]

[1] LACy, Laboratoire de l'Atmosphère et des Cyclones (UMR 8105 CNRS, Université de La Réunion, Météo-France), Saint-Denis de La Réunion 97744, France; jean.cadet@univ-reunion.fr (J.-M.C.); hassan.bencherif@univ-reunion.fr (H.B.);

[2] School of Chemistry and Physics, University of KwaZulu-Natal, Durban 4041, South Africa

[3] Université de la Réunion, Saint-Denis de La Réunion 97744, France; nicolas.p.cadet@gmail.com (N.C.);

[4] Conseil Régional de la Réunion, 5 Avenue René Cassin, Sainte-Clotilde, 97490, La Réunion, France ; matthias.belus@cr-reunion.fr (M.B.);

[5] Department of Geography, Geoinformatics and Meteorology, University of Pretoria, Pretoria 0002, South Africa; caradee.wright@mrc.ac.za (C.Y.W.);

[6] Environment and Health Research Unit, South African Medical Research Council, Pretoria 0001, South Africa; caradee.wright@mrc.ac.za (C.Y.W.);

[*] Correspondence: jean.cadet@univ-reunion.fr; Tel.: +262-692-93-82-97

Abstract: Reunion Island is a popular tourist destination with sandy beaches, an active volcano (Piton de la Fournaise), and Piton des Neiges, the highest and most dominant geological feature on the island. Reunion is known to have high levels of solar ultraviolet radiation (UVR) with an ultraviolet index (UVI) which can reach 8 in winter and 16 in summer, under certain conditions. UVR has been linked to skin cancer, melanoma and eye disease such as cataracts. The World Health Organization (WHO) devised the UVI as a tool for expressing UVR intensity. Thresholds ranging from low (UVI 1-2) to extreme (UVI >11) were defined depending on the risk to human health. The purpose of the study was to assess UVR exposure levels over three of the busiest tourist sites on the island. UVR was measured over several hours along popular hiking trails around Piton de la Fournaise (PDF), Piton des Neiges (PDN) and St-Leu Beach (LEU). The results were compared with those recorded by the local UV station at Saint-Denis. In addition, cumulative Standard Erythemal Dose (SED) was calculated, i.e. the minimal dose to cause sunburn as per the Fitzpatrick Skin Phototype classification. Results showed that UVI exposure at PDF, PDN and LEU were extreme (>11) and reached maximum UVI levels of 21.1, 22.5, and 14.5, respectively. Cumulative SEDs were multiple times higher than the thresholds established by the Fitzpatrick Skin Phototype classification. UVI measurements at the three study sites showed that Reunion Island is exposed to extreme UVR conditions. Public awareness campaigns are needed to inform the population of the health risks related to UVR exposure.

Keywords: Solar UV radiation; Tropics; UV exposure; Human Health; Mountain; Volcano; Beach; Hike

1. Introduction

The main natural source of ultraviolet radiation (UVR) on earth comes from the sun. UVR represents 5% of solar spectral irradiance. Despite this small percentage, UVR is both essential and dangerous for the biosphere. UVR wavelength range is 100-400 nm and is divided into three wavebands, depending on its transmission capability in the atmosphere and its biological effects on humans. UVA (315-400 nm) represents 95% of the UVR reaching Earth, most UVB (280-315 nm) is absorbed by the atmosphere and UVC (100-280nm) does not reach Earth's surface due to the ozone layer [1,2]. When going through the atmosphere, UVR is subject to several amplitude variations. Surface UVR is modulated by several parameters: atmospheric parameters such as ozone, aerosols or clouds [3-5]; geographic parameters (such as latitude or altitude); temporal parameters (seasons or time of the day, i.e. solar zenith angle [6]).

Surface UVR has beneficial effects on human health. Vitamin D synthesis requires UVR and is known to be an important factor to have healthy bones. Vitamin D has also a huge impact on brain chemistry, for example in brain serotonin levels which fight anxiety and depression [7]. In medicine, UVR has been used in phototherapy for decades [8,9]. Despite these positive effects, the adverse effects of UVR can be critical for human health. The characteristics of UVR increase the risk of skin cancer, such as melanoma, eye disease, such as cataracts or immunodeficiency when people are over exposed to UVR [10,11]. The risk related to UVR depends on skin phototype which characterizes sunburn susceptibility (**Table 1** shows the Fitzpatrick Skin Phototype classification [12]).

Human behavior is a factor that can lead to over exposure to UVR. Indeed, the increase of outdoor activities synonymous with good health and sun tanning for aesthetic goals have increased the level of UVR exposure [13-15]. Artificial UVR sources also cause over exposure to UVR, such as welding torches and sunbeds. In 2015, the use of sunbeds was linked to 4% of melanoma in France [16]. Sunbeds are also known to accelerate skin ageing. Addictive use of sunbeds also contributes to an increase in UVR exposure [17].

Reunion Island (**Figure 1**) is a tropical island in the southwest of the Indian Ocean, and is well-known as a touristic destination due to its varied attractions such as subtropical rainforests, an active volcano and lagoons. Listed as a world UNESCO heritage site since 2010, the wide biodiversity of plants and animals, with their high level of endemism, generates a great interest for the destination [18]. In this context, more than 500,000 tourists (2018 data [19]) visit Reunion Island every year. Several outdoor activities are possible all-year-round due to the tropical climate. Tourists as well as the local population (+800,000) may experience intensive UVR exposure.

The World Health Organization (WHO) defined the UV Index (UVI) as a simple tool for public awareness. UVI starts from zero when there is no UVR and increases with UVR intensity. Different thresholds (i.e., 1–2: low, 3–5: moderate, 6–7: high, 8–10: very high, >11: extreme) have been defined depending on the risk to human health and the use of suitable protection [20]. Sea level climatological averages showed that UVI can reach 8 during winter and 16 during summer on Reunion Island [21,22]. Reunion is a mountainous island where Cadet et al. [6] reported a maximum UVI of 20 at ~2900m height. However, UVI is not well known by the population and even by the dermatologists [23].

In Reunion Island, in 2015, the invasive melanoma rate was 6.1 cases per 100,000 people in a female standard population and 7.1 cases per 100,000 people in a male standard population, and a positive trend was found (statistics were not deemed comprehensive and no data have been available since 2015) [6,24].

In this context of high risk related to UVR, and taking into account the popularity of Reunion Island as a touristic destination, this study aims to assess the UVR exposure over three sites that are popular with local and foreign tourists throughout the year: the Piton de la Fournaise volcano (2630m), the highest summit Piton des Neiges (3070m) and Saint-Leu Beach.

Table 1: Fitzpatrick Skin phototype classification [12]

Phototype	Characteristics	History of sunburn	Minimal dose to elicit sunburn (SED)
I	Ivory white skin, light eyes	Burns easily	2-3
II	White skin, hazel/brown eyes	Burns easily	2.5-3
III	White skin, brown eyes	Burns moderately	3-5
IV	Lightly skin, dark eyes	Burns minimally	4.5-6
V	Moderate brown skin, dark eyes	Rarely burns	6-20
VI	Strong brown/black skin, dark eyes	Never burns	6-20

Figure 1. Reunion Island location.

2. Experiments

2.1. Instruments

2.1.1. Solarmeter Model 6.5 UV Index Meter

A handheld Solarmeter Model 6.5 UV Index Meter (SN#10414) was used during the field experiments. This instrument is manufactured by Solarmeter® (Glenside, PA, USA), a trademark of Solar Light Company Inc. A silicon carbide photodiode records erythemal UV irradiance in the 280 to 400 nm wavelength range. The instrument records erythemal-weighted UVR and the UVI is calculated following the standard formula (Equation 1) [25]. Erythemal-weighted UVR is obtained by integrated solar irradiance with erythemal action spectrum. The accuracy traceable to the National Institute of Standards and Technology (NIST) is 10% and a previous study [26] demonstrated a good correlation with the reference instrument.

$$UVI = k_{er}.\int_{250\,nm}^{400\,nm} E_\lambda.S_{er}(\lambda)\,.d\lambda \,, \qquad (1)$$

where k_{er} is a constant equal to 40 W^{-1}.m^2, E_λ is the solar spectral irradiance expressed in W.m^{-2} for each wavelength (λ) measurement, S_{er} is the erythema action spectrum depending on λ, and dλ is the wavelength interval.

2.1.2. Bentham Spectroradiometer DTMc300

UVI from a spectroradiometer Bentham DTMc300 was also used. This spectroradiometer is manufactured by Bentham Instrument Ltd. Co. (Reading, England, UK) and is operated by Observatoire de Physique de l'Atmosphère de la Réunion (OPAR) in Saint-Denis, Reunion. The instrument is affiliated with the Network for the Detection of Atmospheric Composition Change (NDACC) since 2015. A calibration is performed every three months with a 150W lamp and a 1000W quartz tungsten halogen lamp from NIST. The wavelength misalignment correction is performed at distance via self-made software [27] by the LOA (Laboratoire d'Optique Atmosphérique) from University of Lille-1, France. UVI is recorded every 15 minutes following the standard formula (Equation 1) [25] using a four-minute wavelength scan in the 280-450 nm wavelength range. The instrument uncertainty is ±5% (coverage factor k=2) [28].

2.2. Methods

Reunion Island is well known by tourists for its various landscapes and outdoor activities: from its sandy beaches to its mountainous inland areas where the highest summit of the island reaches 3070m at the top of the Piton des Neiges. The numerous and well-maintained trails winding through the island make the island's summits easily accessible for all nature enthusiasts all year round, making them among the busiest sites on the island. The Office National des Forêts (ONF - National Forestry Office) estimates that 1,200,000 hikers use the 850-km hike path network every year [29]. The Piton de la Fournaise, one of the world's most active and accessible volcanoes, illustrates this passion for high altitude hiking as it is the most visited place on the island, with approximately 400,000 visitors per year [29]. As for the beach area, it is located on the west coast of the island. This is because of the existence of a coral reef, which makes the shoreline attractive and very popular, especially on weekends and public holidays. The conditions to enjoy these sites are favorable all year as the island benefits from a tropical climate. It is in this context that we decided to assess the UVR exposure on some of the most visited sites to better comprehend what the visitors are exposed to along the numerous altitude hiking trails or when they spend time at the beach. We therefore chose to carry out our surveys on three popular sites: the hike that leads to one of the world's most active volcano, Piton de la Fournaise (hereafter referred to as PDF), as the most visited natural site, the hike that allows visitors to climb up the Piton des Neiges (PDN), the highest summit of the island, and on the beach in St-Leu (LEU), one of the most frequented beaches. These sites are shown in **Figure 2**.

The OPAR's spectro-radiometer UVI data was used for this study. Located at Saint-Denis (hereafter referred to as SDN), the instrument affiliated to NDACC provides high quality data, which have been used in several studies. We used UVI from this spectro-radiometer as a comparison to our field measurement campaign.

The field measurement campaign took place in December 2019. The measurement protocol used in this study was the same as in previous studies [6,30]. Ambient erythemal UVR measurements were made using a handheld Solarmeter Model 6.5 UV Index Meter (SN#10414). Measurements were made every 10 minutes by volunteers following the supplier measurement recommendations. Cumulative Standard Erythemal Doses (SED) were calculated from UVI following Equation 2. One SED is equivalent to 100 J.m^{-2}.

$$UV_d = \sum_i \frac{\Delta t \times UVI}{k_{er} \times 100}, \qquad (2)$$

where UV_d is the cumulative dose (SED unit), Δt the interval time between two measurements, k_{er} the constant defined in equation 1 and 100 a factor for the conversion from [J.m^{-2}] to [SED].

The UVI from the Bentham DTMc300 at the OPAR UV station (hereafter referred to as SDN) was compared to the experiments, only on an indicative basis as the different sites do not have the same

environment and atmospheric conditions. Hourly mean and standard deviation (Equations 3 and 4) of SDN UVI will be computed using December 2019 data.

$$\overline{UVI} = \frac{1}{n}\sum\nolimits_{i=1}^{n} UVI_i \,, \tag{3}$$

$$\sigma = \sqrt{\frac{1}{n-1}\sum\nolimits_{i=1}^{n}(UVI_i - \overline{UVI})^2} \,, \tag{4}$$

where $\overline{UVI}$ is the mean of UVI and σ the standard deviation, n is the number of UVI observations during the measurement campaign (December 2019).
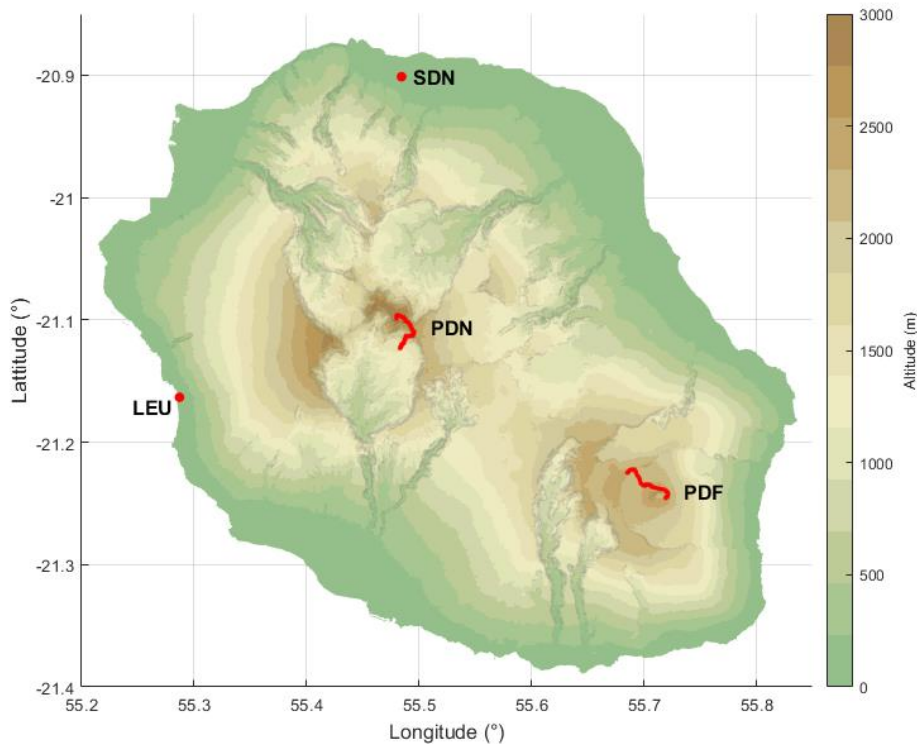
Figure 2. Measurement campaign locations at Reunion Island. The red dots show St-Leu Beach (LEU) and OPAR UV station at Saint-Denis (SDN). The red lines show the hike paths during the Piton de la Fournaise (PDF) and Piton des Neiges (PDN) hikes. The color bar on the right side displays the altitude in meters.

3. Results and Discussion

The hike to PDF took place on 15/12/2019 and lasted 6h (**Figure 3a,b**). The environment is completely exposed to the sun except during the first and the last 10 minutes, where short vegetation and relief can interfere with UVR measurement. The grey area at the bottom of **Figure 3a** highlights the presence of cloud (cumulus) from the typical diurnal cloud formation of the island [31,32]. Clouds may have reduced the UVR, but it could also be increased by cloud scattering [33]. The UVI was extreme (>11) for 3.5 hours and reached a maximum value of 21.1. The total cumulative dose during this hike was 57 SED (**Figure 3b**) (**Table 2**).

The hike to PDN took place four days later on 19/12/2019 and lasted 8h30 (**Figure 3c,d**). Different environmental situations affected the UVR during this hike experiment. The first and the third grey areas (from 6 a.m. to 8.50 a.m. and from 1 p.m. to 2.30 p.m.) depicted at the bottom of **Figure 3c** show the presence of a dense tropical forest and relief where UVI was strongly attenuated. There was

almost no direct sunlight during these periods of time. Other than these periods of respite, there was no vegetation and no relief which can affect UVR measurement. From 11.10 a.m. to 2.30 p.m., in the downward direction of the hike, UVI measurements were performed in the presence of cumulus cloud cover that stretched from the summit to the base of PDN. During the descent phase, UVI first increased due to increased cloud scattering, then decreased. The UVI was extreme (>11) for 3.5 hours and reached a maximum value of 22.5. The total cumulative dose during this hike was 65 SED (**Figure 3d**) and (**Table 2**).

The beach UVR campaign at St-Leu site took place on 28/12/2019 and was the longest experiment in duration, i.e. 9hrs. As seen from the grey shaded areas depicted at the bottom of Figure 3e, some morning clouds had developed and then quickly dissipated, thereby reducing UVR. The UVI was extreme (>11) during three consecutive hours and reached a maximum value of 14.5. The total cumulative dose during this experiment was 64 SED (**Figure 3f**) (**Table 2**).

Taking into account the differences in environmental and meteorological characteristics from one experimental site to another, in addition to differences in observation duration, these results cannot be inter-compared. However, regardless of location and height, all experiments showed situations of very high and extreme exposure to UV radiation. As expected, the PDN hike showed the highest UV index (22.4) at the highest summit of the island (3070m). Regarding exposure, the beach experience at St-Leu highlighted the longest exposure time. In fact, as seen in Figure 3e, we observed more than 4.5 hours of continuous exposure to very high UVI values (higher than 8), during the local 10h00-14h30 time period, resulting in a cumulative dose of ~50 SEDs. Moreover, for all sites, the obtained cumulative doses were extremely high (higher than 50 SED) (see **Figure 3b,d,f**).

UVR data at SDN showed a December-2019 UVR level higher than the December climatological UVR level (December averaged values derived over 11-years of continuous UVR observations from 2009 to 2019) (**Figure 4**). It was observed that the UVI values averaged over December 2019 were higher than the climatological values, but within one standard deviation. The orange shaded area in **Figure 4a** highlights a higher dispersion in the afternoon. As reported by Cadet et al. [22], the observed daily variability could be induced by cloud cover which was higher in the afternoon over the SDN site. This situation is explained by the position of Reunion Island in the east-west trade wind flow and the topography of the island [31-33].

Schoolchildren and outdoor workers are subject to UVR risk. An estimation of the possible exposure can be computed from the daily ambient UVR (Bentham DTMc300 spectro-radiometer) following Wright et al. [34]. Schoolchildren receive 5% of daily ambient UVR whereas outdoor workers receive 20%. Possible UVR exposures are 3 SED and 12 SED for schoolchildren and outdoor workers respectively. These exposures can induce sunburn depending on skin phototype (Table). Several factors can influence the percentage of UVR. Previous studies showed that outdoor workers may experience 10% to 70% of the daily ambient UVR depending on their activity [35].

Météo-France provides UV Index forecasting. The forecast is provided by the 3-D MOCAGE model [36]. The latter is a chemistry transport model which is able to reproduce multiple chemical, dynamical and physical processes such as convection, chemistry and climate interactions or emissions and depositions. It is used both for research and operational purposes at Météo-France. The UV Index calculation in MOCAGE are based on lookup table. These are pre-computed tables generated with the TUV model for multiple values of ozone profile, altitude, solar zenith angle, surface albedo and aerosols. These tables are then used during the MOCAGE simulation in order to determine UV index at a model grid point for specific values of ozone, solar zenith angle, albedo, altitude and aerosols [5]. Depending on the nebulosity, a correction is applied on the UV index value [37]. The maximum of UVI recordings made during the experiment at PDF and LEU were 21.1 and 14.5, while Météo-France UVI forecast was 18 and 16, respectively. The maximum UVI recorded at

PDN experiment was 22.4, while UVI forecast at the beginning of the PDN hike (Cilaos village, 1200m) was 16. On an indicative basis, by using UVI gradient with altitude [38], UVI forecast could be 20 at PDN summit. Overall, during December 2019 at SDN, Météo-France forecasts underestimated UVI values by 10% in comparison to the OPAR Bentham DTMc300 spectro-radiometer. The UVI forecast bias with the handheld radiometer and the spectro-radiometer can be explained by 1) the instrument's uncertainties, 10% and 5% respectively, 2) by the difficulties to estimate the cloud effect on UVI (direct attenuation or enhancement by multiple scattering) in a tropical environment where cloud cover is highly variable, especially at altitude, 3) by the difficulty for the model to take into account cloud covering at short space scales with high altitude variation and 4) by the difficulties of the MOCAGE model in estimating ozone levels in tropics regions of the southern hemisphere.

On an indicative basis, we used the UVI climatology at SDN (2009-2019) and altitude profile of the three experiments (PDF, PDN and LEU) to compute the cumulative exposure doses. We used a UVI gradient from Blumthaler et al. (1997) [38]: +15.1%/1000m at 60° solar elevation and +18.6%/1000m at 20° solar elevation. We obtained the cumulative exposure doses of 52, 67 and 51 SED for PDF, PDN and LEU, respectively. These results were comparable to the cumulative exposure doses measured. However, these results should be taken with reservation as the use of a simple coefficient may not be sufficient [39]. UVI depends on other parameters such as ozone, cloud, albedo and aerosols. The atmospheric chemical composition is very different on each side of the boundary layer [40-42]. The low aerosol load above the boundary layer induces higher UVR.

For comparison, we looked at the same time period of the three experiments, i.e. 9 a.m. to 1 p.m. (6h duration). The partial cumulative doses at PDF, PDN and LEU were 53, 59 and 39 respectively. Differences between these results are compatible with the UVR gradient with altitude proposed by Blumthaler et al. (1997) [38].

Table 2. Summary of the experiment results, with the associated cumulative doses.

	Activity	Date	Duration	Altitude	Cumulative dose
PDF	Hike	15/12/2019	6h	2280-2480 m	57 SED
PDN	Hike	19/12/2019	8.5h	1370-3070 m	65 SED
LEU	Beach	28/12/2019	9h	1 m	64 SED
SDN	UV station	12/2019	11h (full day)	85 m	59 SED
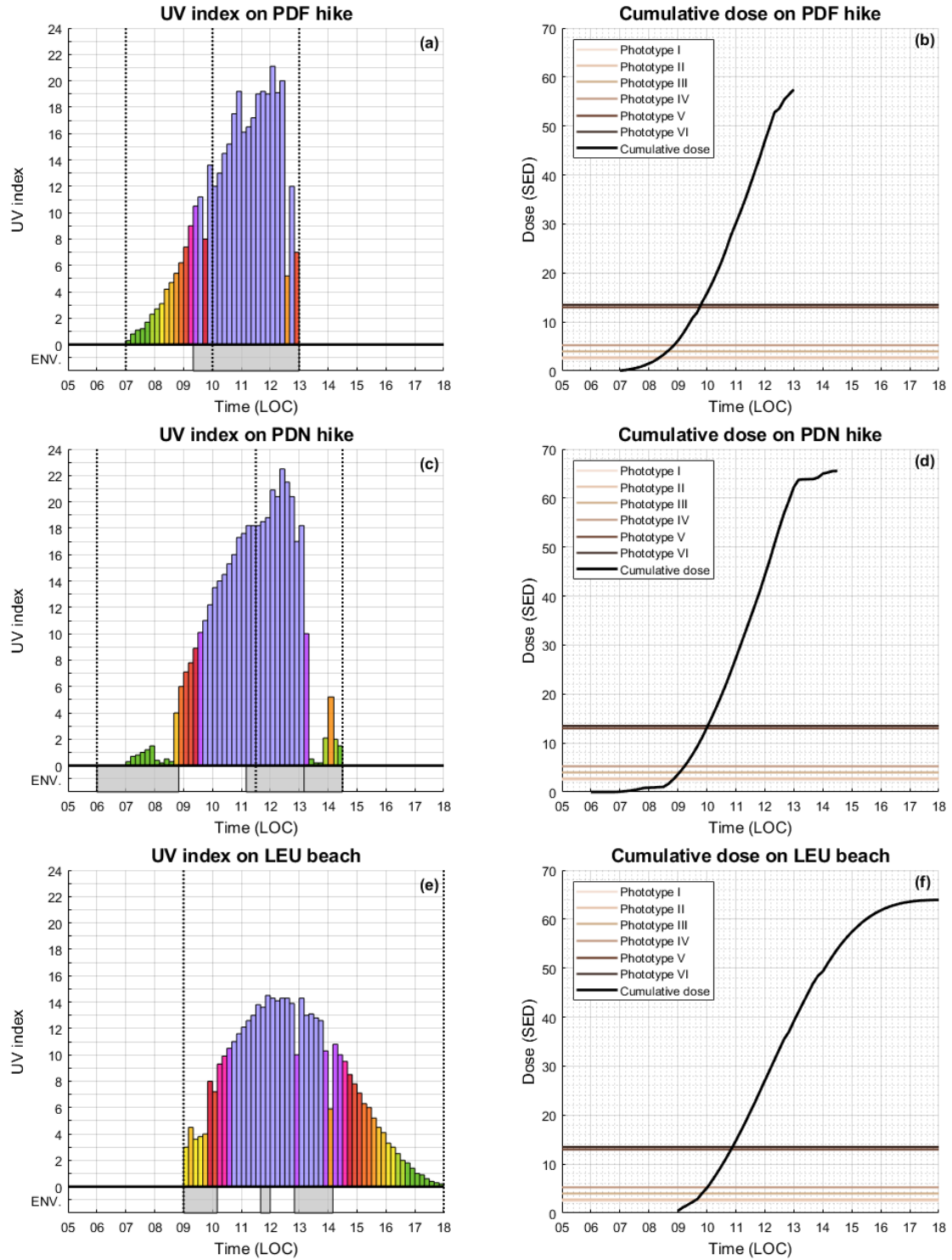
Figure 3. (a), (c) and (e) show UVI recorded at PDF, PDN and LEU respectively. The colors of the histograms also represent the UVI following the standard UVI color scale. Vertical dotted lines show the beginning and the end of the activities. For PDF and PDN, a third vertical dotted line shows the U-turn point, between the ascending and descending part of the hikes. The grey surfaces, ENV., at the bottom of the figures show environmental effects affecting UVR, mainly cloud cover and shade. Cumulative UV doses at PDF, PDN and LEU are shown in (b), (d) and (f) respectively. The black curves on the right plots represent the cumulative exposure doses, while the superimposed horizontal lines show the threshold for one exposure dose to sunburn as a function of skin phototype (Table).
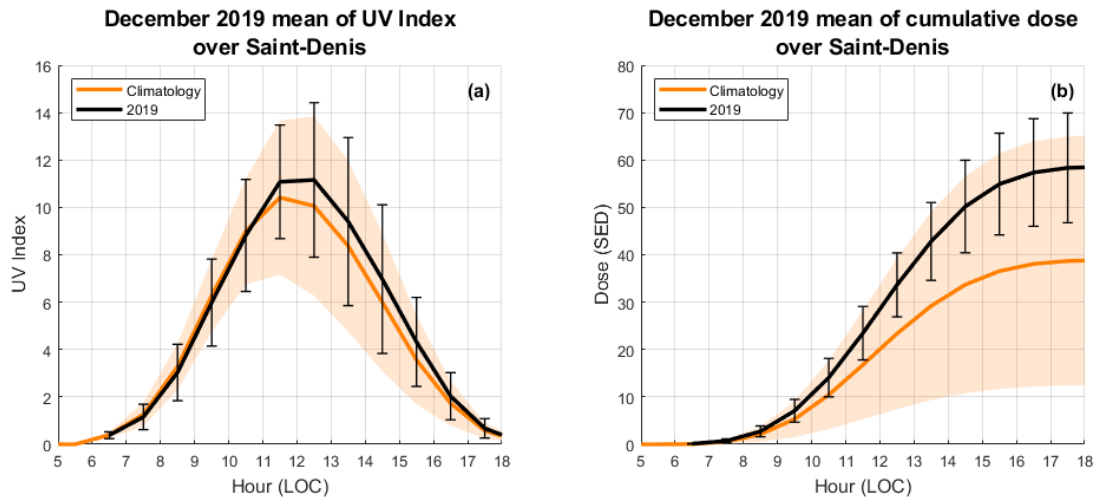
Figure 4. (a) represents a comparison of UVI between the December 2019 mean (black) and the December climatological mean (orange) at Saint-Denis; (b) represents a comparison of the cumulative exposure dose (SED) between the December 2019 mean (black) and the December climatological mean (orange) over Saint-Denis derived from UVI data (a). The orange lines represent the December climatological mean and the shaded areas one standard deviation as derived from 2009-2019 observations. The black lines represent the December 2019 mean and the vertical black bars one standard deviation.

4. Conclusions

Reunion Island is a popular tourist destination for its sandy beaches, active volcano and mountains. Over a million people go through the hike path network every year. In this context where people are extremely exposed, UVR assessment was performed over three popular sites: the volcano Piton de la Fournaise, the highest summit Piton des Neiges and Saint-Leu beach. These measurements took place during December 2019. Measurements showed that Reunion Island is exposed to extreme UVR conditions. The UVR assessment performed revealed that total UVR exposure can reach 65 SED. These exposure doses correspond to several times the minimal erythemal dose to elicit sunburn for each skin phototype. Public awareness of the risks related to UVR exposure becomes crucial when people do not use suitable protection since extreme UVR exposure can cause first-, second-, or third-degree burns and increase the risk of long-term physiological diseases [43]. Anecdotally, most people are usually not informed well of the dangers of long-term exposure to UVR especially in a tropical environment. Météo-France provides UVI forecasts [5], but this information is only available on Météo-France website, making them, unfortunately, less accessible or known. This information would be more useful to the population if it is broadcasted along with the daily weather (i.e. temperature, rainfall, wind etc.) forecasts. As the entire population could be exposed to UVR when spending time outside, be it for professional or leisurely activities, it is fair to say that a daily UVI forecast would be in the public health interest. In the case of UV experiment at Saint-Leu beach, for example, we observed about 4.5 hours of continuous exposure to very high UVI values, between 10h00 and 14h30 local time, resulting in a cumulative dose of ~50 SEDs. Therefore, the public must be informed of the danger of UV exposure and it should be recommended to avoid sun bath and UV exposure during this time slot. Along with more awareness campaigns and more efficient measuring devices placed around the island, a general understanding of UVR will improve, thereby reducing the risks linked to excess exposure resulting from insufficient UVR protection. As the Island's trails and beaches are where tourists and locals are most exposed to UVR, signboards, placed in key areas, would be useful in raising awareness and improving people's attitude towards UVR exposure risks. These notices, placed at the beginning of hiking trails and entrances to beaches would summarize the risks and the protective measures that should be taken regarding solar UVR exposure. It is needless

to say that Reunion observations and the above recommendations may be relevant to many other sites in tropical countries and territories.

References

1. Kerr, J. B.; Fioletov, V. E.; Surface ultraviolet radiation. *Atmosphere-Ocean* **2008**, 46, 159-184, doi: 10.3137/ao.460108.
2. International Commission on Non-Ionizing Radiation Protection. Guidelines on limits of exposure to ultraviolet radiation of wavelength between 180 nm and 400 nm. *Health Phys.* **2004**, 86, 171-186.
3. Bais, A. F.; Lucas, R. M.; Bronman, J. F.; Williamson, C. E.; Sulzberger, B.; Austin, A. T.; Wilson, S. R.; Andrady, A. L.; Bernhard, G.; Richard, L.; et al.; Royal Society of Chemistry: London, United Kingdom. Environmental effects of ozone depletion, UV radiation and interactions with climate change: UNEP Environmental Effects Assessment Panel, update 2017. *Photochemical and Photobiological Sciences* **2018**, 17, 127-179, doi: 10.1039/C7PP90043K.
4. Tarasick, D. W.; Fioletov, V. E.; Wardle, D. I.; Kerr, J. B.; McArthur, L. J.; McLinden, C. A.; Climatology and trends of surface UV radiation: Survey article. *Atmosphere-Ocean* **2010**, 41, 121-138, doi: 10.3137/ao.410202
5. Jégou, F.; Godin-Beekmann, S.; Corrêa, M. P.; Brogniez, C.; Auriol, F.; Peuch, V. H.; Haeffelin, M.; Pazmiño, A.; Saiag, P.; Goutail, F.; Mahé, A.; Validity of satellite measurements used for the monitoring of UV radiation risk on health. *Atmospheric Chemistry and Physics* **2011**, 11, 13377-13394, doi: 10.5194/acp-11-13377-2011.
6. Cadet, J.-M.; Bencherif, H.; du Preez, D. J.; Portafaix, T.; Sultan-Bichat, N.; Belus, M.; Brogniez, M.; Auriol, F.; Metzger, J.-M.; Ncongwane, K.; Coetzee, G. J. R.; Wright, C. Y.; Solar UV radiation in Saint-Denis, La Réunion and Cape Town, South Africa: 10-years climatology and human assessment at altitude. *Atmosphere* **2019**, 10, 589, doi: 10.3390/atmos10100589.
7. Lansdowne, A.; Provost, S.; Vitamin D3 enhances mood healthy subjects during winter. *Psychopharmacology* **1998**, 135, 319-323, doi: 10.1007/s002130050517.
8. Bruern K.; Werfel, T.; Phototherapy. *Kanerva's Occupational Dermatology* **2019**, 1279-1288, doi: 10.1007/978-3-319-68617-2_90.
9. Rajakumar, K.; Greenspan, S. L.; Thomas, S. B.; Holick, M. F.; Solar Ultraviolet Radiation AND Vitamin D: A Historical Perspective. *American journal of public health* **2007**, 97, 1746-1754, doi: 10.2105/AJPH.2006.091736.
10. Gallagher, R. P.; Lee, T. K.; Adverse effects of ultraviolet radiation: a brief review. *Progress in Biophysics and Molecular Biology* **2006**, 92, 119-131, doi: 10.1016/j.pbiomolbio.2006.02.011.

11. Lucas, R.; McMichael, T.; Smith, W.; Armstrong, B.; World Health Organization; Solar Ultraviolet Radiation: Global burden of disease from solar ultraviolet radiation. *Environmental Burden of Disease* **2006**, 13, ISSN: 1728-1652. Available on: https://www.who.int/uv/health/solaruvradfull_180706.pdf (accessed on 13/05/2020).

12. Fitzpatrick, T. B.; Skin Phototypes. In Proceedings of the 20th World Congress of Dermatology, Paris, France. 1-5 July 2002.

13. Albert, M. R.; Ostheimer, K. G.; The evolution of current medical and popular attitudes toward ultraviolet light exposure: part 1. *J. Am. Acad. Dermatol.* **2002**, 47, 930-7, doi: 10.1067/mjd.2002.127254.

14. Albert, M. R.; Ostheimer, K. G.; The evolution of current medical and popular attitudes toward ultraviolet light exposure: part 2. *J. Am. Acad. Dermatol.* **2003**, 48, 909-18, doi: 10.1067/mjd.2003.272.

15. Albert, M. R.; Ostheimer, K. G.; The evolution of current medical and popular attitudes toward ultraviolet light exposure: part 3. *J. Am. Acad. Dermatol.* **2003**, 49, 1096-1106, doi: 10.1016/S0190-9622(03)00021-5.

16. Arnold, M.; Kvaskoff, M.; Thuret, A.; Guénel, P.; Bray, F.; Soerjomataram, I.; Cutaneous melanoma in France in 2015 attributable to solar ultraviolet radiation and the use of sunbeds. *Journal of the European Academy of Dermatology and Venerology* **2018**, 32, 1681-1686, doi: 10.1111/jdv.15022.

17. Aubert, P. M.; Seibyl, J. P.; Price, J. L.; Harris, T. S.; Filbey, F. M.; Jacobe, H.; Devous Sr., M. D.; Adinoff, B.; Dopamine efflux in response to ultraviolet radiation in addicted sunbed users. *Psychiatry Research: Neuroimaging* **2016**, 251, 7-14, doi: 10.1016/j.pscychresns.2016.04.001.

18. United Nations Educational, Scientific and Cultural Organization: Pitons, cirques and remparts of Reunion Island. Available online: https://whc.unesco.org/en/list/1317/ (accessed on 10/05/2020)

19. Comité Régional du Tourisme; *2018 Fréquentation Touristique*; Comité Régional du Tourisme: Saint-Paul, La Réunion, 2019. Available online: https://pro.reunion.fr/actualites/etudes-et-indicateurs/chiffres-du-tourisme-2018-le-bilan (accessed on 10/05/2020).

20. Fioletov, V.; Kerr, J. B.; Fergusson, A.; The UV Index: Definition, Distribution and Factors Affecting it. *Can. J. Public Health* **2010**, 2010, 101, 15-19, doi: 10.1007/BF03405303.

21. Lamy, K.; Portafaix, T.; Brogniez, C.; Godin-Beekmann, S.; Bencherif, H.; Morel, B.; Pazmino, A.; Metzger, J.-M.; Auriol, F.; Deroo, C.; Duflot, V.; Goloub, P.; Long, C. N.; Ultraviolet radiation modelling from ground-based and satellite measurements on Reunion Island, southern tropics. *Atmospheric Chemistry and Physics* **2018**, 18, 227-246, doi: 10.5194/acp-18-227-2018.

22. Cadet, J.-M.; Portafaix, T.; Bencherif, H.; Lamy, K.; Brogniez, C.; Auriol, F.; Metzger, J.-M.; Boudreault, L.-E.; Wright, C. Y.; Inter-Comparison Campaign of Solar UVR Instruments under Clear Sky Conditions at Réunion Island. *Int. J. Environ. Res. Public Health* **2020**, 17, 2867, doi: 10.3390/ijerph17082867.

23. Sin, C.; Beauchet, A.; Marchal, A.; Sigal, M. L.; Mahé, E.; Compréhension et utilisation de l'indice universel de rayonnement solaire (« indice ultraviolet ») par les dermatologues français métropolitains. *Annales de dermatologie et de vénéréologie* **2013**, 140, 15-20, doi: 10.1016/j.annder.2012.09.010.

24. Warocquier, J.; Miquel, J.; Chirpaz, E.; Beylot-Barry, M.; Sultan-Bichat, N.; Groupe de travail des dermatologues et anatomopathologistes de l'île de la Réunion; Données épidémiologiques des mélanomes cutanés à la Réunion en 2015. *Annales de Dermatologies et de Vénéréologie* **2016**, 143, S323-S314, doi: 10.1016/j.annder.2016.09.476.

25. World Health Organization (WHO) *Global solar UV index: a practical guide*; World Health Organization (WHO): Geneva, Switzerland, 2002. Available online: https://www.who.int/uv/publications/en/UVIGuide.pdf (accessed on 08 May 2020).

26. de Paula Corrêa, M.; Godin-Beekmann, S.; Haeffelin, M.; Brogniez, C.; Verschaeve, F.; Saiag, P.; Pazmiño, A.; Mahé, E.; Comparison between UV index measurements performed by research-grade. *Photochemical & Photobiological Sciences* **2010**, *9(4)*, 459-463, doi: 10.1039/B9PP00179D.

27. Houët, M. *Spectroradiométrie du Rayonnement Solaire UV au Sol: Améliorations Apportées à L'instrumentation et au Traitement des Mesures, Analyse pour L'évaluation du Contenu Atmosphérique en Ozone et en Aérosols*; Université de Lille: Lille, France, 2003.

28. Brogniez, C.; Auriol, F.; Deroo, C.; Arola, A.; Kujanpää, J.; Sauvage, B.; Kalakoski, N.; Pitkänen, N.R.A.; Catalfamo, M.; Metzger, J.-M.; et al. Validation of satellite-based noontime UVI with NDACC ground-based instruments: Influence of topography, environment and satellite overpass time. *Atmos. Chem. Phys.* **2016**, *16*, 15049–15074, doi: 10.5194/acp-16-15049-2016.

29. ONF Réunion. Accessible online: http://www1.onf.fr/la-reunion/@@index.html (accessed on 14/05/2020)

30. Mahé, E.; de Paula Corrêa, M.; Godin-Beekmann, S.; Haeffelin, M.; Jégou, F.; Saiag, P.; Beauchet, A. Evaluation of tourists' UV exposure in Paris. *J. Eur. Acad. Dermatol. Venereol.* **2013**, 27, e294-e304, doi: 10.1111/j.1468-3083.2012.04637.x.

31. Jumeaux, G.; Quetelard, H.; Roy, G. Atlas Climatique de La Réunion; Météo-France Direction Interrégionale de la Réunion: Sainte-Clotilde, La Réunion, 2002.

32. Cadet, B.; Goldfarb, L.; Faduilhe, D.; Baldy, S.; Réchou, A.; Giraud, V.; Keckhut, P. A sub-tropical cirrus clouds climatology from Reunion Island (21S, 55E) LiDAR data set. *Geophys. Res. Lett.* **2003**, 30, 1130, doi: 10.1029/2002GL016342.

33. Cede, A.; Blumthaler, M.; Luccini, E.; Piacentini, R. D.; Nuñez, L. Effects of clouds on erythemal and total irradiance as derived from data of the Argentine Network. *Geophys. Res. Lett.* **2002**, 29, 76-1-76-4, doi: 10.1029/2002GL015708.

34. Wright, C.Y.; Brogniez, C.; Ncongwane, K.P.; Sivakumar, V.; Coetzee, G.; Auriol, F.; DeRoo, C.; Sauvage, B.; Metzger, J.-M.; Metzger, J. Sunburn Risk Among Children and Outdoor Workers in South Africa and Reunion Island Coastal Sites. *Photochem. Photobiol.* **2013**, 89, 1226–1233, doi: 10.1111/php.12123.

35. Larkö, O.; Diffey, B. L.; Natural UV-B radiation received by people with outdoor, indoor, and mixed occupations and UV-B treatment of psoriasis. *Clin. Exp. Dermatol.* **1993**, 8, 279-285, doi: 10.1111/j.1365-2230.1983.tb01780.x

36. Josse, B.; Simon, P.; Peuch, V.-H.; Radon global simulations with the multiscale chemistry and transport model MOCAGE. *Tellus B: Chemical and Physical Meteorology* **2004**, 56, 339-356, doi: 10.3402/tellusb.v56i4.16448.

37. Peuch, V.-H.; Cathala, M.-L.; Dessens, O.; Josse, B.; Simon, P.; Peuch, A.; Pailleux, J.; Cammas, J.-P.; Simulations and forecasts in the UTLS and stratosphere with the chemistry and transport model MOCAGE, Proceedings of the ECMWF/SPARC Workshop on Modelling and Assimilation for the Stratosphere and Tropopause, 23 to 26 June 2003, Reading, England, 2004; Accessible online: https://www.ecmwf.int/en/elibrary/11664-simulations-and-forecasts-utls-and-stratosphere-chemistry-and-transport-model (accessed on 09/08/2020).

38. Blumthaler, M.; Ambach, W.; Ellinger, R.; Increase in solar UV radiation with altitude. *Journal of Photochemistry and Photobiology B: Biology* **1997**, 39, 130-134, doi: 10.1016/S1011-1344(96)00018-8.

39. Pfeifer, M. T.; Koepke, P.; Reuder, J.; Effects of altitude and aerosol on UV radiation. *Journal of Geophysical Research: Atmospheres* **2006**, 111, D01203, doi: 10.1029/2005JD006444.

40. Guilpart, E.; Vimeux, F.; Metzger, J.-M.; Evan, S.; Brioude, J.; Cattani, O.; Dynamic of the atmospheric boundary layer from the isotopic composition of surface water vapor at the Maïdo Observatory (La Réunion, Indian Ocean); EGU General Assembly 2016: Vienna, Austria, 2016. Available online: https://ui.adsabs.harvard.edu/abs/2016EGUGA..18.6075G/abstract (accessed on 08 June 2020).

41. Duflot, V.; Tulet, P.; Flores, O.; Barthe, C.; Colomb, A.; Deguillaume, L.; Vaitilingom, M.; Perring, A.; Huffman, A.; Hernandez, M.; et al.; Preliminary results from the FARCE 2015 campaign: multidisciplinary study of the forest–gas–aerosol–cloud system on the tropical island of La Réunion. *Atmospheric Chemistry and Physics* **2019**, 19, 10591-10618, doi: 10.5194/acp-19-10591-2019.

42. Rocco, M.; Colomb, A.; Baray, J.-L.; Amelynck, C.; Verreyken, B.; Borbon, A.; Pichon, J.-M.; Bouvier, L.; Schoon, N.; Gros, V.; Sarda-Esteve, R.; Tulet, P.; Metzger, J.-M.; Duflot, V.; Guadagno, C.; Peris, G.; Brioude, J. Analysis of Volatile Organic Compounds during the OCTAVE Campaign: Sources and Distributions of Formaldehyde on Reunion Island. *Atmosphere* **2020**, 11, 140, doi: 10.3390/atmos11020140.

43. Sanchez-Pérez, J. F.; Vicente-Agullo, D.; Barbera, M.; Castro-Rodriguez, E.; Canovas, M.; Relationship between ultraviolet index (UVI) and first-, second-and third-degree sunburn using the Probit methodology. *Scientific reports* **2019**, 9, 1-13, doi: 10.1038/s41598-018-36850-x.

CONCLUSION

Le rayonnement solaire ultraviolet solaire joue un rôle quotidien dans notre vie sur Terre. Acteur majeur dans le processus de synthèse de vitamine D, le rayonnement solaire ultraviolet devient alors nécessaire à notre bonne santé. En revanche, la surexposition à celui-ci est très dangereuse, car elle peut provoquer de nombreuses pathologies : cancer de la peau, cataractes, immunodéficience, etc. Qui plus est, l'évolution des comportements au fil du temps a amené la population à s'exposer davantage au rayonnement solaire, par l'augmentation d'activité en extérieur, ou encore par l'utilisation de cabines de bronzage. La connaissance du risque lié au rayonnement ultraviolet, ainsi que sa mesure précise, est donc primordiale. Les nombreuses interactions avec l'atmosphère rendent la mesure et la quantification du rayonnement ultraviolet complexes. En effet, il réagit avec de plusieurs paramètres atmosphériques, tel que l'ozone, les aérosols ou les nuages, par exemple. Les paramètres géographiques et temporels sont également très importants. L'irradiance solaire n'est en effet pas la même au niveau de l'équateur qu'aux pôles, à midi qu'au levé/couché du soleil.

La première partie de ce travail a été consacrée à l'évaluation de différents instruments de mesures du rayonnement ultraviolet, au sol et à bord de satellite. Une comparaison entre des radiomètres larges bandes Solar Light UV-Biometer Model 501 du réseau instrumentés du SAWS en Afrique du Sud et l'instrument OMI à bord du satellite Aura a été effectuée. Les résultats ont montré un bon accord entre les deux jeux de données. Cependant, il a été mis en évidence d'une part, la nécessité de calibrations et d'exercice d'inter-comparaisons plus réguliers, et d'autre part, la limite des mesures par satellites, notamment la difficulté d'évaluer la donnée sur des échelles d'espace très petites. Par la suite, une campagne d'inter-comparaison a été effectuée à La Réunion. Cette campagne a permis d'évaluer la performance sur une année de 4 radiomètres larges bande, en comparaison à un spectro-radiomètre de référence. Les résultats d'inter-comparaison sont très encourageants pour trois des quatre radiomètres. En effet, il a été trouvé un faible écart avec la référence ainsi qu'une très bonne stabilité temporelle. Là aussi, la calibration des radiomètres a joué un rôle déterminant dans les résultats.

Les données de ces différents instruments ont par la suite été utilisées pour le calcul de climatologie et de tendance, notamment à La Réunion. En effet, La Réunion est une île

montagneuse qui cumule des paramètres géographiques et atmosphériques favorisant une forte intensité du rayonnement solaire. La climatologie a montré que les indices UV, utilisés pour la quantification du rayonnement UV, sont de 8 en hivers et peuvent aller jusqu'à 16 en été. Pour rappel, le seuil d'exposition extrême fixé par l'OMS est un indice UV de 11. En été, le rayonnement UV est au moins extrême 80% du temps. Le calcul de tendance a montré pour La Réunion une augmentation d'intensité sur une période de 10 ans. Cette augmentation peut être due à un changement de paramètres atmosphériques. Cependant, une étude plus complète et focalisée de tendance doit être réalisée.

Le rayonnement ultraviolet étant de très forte intensité à la Réunion, la population y est donc fortement exposée. De plus, La Réunion est une destination touristique prisée, dont la plupart des activités se font en extérieur. La dernière partie de ce travail a été d'évaluer l'exposition de la population sur les lieux fréquentés. Quatre sites populaires ont été choisis. Les mesures ont été effectuées à l'aide d'un radiomètre portatif. Il a été trouvé des doses très importantes d'exposition au rayonnement UV, dépassant de multiples fois le seuil d'exposition pouvant engendrer des dommages cutanés. La prévention de la population revêt alors une importance capitale.

Cependant, les moyens employés pour la prévention de la population sont faibles voire inexistant. Les nombreuses possibilités d'activités en plein air laissent imaginer que des messages d'information et de prévention des risques liés au rayonnement ultraviolet sur ces sites ne pourraient qu'être bénéfiques pour la santé publique. De plus, la diffusion de prévisions d'indice UV sur les chaînes d'informations pourrait contribuer à l'amélioration des connaissances de la population.

Parallèlement, des études paramétriques plus poussées peuvent être réalisés afin de mieux comprendre et évaluer le rayonnement UV sur une île tropicale comme La Réunion, notamment en fonction de la nébulosité. Des campagnes de terrains de plus grande ampleur peuvent également contribuer à l'amélioration des connaissances sur des sites exposées, où l'environnement a aussi un rôle à jouer, par exemple sur des sites à forte végétation.

Le rayonnement ultraviolet est omniprésent, nécessaire et vital. Sa complète maîtrise ne pourra qu'être bénéfique à l'amélioration de la santé publique.

BIBLIOGRAPHIE

AFSSE. (2005). *Ultraviolets - Etat des connaissances sur l'exposition et les risques sanitaires.* Consulté le 11 05, 2018, sur http://www.ladocumentationfrancaise.fr/rapports-publics/054000600/index.shtml

Albert, M. R., & Ostheimer, K. G. (2002, December). The evolution of current medical and popular attitudes toward ultraviolet light exposure: part 1. *J Am Acad Dermatol, 47*(6), 930-7. doi:10.1067/mjd.2002.127254

Albert, M. R., & Ostheimer, K. G. (2003, June). The evolution of current medical and popular attitudes toward ultraviolet light exposure: part 2. *J Am Acad Dermatol, 48*(6), 909-18. doi:10.1067/mjd.2003.272

Albert, M., & Ostheimer, K. (2003). The evolution of current medical and popular attitudes toward ultraviolet light exposure: Part 3. *Journal of the American Academy of Dermatology*, 1096-1106.

Anton, M., Cachorro, V. E., Vilaplana, J. M., Toledano, C., Krotkov, N. A., Arola, A., . . . de la Morena, B. (2010). Comparison of UV irradiances from Aura/Ozone Monitoring Instrument (OMI) with Brewer measurements at El Arenosillo (Spain) - Part 1: Analysis of parameter influence. *Atmos. Chem. Phys., 10*, 5979-5989.

Armstrong, B. K., & Kricker, A. (1993). How much melanoma is caused by sun exposure ? *Melanoma research, 3*(6), 395-401.

Arnold, M., Kvaskoff, M., Thuret, A., Guenel, P., Bray, F., & Soerjomataram, I. (2018, April 28). Cutaneous melanoma in France in 2015 attributable to solar ultraviolet radiation and the use of sunbeds. *Journal of The European Academy of Dermatology and Venereology, 32*(10), 1681-1686. doi:10.1111/jdv.15022

Arola, A., Kazadzis, S., Lindfors, A., Krotkov, N., Kujanpää, N., Tamminen, J., . . . Brogniez, C. (2009). A new approach for absorbing aerosols in OMI UV. *Geophys. Res. Lett., 36*, L22805.

ARVAM. (2015). *Crèmes solaires, perturbateurs endocriniens, santé humaine et impact sur les récifs coralliens.*

Aubert, P. M., Seibyl, J. P., Price, J. L., Harris, T. S., Filbey, F. M., Heidi, J., . . . Adinoff, B. (2016, May 30). Dopamine efflux in response to ultraviolet radiation in addicted sunbed users. *Psychiatry Research: Neuroimaging, 251*, 7-14. doi:10.1016/j.pscychresns.2016.04.001

Bais, A. F., Blumthaler, M., Gröbner, J., Seckmeyer, G., Webb, A. R., Gorts, P., . . . Wuttke, S. (2003). Quality Assurance of spectral ultraviolet measurements in Europe through the development of a transportable unit (QASUME). *Ultraviolet Ground- and Space_based Measurements, Models, and Effects II, 4896*, 232-238. doi:10.1117/12.468641

Bais, A. F., Gardiner, B. G., Slaper, H., Blumthaler, M., Bernhard, G., McKenzie, R. L., . . . Redondas, A. (2001, June 01). SUSPEN intercomparison of ultraviolet spectroradiometers. *Journal of Geophysical Research: Atmospheres, 106*(D12), 12509-12525. doi:10.1029/2000JD900561

Bais, A. F., Lucas, R. M., Bornman, J. F., Williamson, C. E., Sulzberger, B., Austin, A. T., & Aucamp, P. J. (2018). Environmental effects of ozone depletion, UV radiation and interactions with climate change: UNEP Environmental Effects Assessment Panel, update 2017. *photochemistry Photobiology Sciences, 17*(2), 127-179. doi:10.1039/C7PP90043K

Bais, A. F., Zerefos, C. S., Meleti, C., Ziomas, I. C., & Tourpali, K. (1993, March). Spectral measurements of solar UVB radiation and its relations to total ozone, SO2 and clouds. *Journal of Geophysical Research: Atmosphères*, 5199-5204. doi:10.1029/92JD02904

Ball, W. T., Staehelin, J., Haigh, J. D., Peter, T., Tummon, F., Stübi, R., . . . Yu, P. (2018, Feb 06). Evidence for a continuous decline in lower stratospheric ozone offsetting ozone layer recovery. *Atmospheric Chemistry and Physics, 18*(2), 1379-1394. doi:10.5194/acp-18-1379-2018

Barnes, M. L., Miura, T., & Giambelluca, T. W. (2016). An assessment of Diurnal and seasonal Cloud Cover Changes over the Hawaiian Islands Using Terra and Aqua MODIS. *Journal of Climate, 29*(1), 77-90. doi:10.1175/JCLI-D-15-0088.1

Barth, J., Cadet, J., Césarini, J., Fitzpatrick, T., McKinlay, A., Mutzhas, M., . . . Urbach, F. (1999). 134/1 TC 6-26 Report: Standardization of the terms UV-A1, UV-A2, and UV-B. *Collection in Photobiology and Photochemistry. Vienna, Austria: Commission Internationale de l'Eclairage*. Consulté le 10 01, 2018, sur www.cie.co.at/publications/cie-collection-photobiology-photochemistry-1999

Bencherif, H., Amraoui, L. E., Kirgis, G., Leclair de Bellevue, J., Hauchecorne, A., Mzé, N., . . . Goutail, F. (2011). Analysis of a rapid increase of stratospheric ozone during late austral summer 2008 over Kerguelen (49.4°S, 70.3°E). *Atmospheric Chemistry and Physics, 11*, 363-373. doi:10.5194/acp-11-363-2011

Bencherif, H., Portafaix, T., Baray, J.-L., Morel, B., Baldy, S., Leveau, J., . . . Diab, R. (2001). LIDAR observations of lower stratospheric aerosols over South Africa linked to large scale transport across the southern subtropical barrier. *Journal Atmospheric Solar Terrestrial Physics, 65*(6), 707-715. doi:10.1016/S1364-6826(03)00006-3

Bernhard, G., & Seckmeyer, G. (1999). Uncertainty of measurements of spectral solar UV irradiance. *Journal of Geophysical Research: Atmospheres, 104*(D12), 14321-14345. doi:10.1029/1999JD900180

Bernhard, G., Arola, A., Dahlback, A., Fioletov, V., Heikkilä, A., Johnsen, B., . . . Tamminen, J. (2015). Comparison of OMI UV onservation with ground-based measurements at high northern latitudes. *ACP, 15*, 7391-7412.

Bessemoulin, P., & Oliviéri, J. (2000, 09). Le rayonnement solaire et sa composante iultraviolette. *La météorologie 8ème série - n°31*, 42-59. Consulté le 10 01, 2018, sur http://documents.irevues.inist.fr/bitstream/handle/2042/36135/meteo_2000_31_42.pdf?sequence=1

Blumthaler, M. (2018, AUG 11). UV Monitoring for Public Health. *International Journal of environmental Research and Public Health, 15*(8), 1723. doi:10.3390/ijerph15081723

Blumthaler, M., Ambach, R., & Ellinger, R. (1996). Increase in solar UV radiation with altitude. *Photochemistry and photobiology*, 130-134. doi:10.1016/S1011-1344(96)00018-8

Bodeker, G. E., & McKenzie, R. L. (1996, February 9). An Algorithm for Inferring Surface UV Irradiance Including Cloud Effects. *Journal of applied meteorology, 35*(10), 1860-1877. doi:10.1175/1520-0450(1996)035<1860:AAFISU>2.0.CO;2

Bodeker, G. E., & Scourfield, M. W. (1998). Estimated past and future variability in UV radiation in South Africa based on trends in total column ozone. *S. Afr. J. Sci., 94*, 24-33.

Börner, F. U., Schütz, H., & Wiedemann, P. (2009, July). A population-based survey on tanning bed use in Germany. *BMC Dermatol, 9*(6). doi:10.1186/1471-5945-9-6

Breiman, L. (2001). Random forests. *Mach. Learn, 45*, 5-32. doi:10.1023/A:1010933404324.

Brogniez, C., Auriol, F., Deroo, C., Arola, A., Kujanpää, J., Sauvage, B., . . . Da Conceicao, P. (2016, 12 06). Validation of satellite-based noontime UVI with NDACC ground-based instruments: influence of topography, environment and satellite overpass time. *Atmospheric Chemistry and Physics, 16*(23), 15049-15074. doi:10.5194/acp-16-15049-2016

Bruern, K., & Werfel, T. (2019). Phototherapy. *Kanerva's Occupationnal Dermatology*, 1279-1288.

Buchard, V., Brogniez, C., Auriol, F., Bonnel, B., Lenoble, J., Tanskanen, A., . . . Veefkind, P. (2008). Comparison of OMI ozone and UV irradiance data with ground-based measurements at two French sites. *Atmos. Chem. Phys., 8*, 4517-4528.

Cadet, B., Goldfarb, L., Faduilhe, D., Baldy, S., Giraud, V., Keckhut, P., & Réchou, A. (2003). A subtropical cirrus clouds climatology from Reunion Island (21°S, 55°E) lidar data set. *Geophysical Research Letters, 30*(3), 1130. doi:10.1029/2002GL016342

Cadet, J., Sage, E., & Douki, T. (2005). Ultraviolet radiation-mediatedd damage to cellular DNA. *Fundamental and Molecular Mechanisms of Mutagenesis, 571*(1-2), 3-17. doi:doi:10.1016/j.mrfmmm.2004.09.012

Cadet, J.-M., Bencherif, H., Du Preez, D. J., Portafaix, T., Brogniez, C., Auriol, F., . . . Wright, C. Y. (2019). Solar UV Radiation in Saint-Denis, La Réunion and Cape Town, South Africa: 10 years Climatology and trends (2009-2018). *French - South African Sciences and Innovations Days.* Pretoria, South Africa.

Cadet, J.-M., Bencherif, H., Du Preez, D. J., Portafaix, T., Sultant-Bichat, N., Belus, M., . . . Wright, C. Y. (2019). Solar UV radiation in Saint-Denis, La Réunion and Cape Town, South Africa: 10 years Climatology and Human Exposure Assessment at Altitude. *Atmosphere, 10*(10), 589. doi:10.3390/atmos10100589

Cadet, J.-M., Bencherif, H., Portafaix, T., Lamy, K., Ncongwane, K. P., Coetzee, G. J., & Wright, C. Y. (2017, November 14). Comparison of Ground-Based and Satellite-Derived Solar UV Index Levels at Six South African Sites. *International journal of environmental research and public health, 14*(11), 1384. doi:10.3390/ijerph14111384

Cadet, J.-M., Portafaix, T., Bencherif, H., Brogniez, C., Sébastien, N., Lallemand, C., & Wright, C. Y. (2018). Inter-comparison campaign of solar UVR instruments at Réunion island (21.0°S, 55.5°E): Findings and recommendations. *European Conference on solar UV monitoring.* Vienna. Consulté le 10 18, 2018, sur http://i115srv2.vu-wien.ac.at/UV_INDEX_ORG/ECUVM2018/Presentations/cadet_poster.pdf

Calbo, J., Pagès, D., & Gonzalez, J.-A. (2004). Empirical studies of cloud effects on UV radiation: A review. *Reviews of Geophysics*. doi:10.1029/2004RG000155

Caldwell, M. M. (1971). Solar UV irradiation and the growth and development of higher plants. *Photophysiology, 6*, 131-177.

Canada.ca. (s.d.). Consulté le 04 26, 2019, sur Canada.ca: https://www.canada.ca/fr/sante-canada/services/securite-soleil/qu-est-que-rayonnement-ultraviolet.html

Cede, A., Blumthaler, M., Luccini, E., Piacentini, R. D., & Nuñez, L. (2002). Effects of clouds on erythemal and total irradiance as derived from data of the Argentine network. *Geophysical Research Letters, 29*(24). doi:10.1029/2002GL015708

Cesana, G., Del Genio, A. D., Ackerman, A. S., Kelley, M., Elsaesser, G., Fridlind, A. M., . . . Yao, M.-S. (2019). Evaluating models' response of tropical low clouds to SST forcingsusing CALIPSO observations. *Atmospheric Chemistry and Physics, 19*(1), 2813-2832. doi:10.5194/acp-19-2813-2019

Césarini, J. P. (1977). Soleil et peau. *Journal de Médecine Esthetique, 14*, 5-12.

Chaillol, I. (2011). *Mesure de l'exposition au rayonnement ultraviolet solaire pour les études épidémiologiques.* Lyon: Université Claude Bernard. Récupéré sur https://tel.archives-ouvertes.fr/tel-00831718

Chambelin, D. (2013). *Navigation Générale* (éd. Institut Aéronautique Jean Mermoz, Vol. 1). Rungis, France: Institut Aéronautique Jean Mermoz.

Chepfer, H., Noel, V., Winker, D., & Chiriaco, M. (2014). Where and when we observe cloud changes due to climate warming? *Geophysical Research Letters, 41*(23), 8387-8395. doi:10.1002/2014GL061792

CIE. (1997). *Standard Erythema Dose: A Review.* Vienna, Austria: Technical Report CIE 125-1997. CIE Central Bureau.

CIE, I. 1. (1999). Erythema reference action spectrum and standard eryhema dose ISO 17166. *Commission Internationale de l'Eclairage*.

Coelho, S. G., Yin, L., Smuda, C., Mahns, A., Kolbe, L., & Hearing, V. J. (2014, 11 21). Photobiological implications of melanin photoprotection after UVB-induced tanning of human skin but not UVA-induced tanning. *Pigment Cell & Melanoma Research, 28*(2), 210-216. doi:10.1111/pcmr.12331

Cooper, O. R., Parrish, D. D., Ziemke, J., Cupeiro, M., Galbally, I. E., Gilge, S., & Naik, V. (2014). Global distribution and trends of tropospherique ozone: An observation-based review. *Elementa: Science of the Anthropocene, 2*, 29. doi:10.12952/journal.elementa.000029

Corrëa, M. d., Godin-Beekmann, S., Haeffelin, M., Bekki, S., Saiag, P., Badosa, J., . . . Mahé, E. (2013). Projected changes in clear-sky erythemal and vitamin D effective UV doses for Europe over the period 2006 to 2100. *Photochemical & Photobiological Sciences, 12*(6), 1053-1064. doi:10.1039/C3PP50024A

de Paula Corrêa, M., Godin-Beekmann, S., Haeffelin, M., Brogniez, C., Verschaeve, F., Saiag, P., . . . Mahé, E. (2010, 02 03). Comparison between UV index measurements performed by

research-grade. *Photochemical & Photobiological Sciences, 9*(4), 459-463. doi:10.1039/B9PP00179D

Diaz, S. B., Paladini, A. A., Braile, H. G., Dieguez, M. C., Deferrari, G. A., Vernet, M., & Vrsalovic, J. (2014, May). Global and direct UV irradiance variation in the Nahuel Huapi National Parl (Patagonia, Argentina) after the eruption of Puyehue-Cordon Caulle (Chile). (Elsevier, Éd.) *Journal of Atmospheric ans Solar-Terrestrial Physics, 112*, 47-56. doi:10.1016/j.jastp.2014.02.006

Diffey, B. L. (1991). Solar ultraviolet radiation effects on biological systems. *Phys. Med. Biol, 36*(3), 299-328. doi:10.1088/0031-9155/36/3/001

Diffey, B. L., & McKinlay, A. F. (1987). A reference action spectrum for ultraviolet induced erythema in human skin. *Human Exposure to UV radiation: Risks and Regulations,*, 83-87.

Diffey, B. L., Jansén, C. T., Urbach, F., & Wulf, H. C. (1996, 09 06). The standard erythemal dose: a new photobiological concept. *Photodermatology, Photoimmunology & Photomedicine, 13*(2), 66-66. doi:10.1111/j.1600-0781.1997.tb00110.x

Dobber, M. R., Voors, R., Dirksen, R. J., Kleipool, Q., & Levelt, P. F. (2008, 04 04). he high-resolution solar referencespectrum between 250 and 550 nm and its application to measurements with the ozone monitoring instrument. *Solar Physics, 249*(2), 281-291. doi:10.1007/s11207-008-9187-7

Du Preez, D., Ajti, J., Bencherif, H., Bègue, N., Cadet, J.-M., Wright, C., & Ajtic, J. (2019, March 6). Spring and summer time ozone and solar ultraviolter radiation variations over Cape Point, South Africa. *Annales Geophysicae, 37*(2), 129-141. doi:10.5194/angeo-37-129-2019

Dubovik, O., Smirnov, A., Holben, B. N., King, M. D., Kaufman, Y. J., Eck, T. F., & Slutsker, I. (2000). Accuracy assessments of aerosol optical properties retrieved from Aerosol Robotic Network (AERONET) Sun and sky radiance measurements. *Journal of Geophysical Research: Atmospheres, 105*(D8), 9791-9806. doi:10.1029/2000jd900040

Duflot, V., Tulet, P., Flores, O., Barthe, C., Colomb, A., Deguillaume, L., . . . al., e. (2019). Preliminary results from the FARCE 2015 campaign: multidisciplinary study of the forest-gas-aerosol-cloud system on the tropical island La Réunion. *Atmospheric Chemistry and Physics, 19*, 10591-10618. doi:10.5194/acp-19-10591-2019

Fan, L., Li, W., Dahlback, A., Stammes, J. J., Stammes, S., & Stammes, K. (2015). Long-term comparisons of UV index values derived from a NILU-UV instrument, NWS, and OMI in the New York area. *Appl. Opt., 54*, 1945-1951.

Fioletov, V. E., McArthur, L. J., Mathews, T. W., & Marrett, L. (2008). On the relation between erythemal and vitamin D action spectrum weighted ultraviolet radiation. *Journal of Photochemistry and Photobiology B: Biology, 95*(1), 9-16. doi:10.1016/j.jphotobiol.2008.11.014

Fioletov, V., Kerr, J. B., & Fergusson, A. (2010). The UV Index: Definition, Distribution and Factors Affecting it. *Canadian Journal Public Health, 101*(4), 15-19. doi:10.17269/cjph.101.1905

Fisher, G. J., Wang, Z., Datta, S. C., Varani, J., Kang, S., & Voorhees, J. J. (1997, 11 13). Phatophysiology of Premature Skin Aging Inducing by Ultraviolet light. *The New England Journal of Medecine, 337*, 1419-1429. doi:10.1056/NEJM199711133372003

Fitzpatrick, T. B. (2002). Skin Phototypes. *20th World Congress of Dermatology, Paris*.

Forsyth, G. G., Kruger, F. J., & Le Maitre, D. C. (2010). *National veldfire risk assessment: Analysis of exposure of social, economic and environmental assets to veldfire hazards in South Africa.* National Resources and the Environment CSIR, Fred Consulting cc.

Fountoulakis, I., & Diémoz, H. (2019, June 5-7). Monitoring of spectral UV irradiance in Aosta, Saint-Christophe, Italy: from measurements to data analysis. *VII Convegno Nazionale Agenti Fisici*.

Fountoulakis, I., Zerefos, C. S., Bais, A. F., Kapsomenakis, J., Koukouli, M.-E., Ohkawara, N., . . . Webb, A. R. (2018). Twenty-five years of spectral UV-B measurements over Canada, Europe and Japan: Trends and effects from changes in ozone, aerosols, clouds and surface reflectivity. *Comptes Rendus Geosciences, 350*(7), 393-402. doi:10.1016/j.crte.2018.07.011

Fountoulakis, L., Bais, A. F., Fragkos, K., Meleti, C., Tourpali, K., & Zempila, M. M. (2016). Short- and long-term variability of spectral solar UV irradiance at Thessaloniki, Greece: effects of changes in aerosols, total ozone and clouds. *Atmospheric Chemistry and Physics, 16*, 2493-2505. doi:10.5194/acp-16-2493-2016

Gallagher, R. P., & Lee, T. K. (2016). Adverse effects of ultraviolet radiation: A brief review. *Biophysics & Molecular Biology, 92*, 119-131. doi:10.1016/j.pbiomolbio.2006.02.011

Gallagher, R. P., Elwood, J. M., Rootman, J., Spinelli, J. J., Hill, G. B., Threlfall, W. J., & Birdsejj, J. M. (1985, 04 01). Risk factors for oculat melanoma: Western Canada melanoma study. *Journal of the National Cancer Institute, 74*(4), 775-778. doi:10.1093/jnci/74.4.775

Gallagher, R. P., Spinelli, J. J., & Lee, T. K. (2005). Tanning Beds, Sunlamps, and Risk of Cutaneous Malignant Melanoma. *Cancer Epidemiology, Biomarkers & Prevention, 14*(3), 562-566. doi:10.1158/1055-9965

Genet, R. (2018). *L'exposition aux ultraviolets artificiels émis par les cabines de bronzage.* Maisons-Alfort. Consulté le 11 12, 2018, sur https://www.anses.fr/fr/system/files/AP2018SA0131.pdf

Gröbner, J., Hülsen, G., Vuilleumier, L., Blumthaler, M., Vilaplana, J. M., Walker, D., & Gil, J. E. (2006). *Report of the PMOD/WRC-COST Calibration and Intercomparison of Erythemal radiometers.* PMOD/WRC-COST, Davos, Switzerland. Consulté le 10 22, 2018, sur ftp://ftp.pmodwrc.ch/pub/publications/PMOD_COST726_BBreport.pdf

Guarnieri, R. A., Padilha, L. F., Guarnieri, F. F., Echer, E., Makita, K., K., P. D., . . . Schuch, N. J. (2003, June). A study of the anticorrelations between ozone and UV-B radiation using linear and exponential fits in southern Brazil. *Advances in Space Research*, 764-768. doi:10.1016/j.asr.2003.06.040

Holick, M. F. (2001). Chapter 2 - A perspective on the beneficial effects of moderate exposure to sunlight: bone health, cancer prevention, mental health and well being. *Comprehensive Series in Photosciences, 3*, 13-37. doi:10.1016/S1568-461X(01)80037-5

Houët, M. (2003). *Spectroradiométrie du rayonnement Solaire UV au sol : Améliorations apportées à l'instrumentation et au traitement des mesures, Analyse pour l'évaluation du contenu atmosphérique en ozone et en aérosols.* Lille, France: Université de Lille.

Hülsen, G., & Gröbner, J. (2014). *Protocol of the intercomparison at Université de La Réunion, Saint-Denis, France on April 08 to 17, 2013 with the travelling reference spectroradiometer QASUMEfrom PMOD/WRC.* Davos, Switzerland: PMOD/WRC. Récupéré sur http://www-old.pmodwrc.ch/wcc_uv/qasume_audit/reports/2013_04_StDenis_LaReunion.pdf

Hülsen, G., & Gröbner, J. (2017). *2nd International UV filter Radiometer comparison UVC-II.* Davos, Switzerland: PMOD/WRC, WCC-UV. Consulté le 10 15, 2018, sur http://projects.pmodwrc.ch/bb2017/media/UVC-II_report.pdf

International Commission on Non-Ionizing Radiation Protection. (2004). Guidelines on limits of exposure to ultraviolet radiation of wavelengths between 180 nm and 400 nm. *Health Phys., 86*, 171-186.

Janjai, S., Wisitsirikun, S., Buntoung, S., Pattarapanitchai, S., Wattan, R., Masiri, I., & Bhattarai, B. K. (2014). Comparison of UV index from OMI with multi-chanel filter radiometers at four sites in the tropics: Effects of aerosols and clouds. *Int. J. Climatol., 34*, 453-461.

Jégou, F., Godin-Beekman, S., Corrêa, M. P., Brogniez, C., Auriol, F., Peuch, V. H., . . . Mahé, E. (2011). Validity of satellite measurements used for the monitoring of UV radiation risk on health. *Atmospheric Chemistry and Phisics, 11*(24), 13377-13394. doi:10.5194/acp-11-13377-2011

Joel Hillhouse, G. C., Thompson, K., Jacobsen, P. B., & Hillhouse, J. (2009, December). Investigating the role of appearance-based factors in predicting sunbathing and tanning salon use. *Journal of Behavioral Medicine, 32*(6), 532-44. doi:10.1007/s10865-009-9224-5.

Joint, I. (1999). *CIE Standard 17166: 1999/CIE S007-1998 Erythema Reference Action Spectrum and Standard Erythema.* Vienna, Austria: ISO.

Josse, B., Simon, P., & Peuch, V.-H. (2004). Radon global simulations with the multiscale chemistry and transport model MOCAGE. *Tellus B: Chemical and Physical Meteorology, 56*, 339-356. doi:10.3402/tellusb.v56i4.16448.

Jumaux, G., Quetelard, H., & Roy, D. (2011). *Atlas climatique de La Réunion.* Météo France, Direction interrégionale de la Réunion.

Karran, P., & Brem, R. (2016, August). Trotein oxidation, UVE and human DNA repair. (Elsevier, Éd.) *DNA repair, 44*, 178-185. doi:10.1016/j.dnarep.2016.05.024

Kazadzis, S., Bais, A., Arola, A., Krotkov, N., Kouremeti, N., & Meleti, C. (2009). Ozone Monitoring Instrument spectral UV irradiance products: Comparison with ground based measurements at an urban environment. *ACP, 9*, 585-594.

Kazadzis, S., Bais, A., Kouremeti, N., Zempila, M., Arola, A., Giannakaki, E., . . . Kazantzidis, A. (2009). Spatial and temporal UV irradiance and aerosol variability within the area of on OMI satellite pixel. *Atmos. Chem. Phys., 9*, 4593-4601.

Kazantzidis, A., Bais, A., Topaloglou, C., Garane, K., Zempila, M., Meleti, C., & Zerefos, C. (2006, October 12). Quality assurance of the Greek UV Network: preliminary results from the pilot

phase operation. *Remote Sensing of Clouds and the Atmosphere XI, 6362*, 636229. doi:10.1117/12.689798

Kazantzidis, A., Tzoumanikas, P., Bias, A. F., Fotopoulos, S., & Economou, G. (2012, September). Cloud detection and classification with use of whole-sky ground-based images. *Atmospheric Research, 113*, 80-88. doi:10.1016/j.atmosres.2012.05.005

Kerr, J. B., & Fioletov, V. E. (2008). Surface ultraviolet radiation. *Atmosphere-Ocean, 46*(1), 159-184. doi:10.3137/ao.460108

Kerr, J. B., & McElroy, C. T. (1993). Evidence for large upward trends of ultraviolet-B radiation linked to ozone depletion. 1032-1034. doi:10.1126/science.262.5136.1032

Kerr, J. B., Seckmeyer, G., Bais, A. F., Bernhard, G., Blumthaler, M., Diaz, S. B., . . . A. (2002). Surface ultraviolet radiation: Past and Future, Chapter 5. *Scientific Assessment of ozone Depletion*. Récupéré sur https://acd-ext.gsfc.nasa.gov/Documents/O3_Assessments/Docs/WMO_2002/10_chapter5.pdf

Koelemeijer, R. B., De Haan, J. F., & Stammes, P. (2003). A database of spectral surface reflectivity in the range 335–772 nm derived from 5.5 years of GOME observations. *Journal of Geophysical Research: Atmospheres, 108*(D2), 4070. doi:10.1029/2002jd002429

Koepke, P., Bais, A., Balis, D., Buchwitz, M., De Backer, H., de Cabo, X., . . . Weber, M. (1998, June). Comparison of Models Used for UV Index Calculations. *Photochemistry and Photobiology, 67*(6), 657-662. doi:10.1111/j.1751-1097.1998.tb09109.x

Koppmann, R., von Czapiewski, K., & Reid, J. S. (2005). A review of biomass burning emissions, part I: gaseous emissions of carbon monoxide, mathane, volatile organic compounds, and nitrogen containing compounds. *Atmospheric Chemistry and Physics Discussion, 5*(5), 10455-10516. doi:10.5194/acpd-5-10455-2005

Krotkov, N. A., Bhartia, P. K., Herman, J. R., Fioletov, V., & Kerr, J. (1998). Satellite estimation of spectral surface UV irradiance in the presence of tropospheric aerosols: 1. Cloud-free case. *Journal of Geophysical Research: Atmospheres, 103*(D8), 8779-8793.

Krueger, A. J., Walter, L. S., Bhartia, P. K., Schnetzler, C. C., Krotkov, N. A., Sprod, I., & Bluth, G. J. (1995, July 20). Volcanic sulfur dioxide measurements from the total ozone mapping spectrometer instruments. *Journal of Geophysical Research: Atmospheres, 100*(D7), 14057-14076. doi:10.1029/95JD01222

Lacagnina, C., Hasekamp, O. P., Bian, H., Curci, G., Myhre, G., van Noije, T., . . . Zhang, K. (2015). Aerosol single-scattering albedo over the global oceans: Comparing PARASOL retrievals with AERONET, OMI, and AeroCom models estimates. *Journal of Geophysical Research: Atmospheres, 120*(18), 9814-9836. doi:10.1002/2015JD023501

Lamy, K., Portafaix, T., Bencherif, H., Godin-Beekman, S., Brigniez, C., Metzger, J.-M., . . . Long, C. N. (2016, Sept). Ultraviolet Radiation modeling from groud based ans satellite measurements of ozone over Réunion Island. *Quadriennial Ozone Symposium 2016*, QOS2016-81-6.

Lamy, K., Portafaix, T., Brogniez, C., Godin-Beekmann, S., Bencherif, H., Morel, B., . . . Long, C. N. (2018). Ultraviolet radiation modelling from ground-based and satellite measurements on

Reunion Island, southern tropics. *Atmospheric Chemistry and Physics, 18*(1), 227-246. doi:10.5194/acp-18-227-2018

Lamy, K., Portafaix, T., Forestier, J.-B., Rakotoniaina, S., & Amélie, V. (2019). *Réseau UV-Indien— Premiers Résultats.* Antananarivo, Madagascar: Meeting Geosciences, Resources; Risques, Technologies.

Lamy, K., Portafaix, T., Josse, B., Brogniez, C., Godin-Beekmann, S., Bencherif, H., . . . Abraham, N. L. (2018). Ultraviolet Radiation modelling using output from the Chemistry Climate Model Initiative. *Atmospheric Chemistry and Physics Discussions*. doi:10.5194/acp-2018-525

Lansdowne, A. T., & Provost, S. C. (1998). Vitamin D3 enhances mood in healthy subjects during winter. *Psychopharmacology, 135*(4), 319-323. doi:10.1007/s002130050517

Larkö, O., & Diffey, B. L. (1993). Natural UV-B radiation received by people with outdoor, indoor, and mixed occupations and UV-B treatment of psoriasis. *Clim, Exp. Dermatol., 8*, 279-285. doi:10.1111/j.1365-2230.1983.tb01780.x

Liandrat, O., Cros, S., Braun, A., Saint-Antonin, L., Decroix, J., & Schmutz, N. (2017). Cloud cover forecast from a ground-based all sky infrared thermal camera. *Remote Sens. Clouds Atmos. XXII, 10424*, 104240B. doi:10.1117/12.2278636.

Lippmann, M. (1989). Health effects of ozone a critical review. (Taylor, & Francis, Éds.) *Japca, 39*(5), 672-695. doi:10.1080/08940630.1989.10466554

Lucas, R. M., & Ponsonby, A.-L. (2002). Ultraviolet radiation and health: friends and foe. *the Medical Journal of Australia, 117*(11), 594-598. Consulté le 11 06, 2018, sur https://www.mja.com.au/system/files/issues/177_11_021202/luc10478_fm.pdf

Lucas, R., McMichael, T., Smith, W., & Armstrong, B. (2006). *Solar Ultraviolet radiation: Global burden of disease from solar ultraviolet radiation.* Geneva: World Health Organization. Consulté le 11 06, 2018, sur http://www.who.int/uv/health/solaruvradfull_180706.pdf

Madronich, S. (1993). *UV radiation in the natural and perturbed atmosphere.* Boca Raton, USA: Lewis Publisher.

Madronich, S., Mayer, B., & Fischer, C. A. (1999). *A climatology of Erythemal Ultraviolet Radiation, 1979-1992.* NATO Advanced Study Institute (ASI), Chemistry and Radiation Changes in the Ozone Layer: Lokympari, Crete, Greece.

Mahé, E., Corrêa, M. P., Godin-Beekmann, S., Haeffelin, M., Jégou, F., Saiag, P., & Beauchet, A. (2013). Evaluation of tourists' UV exposure in Paris. *Journal of the European Academy of Dermatology and Venereology, 27*(3), e294-e304. doi:10.1111/j.1468-3083.2012.04637.x

Marchand, M., Keckhut, P., Lefebvre, S., Claud, C., Cugnet, D., Hauchecorne, A., . . . Bekki, S. (2012). Dynamical amplification of the stratospheric solar response simulated with the Chemistry-Climate Model LMDz-Reprobus. *Journal of Atmospheric and Solar-Terrestrial Physics, 75*, 147-160. doi:10.1016/j.jastp.2011.11.008

Marionnet, C., Tricaud, C., & Bernerd, F. (2015). Exposure to Non-Extreme Solar UV Daylight: Spectral Characterization, Effects on Skin Photoprotection. *International Journal of Molecular Sciences, 16*(1), 68-90. doi:10.3390/ijms16010068

Matsumura, y., & Ananthaswamy, H. N. (2004, March 15). Toxic effects of ultraviolet radiation on the skin. *Toxicology and Applied Pharmacology, 195*(3), 298-308. doi:10.1016/j.taap.2003.08.019

McKenzie, R. L., Liley, J. B., & Björn, L. O. (2009, 01 16). UV Radiation: Balancing Risks and Benefits. *Photochemistry and Photobiology, 85*(1), 88-98. doi:10.1111/j.1751-1097.2008.00400.x

McKenzie, R. L., Paulin, K. L., & Madronich, S. (1998). Effects of snow cover on UV irradiance and surface albedo: A case study. *Journal of Geophysical Research: Atmospheres, 103*, 28785-28792. doi:10.1029/98JD02704

McKenzie, R. L., Smale, D., & Kotkamp, M. (2004). Relationship between UVB and erythemally weighted radiation. *Photochem. Photobiol. Sci., 3*, 252-256.

McKenzie, R., Connor, B., & Bodeker, G. (1999, 09 10). Increased summertime UV radiation in New Zealand in Response to ozone loss. *Science*, 1709-1771. doi:10.1126/science.285.5434.1709

McKenzie, R., Kotkamp, M., Seckmeyer, G., Erb, R., Roy, C., Gies, H., & Toomey, S. (1993). First southern hemisphere intercomparison of measured solar UV spectra. *Geophy. Res. Lett., 20*, 2223-2226.

McPeters, R. D., & Labow, G. J. (2011). Climatology 2011: An MLS and sonde derived ozone climatology for satellite retrieval algorithms. *Journal of Geophysical Research: Atmospheres, 117*(D10). doi:10.1029/2011JD017006

Ncongwane, K. P. (2015). *Erythemally-Weighted UV Radiation Measurements at Six South African Sites. Master's Thesis, University of KwaZulu-Natal, Durban, South Africa.*

Ncongwane, K. P., & Coetzee, G. (2010). A quantitative analysis of the SAWS GAW UV network and data since 1994. . *In proceedings of the South African Society for Atmospheric Sciences Conference (SASAS), Gariep Dam, South Africa, 20-22 September 2010*, 20-22.

NICD. (2019, 05 07). *National Cancer Registry - Cancer Statistics.* Récupéré sur National Institute For Communicable Diseases: http://www.nicd.ac.za/centres/national-cancer-registry/

Norval, M., Kellett, P., & Wright, C. Y. (2013). The incidence and body site of skin cancers in the population groups of South Africa. *Photodermatology, Photoimmunology & Photomedicine*.

OMI. (2002). *Ozone Monitoring Instrument (OMI). OMI Algorithm Theoretical Basis Document Version III; Stammes, P., Noordhoek, R., Eds.; ATBD-OMI-03, Version 2.0, August 2002.* Ozone Monitoring Instrument (OMI):Netherlands's Agency for Aerospace Programs (NIVR), Netherland, and Finnish Meteorological Institute (FMI): Helsinki, Finland. Récupéré sur http://eospso.gsfc.nasa.gov/sites/default/files/atbd/ATBD-OMI-03.pdf

OMS. (2002). *L'indice universel de rayonnement UV solaire.* Consulté le 10 08, 2018, sur http://www.who.int/uv/publications/French_final.pdf

ONF. (s.d.). Récupéré sur http://www1.onf.fr/la-reunion/@@index.html

Ozone Monitoring Instrument (OMI) Team. (2012). *Data User's Guide.* Netherlands's Agency for Aerospace Programs (NIVR), Netherland, and Finnish Meteorological Institute (FMI): Helsinki, Finland.

Pfeifer, M. T., Koepke, P., & Reuder, J. (2006). Effects of altitude and aerosol on UV radiation. *Journal of Geophysical Research: Atmospheres, 111*(D1). doi:10.1029/2005JD006444

Prause, A. R., & Scourfield, M. W. (2002). Surface erythema irradiance and total column ozone above Durban, South Africa, for the period 1996-1998. *S. Afr. J. Sci., 98*, 186-188.

Rajakumar, K., Greenspan, S. L., Thomas, S. B., & Holick, M. F. (2007, October). SOLAR Ultraviolet Radiation AND Vitamin D: A Historical Perspective. *Am J Public Health, 97*(10), 1746-1754. doi:10.2105/AJPH.2006.091736

Réchou, A., & Kirkwood, S. (2015). Investigation of weather anomalies in the low-latitude islands of the Indian Ocean in 1991. *Annales Geophysicae, 33*, 789-804. doi:10.5194/angeo-33-789-2015

Rocco, M., Colomb, A., Baray, J.-L., Amelynck, C., Verreyken, B., Borbon, A., . . . Brioude, J. (2020). Analysis of Volatile Organic Coumpounds during the OCTAVE Campaign: Sources and Distributions of Formaldehyde on Reunion Island. *Atmosphere, 11*, 140. doi:10.3390/atmos11020140

Sanchez-Pérez, J. F., Vicente-Agullo, D., Barbera, M., Castro-Rodriguez, E., & Canovas, M. (2019). Relationship between ultraviolet index (UVI) and first-, second- and thrid- degree sunburn using the Probit methodology. *Scientific reports, 9*, 1-13. doi:10.1038/s41598-018-36850-x

Schmalwieser, A. W., Gröbner, J., Blumthaler, M., Klotz, B., De Backer, H., Bolsé, D., . . . O'Hagan, J. (2017, August 14). UV Index monitoring in Europe. *Photochemical and Photobiological Sciences, 16*(9), 1349-1370. doi:10.1039/C7PP00178A

Schwarz, T. (2010, 01 01). The Dark and the Sunny Sides of UVR-Induced Immunosuppression: Photoimmunology Revisited. (Elsevier, Éd.) *Journal of Investigative Dermatology, 130*(1), 49-54. doi:10.1038/jid.2009.217

Seckmeyer, G., Bernhard, A., Blumthaler, M., Booth, C., Lantz, K., & Webb, A. (2005). *Instruments to Measure Solar Ultraviolet Radiation. Part 2: Broadband Instruments Measurieng Erythemally Weighted Solar Irradiance;.* Geneva, Switzerland: World Meteorological Organization (WMO).

Shindell, D., Rind, D., Balachandran, N., Lean, J., & Lonergan, P. (1999, APR 09). Solar Cycle Variability, Ozone, and Climate. *Science, 284*(5412), 305-308. doi:10.1126/science.284.5412.305

Shipowick, C. D., Moore, C. B., Corbett, C., & Bindler, R. (2009, August). Vitamin D and depressive symptoms in women during the winter: A pilot study. *Applied Nursing Research, 22*(3), 221-225. doi:10.1016/j.apnr.2007.08.001

Sin, C., Beauchet, A., Marchal, A., Sigal, M. L., & Mahé, E. (2013). Compréhension et utilisation de l'indice universel de rayonnement solaire (« indice ultraviolet ») par les dermatologues français métropolitains. *Annales de dermatologie et de vénéréologie, 140*, 15-20.

Sinha, R. P., & Häder, D.-P. (2002, Mars 13). UV-induced DNA damage and repair: a review. *Photochemical & Photobiological Sciences, 1*(4), 225-236. doi:10.1039/b201230h

Sitas, F. (1994). Histologically diagnosed cancers in South Africa. *S. Afr. Med. J., 84*, 334-348.

Slaper, H., Velders, J. M., Daniel, S. J., de Gruilj, F. R., & van der Leun, J. C. (1996). Estimates of ozone depletion and skin cancer incidence to examine the Vienna Convention achievements. *Nature, 384*(6606), 256.

Sola, Y., & Lorente, J. (2015, February). Contribution of UVA irradiance to the erythema and photoaging effects in solar and sunbed exposures. *Journal of Photochemistry and Photobiology B: Biology, 143*, 5-11. doi:10.1016/j.jphotobiol.2014.10.024

Stamnes, K., Tsay, S.-C., Wiscombe, W., & Jayaweera, K. (1988). Numerically stable algorithm for discrete-ordinate-method radiative transfer in multiple scattering and emitting layered media. *Applied optics, 27*(12), 2502-2509. doi:10.1364/AO.27.002502

Steinmetz, M. (1997, November). Continuous solar UV monitoring in Germany. *Journal of Photochemistry and Photobiology B: Biology, 41*(1-2), 181-187. doi:10.1016/S1011-1344(96)07455-6

Takemura, T., Nakajima, T., Dubovik, O., Holben, B. N., & Kinne, S. (2002). Single-scattering albedo and radiative forcing of various aerosol species with a global three-dimensional model. *Journal of Climate, 15*(4), 333-352. doi:10.1175/1520-0442(2002)015<0333:SSAARF>2.0.CO;2

Tarasick, D. W., Fioletov, V. E., Wardle, D. I., Kerr, J. B., McArthur, L. J., & McLinden, C. A. (2010, 11 21). Climatology and trends of surface UV radiation: Survey article. *Atmosphere-Ocean, 41*(2), 121-138. doi:10.3137/ao.410202

Tesfaye, M., Sivakumar, V., Botai, J., & Mengistu Tsidu, G. (2011). Aerosol climatology over South Africa on 10 years of Multiangle Imaging Spectroradiometer (MISR) data. *Journal of Geophysical Research, 116*. doi:10.1029/2011JD016023

Tewari, A., Grage, M. M., Harrison, G. I., Sarkany, R., & Young, A. R. (2013, November 22). UVA1 is skin deep: molecular and clinical implications. *Photochemical & Photobiological Sciences, 12*, 95-103. doi: 10.1039/C2PP25323B

Toihir, A. M., Bencherif, H., Sivakumar, V., Amraoui, L. E., Portafaix, T., & Mbatha, N. (2015). Comparison of total column ozone obtained by the IASI-MetOp satellite with ground-based and OMI satellite observations in the southern tropics subtropics. *Ann. Geophys., 33*, 1135-1146.

Toihir, A. M., Portafaix, T., Sivakumar, V., Bencherif, H., Pazmiño, A., & Bègue, N. (2018). Variability and trend in ozone over the southern tropics and subtropics. *Annales Geophysicae, 36*(2), 381-404. doi:10.5194/angeo-36-381-2018

Tourisme, C. R. (2018). Récupéré sur Fréquentation touristique 2018: https://pro.reunion.fr/actualites/etudes-et-indicateurs/chiffres-du-tourisme-2018-le-bilan

Tucker, M. A., Shields, J. A., Hartge, P., Augsburger, J., Hoover, R. N., & Fraumeni, J. F. (1985). Sunlight exposure as risk factor for intraocular malignant melanoma. *New England Journal of Medicine, 313*(13), 789-792. doi:10.1056/NEJM198509263131305

UNESCO. (s.d.). Récupéré sur Pitons, ccirques et remparts of Reunion Island: https://whc.unesco.org/en/list/1317/

Utrillas, M. P., Marin, M. J., Esteve, A. R., Tena, F., Cañada, J., Estellés, V., & Martinez-Lozano, J. A. (2007, 12 28). Diffuse UV erythemal radiation experimental values. *JGR Atmospheres, 112*(D24). doi:10.1029/2007JD008846

Varotsos, C. (1994). Solar ultraviolet radiation and total ozone, as derived from satellite and ground-based instrumentation. *Geophys. Res. Lett., 21*, 1787-1790.

Vasaras, A., Bais, A., Feister, U., & Zerefos, C. (2001). Comparison of two methods for cloud flagging of spectral UV measurements. *Atmos. Res., 57*, 31-42.

Vernet, M., Brody, E. A., Holm-Hansen, O., & Mitchell, B. G. (1994, January 01). The response of Antarctic phytoplankton to ultravioler radiation: absorption, photosynthesis, and taxonomic composition. (C. S. Weiler, & P. A. Penhale, Éds.) *Ultraviolet radiation in Antarctica: measurements and biological effects, 62*, 143-158. doi:10.1029/AR062p0143

Vilaplana, J., Serrano, A., Anton, M., Cancillo, M., Parias, M., & Gröbner, J. (2007). *Report of the "El Arenosillo"/INTA-COST Calibration and Inter-Comparison Campaign ofUVERBroadband Radiometers.* Huelva, Spain: El Arenosillo.

Von Schirnding, U., Strauss, N., Mathee, A., Robertson, P., & Blignaut, R. (1991). Sunscreen use and environmental awareness among beach-goes in Cape Town, South Africa. *Public Health Rev., 19*, 209-217.

Warocquier, J. (2016). Données épidémiologiques des mélanomes cutanés à la Réunion en 2015. *Médecine hunamine et pathologie*.

Waroquier, J., Miquel, J., Chirpaz, E., Beylot-Barry, M., & Sultan-Bichat, N. (2015). Données épidémiologiques des mélanomes cutanés à la Réunion en 2015. *Annales de Dermatologie et de Vénéréologie, 143*(12), S313-S314. doi:10.1016/j.annder.2016.09.476

Webb, A. R., Kline, L., & Holick, M. F. (1988). Influence of Season and Latitude on the Cutaneous Synthesis of Vitamin D3: Exposure to Winter Sunlight in Boston and Edmonton Will Not Promote Vitamin D3 Synthesis in Human Skin. *The Journal of Clinical Endocrinology & Metabolism, 67*(2), 373-378. doi:10.1210/jcem-67-2-373

Webb, A. R., Slaper, H., Koepke, P., & Schmalweiser, A. W. (2011). Know your standard: Clarifying the CIE Erythema Action Spectrum. *Photochemistry and Photobiology, 87*(2), 483-486. doi:10.1111/j.1751-1097.2010.00871.x

Webb, A., Gröbner, J., & Blumthaler, M. (2006). *Practical Guide to Operating Broadband Instruments Measuring Erythemally Weighted Irradiance.* Luxembourg, Luxembourg: Office for Official Publication of the European Communities. doi:EUR 22595, ISBN 92-898-0032-1.

Webb, A., Gröbner, J., & Blumthaler, M. (2007). *A practical guide to operating broadband instruments measuring erythemally weighted irradiance.* EUR-OP.

Weihs, P., Blumthaler, M., Rieder, H. E., Kreuter, A., Simic, S., Laube, W., . . . Tanskanen, A. (2009). Measurements of UV irradiance within the area of one satellite pixel. *ACP, 8*, 5615-5626.

WHO (World Health Organization). (2002). *Global Solar UV Index: A practical Guide.* Geneva, Switzerland: WHO report. Récupéré sur http://www.who.int/uv/publications/en/

WHO. (1994). Environmental health criteria 160: ultraviolet radiation. *Geneva: WHO*, 15-43.

WMO. (1975). *Modifications de la couche d'ozone résultant des activités de l'homme et leurs éventuelles conséquences géophysiques.*

WMO. (2014). *Assessment for Decision-Makers: Scientific Assessment of Ozone Depletion.* World Meteorological Organization, Geneva, Switzerland.

Wright, C. Y., Brogniez, C., Ncongwane, K. P., Venkataraman, S., Coetzee, G., Metzger, J.-M., . . . Sauvage, B. (2013, 06 29). Sunburn Risk Among Children and Outdoor Workers in South Africa and Reunion Island Coastal Sites. *Photochemistry and Photobiology, 89*(5), 1226-1233. doi:10.1111/php.12123

Wright, C. Y., Coetzee, G., & Ncongwane, K. (2011). Ambiant solar UV radiation and seasonal trends in potential sunburn risk among schoolchildren in South Africa. *S. Afr. J. Child Health, 5*, 33-38.

Young, A. R. (2006). Acute effects of UVR on human eyes and skin. *Progress in Biophysics and Molecular Biology, 92*(1), 80-85. doi:10.1016/j.pbiomolbio.2006.02.005

Zaratti, F., Piacentini, R. D., Guillén, H. A., Cabrera, S. H., Liley, J. B., & McKenzie, R. L. (2014). Proposal for a modification of the UVI risk scale. *Photochemical & Photobiological Sciences, 13*(7), 980-985. doi:10.1039/C4PP00006D

Zempila, M. M., Koukouli, M. E., Bais, A., Fountoulakis, I., Arola, A., Kouremeti, N., & Balis, D. (2016). OMI/Aura UV product validation using NILU-UV ground-based measurements in Thessaloniki, Greece. *Atmos. Environ., 140*, 283-297.

Zempila, M., Giannaros, T., Bais, A., Melas, D., & Kazantzidis, A. (2016). Evaluation of WRF shortwave radiation parameterizations in predicting Global Horizontal Irradiance in Greece. *Renew. Energy, 86*, 831-840.

Zerefos, C. S. (2002). Long-term ozone and UV variations at Thessaloniki, Greece. *Physics and Chemistry of the Earth*, 455-460. doi:10.1016/S1474-7065(02)00026-8

RESUME

Les causes potentielles de l'augmentation des cancers de la peau sont nombreuses, comme les changements comportementaux ou les modifications de l'intensité des rayonnements ultraviolets (UV) à la surface, en réponse aux perturbations de paramètres environnementaux (ozone stratosphérique, nébulosité, aérosols) dues au changement climatique ou aux activités anthropiques. Compte tenu de leur position géographique, les régions tropicales reçoivent le maximum de rayonnement solaire incident et donc d'UV. Le risque UV dans ces régions est très élevé, du fait de plusieurs facteurs dont la démographie ou les habitudes d'activités en extérieur. La mesure précise de l'intensité du rayonnement ultraviolet est donc primordiale. Un des objectifs de ce travail a été l'évaluation de la qualité de différents instruments par comparaison à un instrument de référence. Un exercice de comparaison satellite a également été réalisé. Une étude de tendance a été faite à partir de la base de données UV de La Réunion. Une tendance à l'augmentation a été trouvée. Cette augmentation peut être due à un changement d'ozone ou encore à un changement de nébulosité liée à l'augmentation de la température des océans. Enfin, il a été réalisé des mesures d'exposition dans des lieux très fréquentés et où l'intensité du rayonnement et le risque UV sont très élevés. La Réunion étant une île montagneuse connue pour ses nombreuses possibilités de randonnées et d'activités en extérieur, des mesures d'exposition ont été réalisées sur des sites fréquentés, par exemple la randonnée Maïdo-Grand Bénare ; réalisée en 7h de marche, au bout desquelles il a été mesuré plus de 60 doses standards érythemales. Selon le phototype, et quel que soit le site, les doses obtenues sont de multiples fois supérieures aux doses minimales erythemales. Il en ressort clairement l'importance de la protection des populations ainsi que la nécessité de campagne de prévention sur le risque UV.

ABSTRACT

The main causes of skin cancer are human behavior change and the increase of surface ultraviolet radiation, in response to atmospheric parameters changes (stratospheric ozone, clouds, or aerosols) due to climate change or anthropogenic activities. Taking into account their geographic position, tropical regions receive the maximum of solar UV irradiance. The risk related to UV is very high, due to the demography or increase in outdoor activities. The precise UV measurement then becomes very important. One of the purpose of this PhD thesis was the evaluation of different UV measurement instruments in comparison to a reference one. Comparison to satellite UV measurements was also performed. A trend study was done by using ground-based UV database at Saint-Denis. An increase trend in UVI was found. This increase may be due to ozone change or to cloud change in response to the increase of sea temperature caused by climate change. Following that comparison work, UV exposure work was done in popular sites where people are exposed to extreme UV radiation, in altitude for example. Réunion island is a mountainous well-known for its several possibilities of hikes and outdoors activities. The measurement performed during the Maïdo - Grand Bénare hike, for example, showed that people can be exposed up to 60 standard erythemal doses, what corresponds to several times the minimal threshold to elicit sunburn whatever the sun phototype. Therefore, the public must be informed of the danger of UV exposure. Along with more awareness campaigns and more efficient measuring devices placed around the island, a general understanding of UVR will improve, thereby reducing the risks linked to excess exposure resulting from insufficient UVR protection.